Cell Reports
Medicine

Article

Traumatic life experiences during critical periods lead to diverse developmental trajectories

Graphical abstract

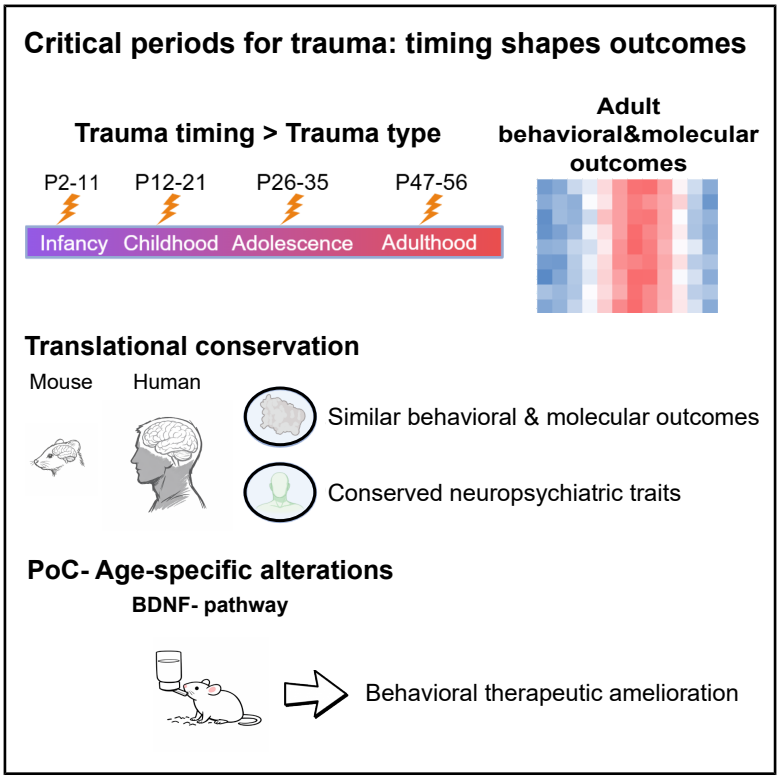

Highlights

- Mostly trauma timing, not type, drives long-term behavioral and molecular changes
- Findings in mice parallel effects of traumatic life events in humans
- BDNF pathway is a potential target for trauma-related psychopathology in young adults

Authors

Giovanni Morelli, Greta Visintin, Elisa Gelli, ..., Andrea Petretto, Valter Tucci, Laura Cancedda

Correspondence

laura.cancedda@iit.it

In brief

Morelli et al. showed that exposure to traumatic events during distinct developmental periods in mice and humans produces long-lasting behavioral and molecular changes, revealing critical periods in which stress timing, rather than its nature, shapes adult brain function. The BDNF pathway represents a potential therapeutic target for trauma in young adulthood.

Morelli et al., 2026, Cell Reports Medicine 7, 102798
June 16, 2026
https://doi.org/10.1016/j.xcrm.2026.102798

CellPress

Please cite this article in press as: Morelli et al., Traumatic life experiences during critical periods lead to diverse developmental trajectories, Cell Reports Medicine (2026), https://doi.org/10.1016/j.xcrm.2026.102798

Cell Reports Medicine

CellPress
OPEN ACCESS

Article

Traumatic life experiences during critical periods lead to diverse developmental trajectories

Giovanni Morelli,[1,10] Greta Visintin,[1,2,10] Elisa Gelli,[3] Angelo Serani,[3] Martina Bartolucci,[4] Sara Uccella,[5,6] Maria D'Apruzzo,[6] Deborah Preiti,[6,7] Mariam Marie Chellali,[1,2] Alessandra Cucinelli,[1,2] Mohit Rastogi,[1,2] Matteo Falappa,[3] Andrea Scalabrini,[8] Gustavo Turecki,[9] Andrea Petretto,[4] Valter Tucci,[3,11] and Laura Cancedda[1,11,12,*]

[1]Brain Development and Disease Laboratory, Istituto Italiano di Tecnologia, Genoa, Italy
[2]University of Genoa, Genoa, Italy
[3]Genetics and Epigenetics of Behavior Laboratory, Istituto Italiano di Tecnologia, Genoa, Italy
[4]Core Facilities - Clinical Proteomics and Metabolomics, IRCCS Istituto Giannina Gaslini, Genoa, Italy
[5]Department of Neurosciences, Rehabilitation, Ophthalmology, Genetics, and Maternal and Child Health (DINOGMI), University of Genoa, Genoa, Italy
[6]Child Neuropsychiatry Unit, IRCCS Istituto Giannina Gaslini, Genoa, Italy
[7]Patologia Neonatale, IRCCS Istituto Giannina Gaslini, Genoa, Italy
[8]Department of Human and Social Sciences, University of Bergamo, Bergamo, Italy
[9]Douglas Institute, Department of Psychiatry, McGill University, Montreal, QC, Canada
[10]These authors contributed equally
[11]These authors contributed equally
[12]Lead contact
*Correspondence: laura.cancedda@iit.it
https://doi.org/10.1016/j.xcrm.2026.102798

SUMMARY

Traumatic events can disrupt neurodevelopment, increasing the risk for neuropsychiatric disorders. However, the relationships between specific types of traumas and the emergence of particular neuropsychiatric traits remain elusive. Here, we examine the long-term consequences of different life-threatening events experienced during four distinct developmental periods in mice. Our findings at the behavioral and molecular/cellular levels in adulthood suggest a crucial role for timing (rather than type) of stress during development in shaping long-term outcomes. Our parallel analysis of individuals exposed to trauma at diverse life stages reveals similar results. Finally, our proteomic data suggest the brain-derived neurotrophic factor (BDNF)-pathway as a promising therapeutic target for ameliorating psychopathology related to trauma experienced specifically in early adulthood in mice and potentially in individuals. Our results point to the existence of critical periods for trauma exposure that uniquely influence adult behavioral outcomes and induce time-specific molecular/cellular patterns in the brain, which may have therapeutic implications.

INTRODUCTION

Brain development is defined by a timely sequence of neurodevelopmental genetic programs and by life experiences that interact closely to shape adult behavior by modifying the molecular and cellular landscape of the individual.[1,2] Since the 20th century, influential observers of human behavior (e.g., Freud, Piaget) have attempted to identify developmental stages at which individuals are especially vulnerable to negative life experiences.[3–5] Analogously, pioneering neurophysiologists discovered critical periods for brain plasticity.[6] These are specific time windows when the developing brain is particularly sensitive to environmental stimuli and life experiences, accompanied by an enhanced ability to modify neuronal connections.[7] In modern neuroscience, it is currently accepted that positive experiences (e.g., nurturing care, stable environments) during critical periods modulate gene expression, cellular signaling, and brain wiring, favoring the manifestation of healthy behavioral skills (e.g., language, musical abilities), which are more challenging to acquire in adulthood.[1,2,8] Conversely, traumatic experiences (e.g., physical/sexual abuse, domestic violence) can disrupt this process, causing long-lasting maladaptive brain modifications and behaviors.[9–13] Specifically, dysfunctional behaviors due to traumatic experiences are characterized by diverse combinations of traits such as aggressiveness/dominance, social impairment, attention deficit, hyperactivity, depression, generalized/repetitive anxiety, and abnormal personality (as in personality disorders [PDs][14–17]). In adults, maladaptive behaviors, PDs, and posttraumatic stress disorder (PTSD[18]) often coexist[19,20] and manifest with unique characteristics independent of the large variety of traumatic life events that can be experienced in life.[21] Indeed, current knowledge suggests that any type of adverse

Please cite this article in press as: Morelli et al., Traumatic life experiences during critical periods lead to diverse developmental trajectories, Cell Reports Medicine (2026), https://doi.org/10.1016/j.xcrm.2026.102798

event can lead to any mental disorder. Additionally, genetic/epigenetic mechanisms account only partially for vulnerability to specific mental health outcomes following exposure to traumatic life experiences.[22–25]

Here, we investigated whether the timing of stress exposure (independent of its type) serves as a significant factor connecting experienced trauma with subsequent adult specific behavioral traits or neuropsychiatric outcomes. We identified the long-term consequences of two diverse types of trauma in mice (i.e., predator-scent exposure or underwater immersion), chosen among adverse life experiences equally applicable to different time windows (infancy, childhood, adolescence, and young adulthood). We compared our observations associated with the timing of stress in mice with the neuropsychiatric outcomes or brain proteomic signatures of people exposed to trauma at different times in life and found distinct alterations in both. These alterations were specifically associated with the timing, rather than the type, of trauma. Finally, our study indicated the brain-derived neurotrophic factor (BDNF) pathway as a promising pharmaceutical target to ameliorate psychopathology resulting from trauma exposure specifically experienced during young adulthood in mice and potentially in people.

RESULTS

The timing of trauma exposure during life induces specific behavioral phenotypes in adult mice

Critical periods during mouse development are correlated with analogous stages in human development. Therefore, we optimized stress paradigms applicable to diverse age groups of C57BL/6J wild-type mice, focusing on infancy (postnatal day [P2–11]), childhood (P12–21), adolescence (P26–35), and young adulthood (P47–56; Figure 1A). Innate predator fear was induced by exposing mice to a fox scent (2,4,5-trimethylthiazole, TMT) for 10 min, whereas acquired trauma was induced by two underwater immersions (IMMs) (2 s each during 2 min of floating). To target infancy and childhood, we also used a similar-duration maternal-separation (MS) paradigm (15 min), a validated preweaning stressor.[26] The control groups included naive and handled mouse litters distinct from stressed litters to avoid the potential influence of stress among control and stressed mates within the same litter. Controls for the TMT group included additional saline-exposed mice. All mice were behaviorally characterized in full adulthood (>P90; Figures 1B–1F).

First, we measured the activation of the stress response in mice at the end of their stress exposure. Corticosterone levels in trauma-exposed mice were significantly higher than those in unstressed, age-matched controls at all ages of trauma (Figures 1G and S1).

In mice stressed at different ages, we next evaluated the long-term behavioral consequences in adulthood ($p > 90$; Table S1). We found that dominance, social interaction, attention, and depression-related behaviors depended on the age of stress exposure, mostly irrespective of the stress type (Figures 1B–1E and S2A–S2D).

With respect to dominance, tested by the tube dominance task in adulthood, infancy-stressed mice exhibited submissive behavior toward age-matched controls, regardless of the experienced trauma. In contrast, stress during adolescence and young adulthood led to increased dominance (Figures 1B, S2A, and S3A). Mice stressed during childhood did not show changes in dominance.

In social interaction tests using the three-chamber apparatus, which we combined into a unique score, mice stressed in infancy or young adulthood displayed social deficits, again irrespective of the trauma, whereas mice stressed during childhood or adolescence did not (Figures 1C, S2B, and S3B). Notably, for social behavior, the type of trauma influenced specific subdomains of social interaction, such as sociability with TMT vs. social novelty with IMM, in mice stressed during young adulthood (Figure S3C, left and right, respectively), and social novelty was affected in mice stressed during adolescence only by IMM (Figure S3C, right).

We assessed attention using the Phenopy system, a home-cage cognitive approach.[27] Adult mice stressed during childhood, adolescence, or young-adulthood (but not mice stressed during infancy) showed significant attention deficits, as their accuracy was impaired when comparing the number of correct trials. The general effect was independent of the type of trauma experienced (Figures 1D, S2C, and S3D). However, a more detailed analysis revealed trauma-related specific differences in attention subdomains. Compared with control mice, mice stressed in infancy showed minor differences across diverse types of trauma, mostly in congruent and incongruent trials. Those stressed in childhood exhibited severe attention impairments across all types of trials and trauma. Adolescence-stressed mice displayed deficits in no-cue and incongruent trials, whereas young adulthood-stressed mice had the most deficits in congruent and incongruent trials when all the traumas were considered (Figures S4A–S4I). These findings were independent of the ability to eventually learn the Phenopy test (Figures S4J–S4L).

We evaluated depression-related (despair) behaviors using tail suspension and forced swim tests, combined into a unique score.[28] We found significant depressive-like traits only in mice stressed during young adulthood, regardless of the type of experienced trauma (Figures 1E, S2D, and S3E–S3G).

For anxiety/obsessive-compulsive disorder (OCD)-related behaviors, we used a scoring approach and combined marble burying and grooming (assessing anxiety-related behaviors in terms of repetitive/OCD-related behaviors), and open field and dark/light tests (assessing generalized anxiety-related behaviors) to include diverse anxiety components. Consistent with the high prevalence of anxiety disorders in persons with a history of trauma exposure,[29,30] we observed increased anxiety/OCD-related behaviors in all animals, independent of the period and type of stress exposure (Figures 1F, S2E, and S3H–S3L), with subtle differences within the same anxiety/OCD subdomains driven by the type of trauma (P12–21 and P47–56 group, Figure S3L; P12–21 group; Figure S3K) or by the type of test (P26–35, Figures S3K and S3L). Figure S2F summarizes the long-term behavioral consequences of our stressor paradigms. Finally, analysis of sex differences revealed that males and females presented overall comparable values (Figure S3, black and red dots, respectively), with limited exceptions (Table S2).

Please cite this article in press as: Morelli et al., Traumatic life experiences during critical periods lead to diverse developmental trajectories, Cell Reports Medicine (2026), https://doi.org/10.1016/j.xcrm.2026.102798

CellPress
OPEN ACCESS

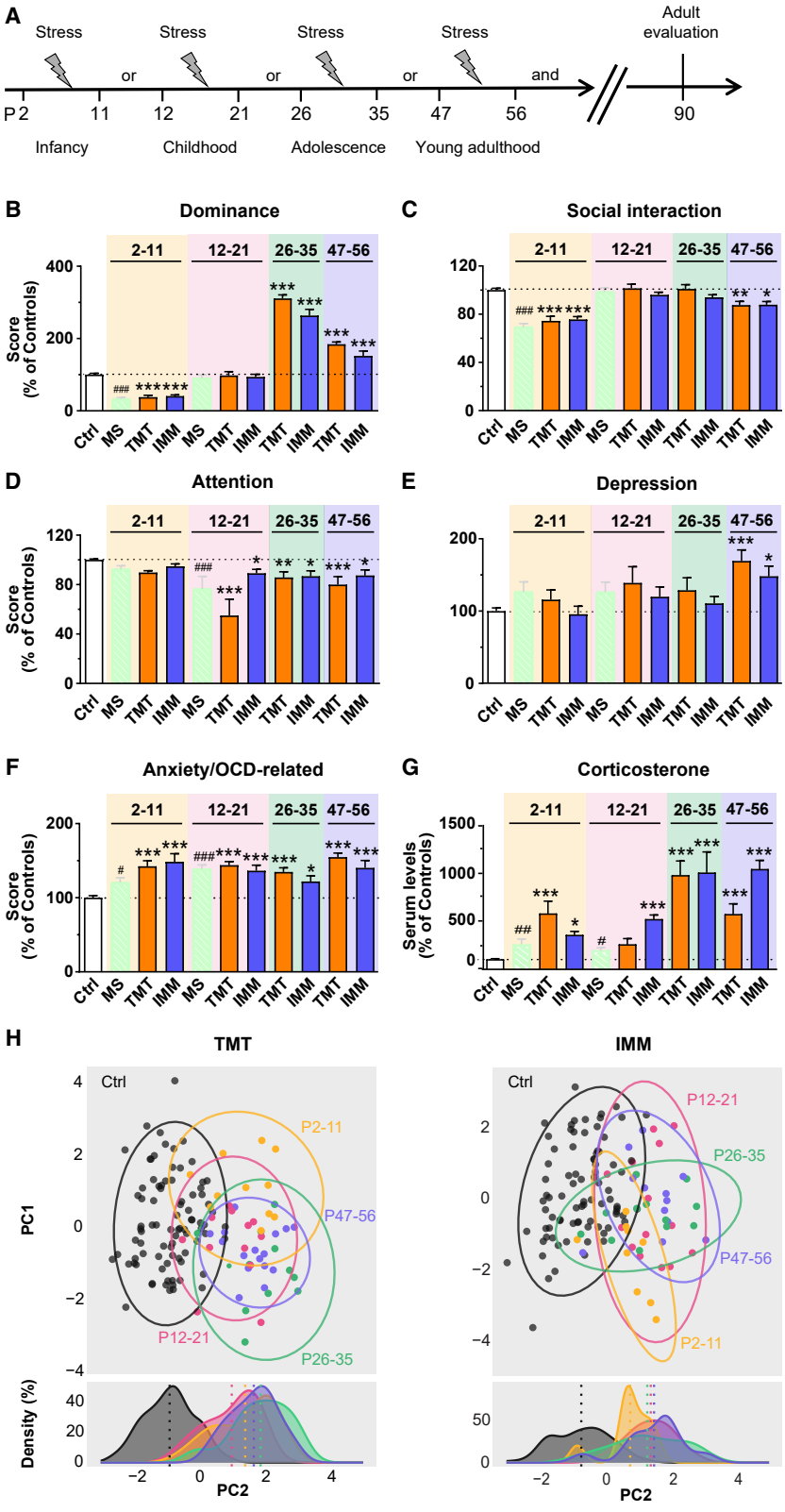

Figure 1. The timing and not the type of trauma exposure earlier in life determines the presence of specific neuropsychiatric-like traits in adult mice

(A) Experimental protocol. Wild-type mice were exposed to a stressor at the indicated developmental times and tested during full adulthood. Stresses included maternal separation (MS; infancy or childhood only), exposure to a predator odor (TMT), or underwater immersion (IMM).

(B–F) Average percentage (+ standard error of the mean [SEM]) of dominance (B), social interaction (C), attention (D), depression (E), and anxiety/OCD (F) scores of adult mice exposed to TMT or IMM at the indicated ages and age-matched controls. The MS data derive from Figure S2 and are reported here for comparison. The percentages were calculated based on the scores created in the experiments presented in Figure S3. Data were derived from at least 2 independent experiments for a total of 9–16 animals per experimental group (total of 209 animals). Exclusively for attention, data were derived from 1 or 2 experiments for a total of 6–9 animals per experimental group (total of 136 animals). Each score is represented as percentage over controls (each age is normalized to its own control) for comparison across ages (TMT and IMM vs. controls: two-way ANOVA, (B) $F_{stress(2,171)} = 43.2$, $p < 0.0001$; (C) $F_{stress(2,169)} = 18.40$, $p < 0.0001$; (D) $F_{stress(2,107)} = 39.94$, $p < 0.0001$; (E) $F_{stress(2,170)} = 9.34$, $p = 0.0001$; (F) $F_{stress(2,170)} = 54.33$, $p < 0.0001$, followed by Dunnett's multiple comparisons test, $^{*}p < 0.05$, $^{**}p < 0.01$, $^{***}p < 0.001$; MS vs. controls: the statistics (#) refer to those in Figure S2).

(G) Average percentage + SEM of mouse serum corticosterone levels at the end of the stress paradigm for all considered ages normalized to the levels of each specific age-matched naive control (non-normalized data in Figure S1). For each age, data were derived from one experiment. (TMT and IMM vs. controls: two-way ANOVA, $F_{stress(2,107)} = 112.4$, $p < 0.0001$, followed by Dunnett's multiple comparisons test, $^{*}p \leq 0.0525$, $^{***}p < 0.001$; MS vs. controls: $F_{stress(1,46)} = 19.77$, $p < 0.0001$, followed by Šídák's multiple comparisons test, $\#p < 0.05$, $\#\#p < 0.01$).

(H) Top: principal-component analysis (PCA) visualization of the first two components for adult mice exposed to TMT or IMM and age-matched controls from behavioral parameters of the same datasets as in (B), (C), (E), and (F). Dots indicate individual mice; colored circles define clusters at the 80th percentile of multivariate *t* distribution of animals exposed to stress at a specific age, whereas the black circle represents the group of controls from all age-of-stress groups. Bottom: graphs showing PC2 densities color-coded for age as in top. Dotted lines: mean distributions of the curves.

See also Tables S2 and S4.

Please cite this article in press as: Morelli et al., Traumatic life experiences during critical periods lead to diverse developmental trajectories, Cell Reports Medicine (2026), https://doi.org/10.1016/j.xcrm.2026.102798

Next, we examined whether differences in the temporal interval between stress exposure and behavioral assessment (different for all our experimental cases) could contribute to the age-dependent outcomes of stress. We conducted a proof-of-concept experiment by exposing mice to TMT during adolescence (P26–35) and performing behavioral tests from P140 (vs. P90 in our standard protocol). Mice exposed to TMT during adolescence showed comparable dominant and anxiety/OCD-related behaviors when evaluated at P90 or P140 (Figures S3M and S3N; Table S3). This indicates that stress-induced maladaptive behaviors persisted over time and did not depend on the temporal lag between stress exposure and behavioral assessment. Consistently, exposing adult animals (P90–99) to TMT and analyzing their behavioral phenotype 4 weeks later (the same temporal lag as in our standard protocol), resulted in fewer effects than those observed in mice exposed to stress during young adulthood (P47–56). Animals stressed during full adulthood showed decreased social interaction and increased anxiety/OCD-related behaviors, mainly due to the generalized component (Table S3), whereas animals stressed during young adulthood showed increased anxiety/OCD-related behaviors mainly due to the repetitive component, as well as increased dominant and depressive-like behaviors, two phenotypes not present following stress exposure during full adulthood (Figures S3O and S3P). These latter findings also point to the existence of specific critical periods for stress-induced outcomes during young vs. full adulthood.

We observed no motor and/or sensory deficits at any age of stress exposure in a modified version of the SmithKline Beecham, Harwell, Imperial College, and Royal London Hospital Phenotype Assessment (SHIRPA) battery test in adult animals stressed earlier in life (Figure S5A; Table S4).

Finally, since PTSD and PD comorbidities include hyperactivity,[31–33] we analyzed this comorbid behavior in our mice. Only mice exposed to TMT during adolescence were hyperactive, as indicated by increased distance traveled in the open field test (Figure S5B) and more trial-independent nose pokes during the Phenopy training phase (Figure S5C).

Recent literature has introduced the psychopathology *p* factor as a general latent dimension derived from a wide range of psychiatric symptoms.[34,35] We adapted this concept to rodents and performed a multidimensional analysis (principal-component analysis [PCA]) of our behavioral data from mice exposed to TMT or IMM; we excluded attention data because they were obtained from a separate cohort of animals due to the isolation required by the Phenopy test. PCA revealed a clear separation between controls and stress-exposed animals, with clustering according to the age of stress exposure, regardless of the nature of the trauma (Figure 1H, top) but with TMT having the greatest impact on overall behavior (Figure 1H, bottom left vs. right).

These findings reveal deficits in specific behavioral domains arising from critical periods for earlier-life stress experienced at various postnatal ages, independent of the stress type.

Mice stressed earlier in life show stress-timing-specific and brain-area-specific patterns of protein expression

Next, we focused on the TMT stressor paradigm and performed a proteomic analysis in adult mice stressed across all four periods of interest and in naive adult controls. We analyzed the amygdala, hypothalamus, hippocampus, and prefrontal cortex (PFC), brain areas primarily involved in stress-related neuropsychiatric disorders.[36,37] First, to assess the general cellular biological effects of traumatic stress by brain region and independent of age of stress exposure, we performed a pathway enrichment analysis on up- and downregulated proteins by interrogating EnrichR-Knowledge Graph (KG) gene-set libraries (Gene Ontology [GO] biological process, Reactome, Mouse Genome Informatics (MGI) mammalian phenotype, DisGenEt, Jensen disease[38]), and we identified common and brain-specific proteins (Figure S6A; Table S5). By grouping together terms enriched by stress exposure (q value < 0.05) within the same cellular context, we found that metabolic abnormalities and other general pathways, such as protein transport and translation, were common to all brain regions (Figure S6B). Nevertheless, we also detected area-specific altered pathways. intellectual disability, dementia, and neurodegenerative diseases (i.e., Parkinson's and Alzheimer's diseases) were terms enriched in the hippocampus, whereas developmental biological processes, such as global developmental delay and neuron projection development, were more strongly affected in subcortical regions (hippocampus and hypothalamus, Figure S6C).

Since our behavioral data highlighted the key role played by the age of stress exposure in shaping long-term consequences, we investigated the effect of the timing of trauma in our proteomic analysis. We examined significantly up- and downregulated proteins in each brain area for at least one age of stress, compared with those in controls. Highly deregulated proteins were present in subcortical regions (amygdala, hypothalamus, hippocampus) in mice stressed during infancy and childhood, whereas the PFC was mostly affected upon stress exposure in adolescence and young adulthood (Figure 2A; Table S5). Consistently, the percentage of deregulated proteins was greater in the subcortical regions of adult mice exposed to stress during infancy and childhood, whereas we observed the opposite trend in adult mice stressed during adolescence and young adulthood, which displayed greater deregulation in the PFC (Figure 2B). Moreover, PCA of proteomic data for each brain area highlighted a separation between controls and animals exposed to stressors earlier in life, with distinct effects on protein expression in diverse brain regions depending on the timing of trauma exposure (Figure 2C, top). In terms of age-group separation, the subcortical regions were sensitive to stress exposure in infancy and childhood, whereas the PFC was mostly affected upon stress exposure in adolescence and young adulthood (Figure 2C, bottom).

In parallel with our behavioral data, the age of trauma exposure represented the major discriminating factor in protein deregulation when we grouped the number of proteins that were differentially regulated in the age-specific, most affected brain areas. We grouped the amygdala, hypothalamus, and hippocampus for P2–11; the amygdala and hypothalamus for P12–21; the amygdala, hypothalamus, and PFC for P26–35; and the amygdala and PFC for P47–56, according to the mean distribution separation of PC2 density from that of controls (Figure 2C, bottom). We subsequently analyzed differentially expressed proteins at one age in the age-specific datasets, considering the diverse brain areas

Please cite this article in press as: Morelli et al., Traumatic life experiences during critical periods lead to diverse developmental trajectories, Cell Reports Medicine (2026), https://doi.org/10.1016/j.xcrm.2026.102798

CellPress
OPEN ACCESS

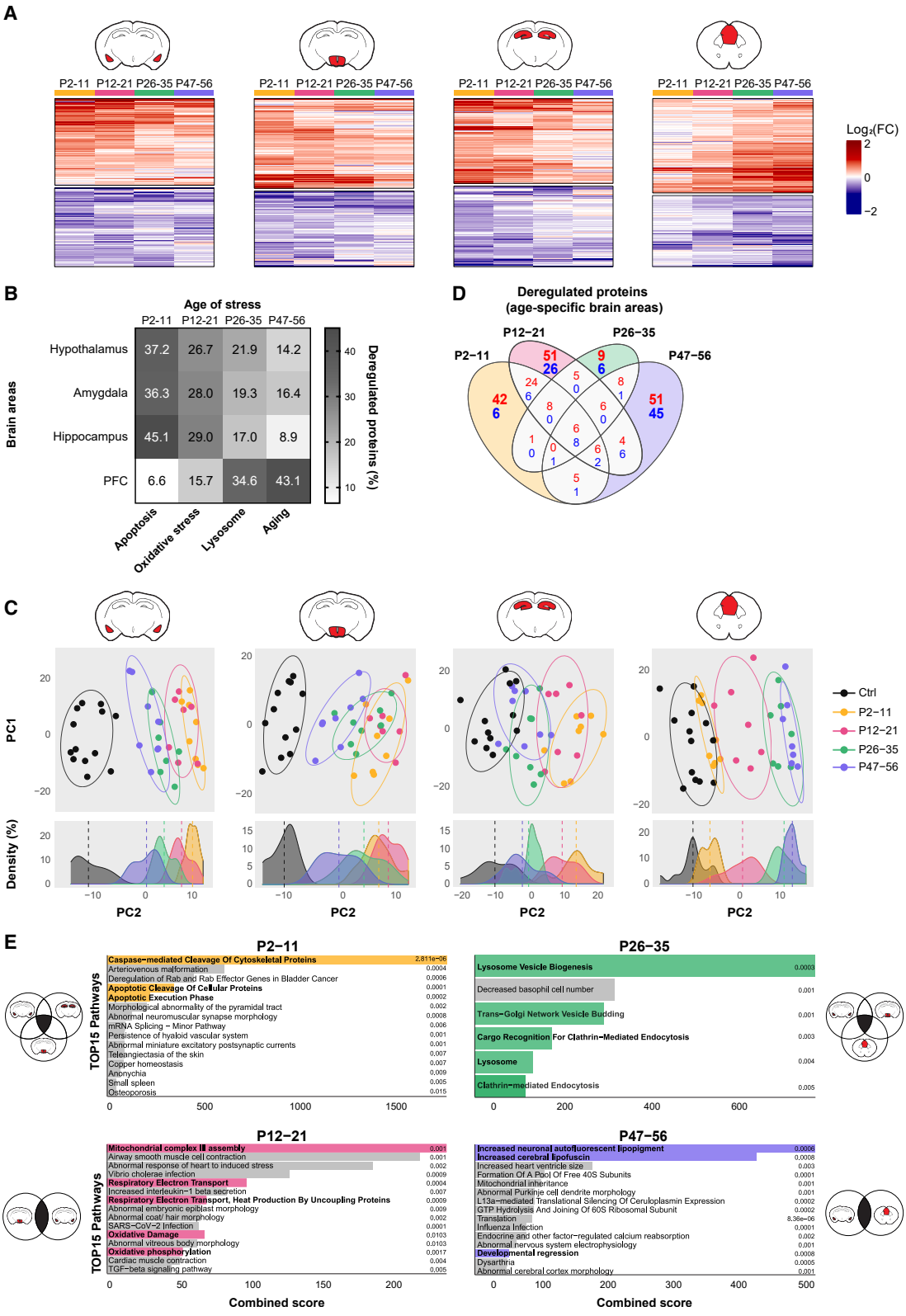

(legend on next page)

Please cite this article in press as: Morelli et al., Traumatic life experiences during critical periods lead to diverse developmental trajectories, Cell Reports Medicine (2026), https://doi.org/10.1016/j.xcrm.2026.102798

described above (Figure 2D). The pathways identified for proteins deregulated in brain areas specific to each stress time window (Figure 2E, cartoons) revealed unique enriched biological processes at each age of stress exposure (Figure 2E; Table S6). Among the 15 highest-scored biological pathways, we found that (1) apoptosis-related pathways were affected in the P2–11 stress-exposed group; (2) oxidative stress ontologies in the P12–21 group; (3) the biogenesis of vesicles in several cellular districts in the P26–35 group; and (4) aging-related signaling, such as proteins related to increased lipofuscin (a marker of neurodegeneration), in the P47–56 group ([39,40]; Figures 2E and 2B, bottom).

These data indicate that both overall impaired metabolism and general biological processes as well as specific deficits were related to the timing of stress exposure, confirming the existence of critical periods for stress-induced long-term consequences at the cellular/molecular level.

TrkB inhibition ameliorates specific behavioral deficits in adult mice exposed to stress during young adulthood

There are currently no targeted medications specifically approved for patients with PTSD and PDs[41] to be combined with psychotherapy.[42] We thus began uncovering putative therapeutic targets in our mice stressed at diverse ages by exploiting our proteomic dataset. We focused on the identification of deregulated proteins or biological processes, which may be specific to each age of stress exposure but involve as many brain areas as possible. This would justify the standard systemic administration of a pharmacological treatment targeting all brain areas. We selected proteins differentially expressed in at least three of the four analyzed brain areas of the proteomic dataset per age of stress. We identified 75 unique proteins altered in infancy, 41 in childhood, 32 in adolescence, and 11 in young adulthood (Figure 3A; Table S7).

The most interesting biological processes enriched by analyzing deregulated (downregulated) proteins in the P2–11 and P12–21 groups of stress exposure highlighted only general neuronal processes such as synaptic regulation or neurotransmitter secretion. Interestingly, in the P26–35 group of stress exposure, together with general calcium and GABAergic signal processing, deregulated (upregulated) proteins were associated mainly with specific processes such as morphine addiction and circadian entrainment (Figure S5D). On the other hand, among the proteins commonly upregulated in the P47–56 group of stress exposure, we detected a coherent set of proteins related to BDNF signaling, which included neurotrophic receptor tyrosine kinase 2 (Ntrk2; tropomyosin receptor kinase B [TrkB]) and the Ras-related protein Rab-11A (Rab11a; Figure 3B). TrkB is a membrane-bound receptor for BDNF and is involved in many developmental processes and in synaptic plasticity.[43] As TrkB expression was increased in the amygdala, hypothalamus, and PFC of adult mice exposed to TMT during young adulthood only, we reasoned that inhibition of this pathway may ameliorate the behavioral phenotypes induced by trauma exposure at this developmental age. We therefore orally administered the Food and Drug Administration (FDA)-approved Trk-inhibitor larotrectinib (10 mg/kg in drinking water,[44] blood-brain barrier penetrant) or its vehicle (0.15% dimethyl sulfoxide (DMSO) in drinking water) as a control to animals exposed to TMT during young adulthood. We performed the treatment one week before behavioral testing and throughout the whole battery of tests (Figure 3C). Larotrectinib treatment fully rescued dominance and depressive-like and anxiety/OCD-related behaviors and partially rescued social deficits (Figures 3D and S7A–S7J).

Next, we tested whether the rescue by Trk inhibition was age- and trauma-specific. We thus first orally administered larotrectinib to adult mice exposed to a different type of stressor, IMM, during young adulthood. We found that the treatment fully rescued dominance, social interaction deficits, and depressive-like, as well as anxiety/OCD-related, behaviors, suggesting that Trk inhibition is beneficial for behavioral alterations in animals stressed during young adulthood in a stress-type-independent manner (Figures S8A–S8M). Next, we performed a complementary experiment by assessing whether larotrectinib was effective at ameliorating stress-related behaviors specifically in response to trauma during young adulthood by orally administering the drug to adult animals exposed to TMT during a different developmental period (i.e., infancy). Accordingly, the treatment was not able to ameliorate the specific behavioral abnormalities of adult mice exposed to TMT during infancy (no amelioration in dominance or social interaction; Figures S9A–S9E). Larotrectinib did partially ameliorate anxiety/OCD-related behaviors in adult mice exposed to TMT during infancy, but anxiety/OCD was a trait common to all ages of trauma exposure (Figures S9F–S9J).

Figure 2. In adult mice, earlier traumas alter specific cellular processes common to diverse brain areas that depend on the insult timing

(A) Protein expression heatmaps (log_2 fold change [FC, right scale bar] vs. controls) for each brain area (amygdala, hypothalamus, hippocampus, prefrontal cortex; color-coded in red) analyzed in proteomic experiments performed on adult animals stressed with TMT. Proteins significantly deregulated in at least one group of stress age are plotted. Up- and downregulated proteins are represented in red and blue, respectively.

(B) Deregulated protein heatmap (numbers in squares, FC threshold = 0.3 and false discovery rate [FDR] p value < 0.05; color-coded on the right) in brain areas analyzed as in (A).

(C) PCA visualization of the first two components of proteomic expression in analyzed brain areas (color-coded on top of the graphs) for each age of stress as in (A). Dots indicate individual mice; colored circles define clusters at the 80th percentile of multivariate t distribution of animals exposed to stress at a specific age, black circle represents the group of controls. Bottom: graphs showing PC2 densities for each analyzed brain area. Dotted lines: mean distribution curves.

(D) Venn diagram with commonly (gray) and age-specific (bold, color-coded as in Figure 1) up- (red) and downregulated (blue) proteins at FDR < 0.05 in the brain areas better segregating (according to the most representative components and centroid distance) from controls based on PC2 density plot in (C). Selected areas: P2–11, hypothalamus, hippocampus, amygdala; P12–21, hypothalamus, amygdala; P26–35, hypothalamus, amygdala, PFC; P47–56, amygdala, PFC.

(E) EnrichR-KG pathway enrichment analysis on specific deregulated proteins for each group of stress age from (D); the top 15 p value significantly enriched terms (all significant enriched terms for P26–35) are shown in the bar-plot. q value (FDR-corrected p value) < 0.1 was set as threshold, and specific values for each term are indicated on the right of each bar. Age-specific colors indicate pathways of special interest. Brain cartoons indicate brain areas considered for the analysis, as in (D). See also Table S5.

Please cite this article in press as: Morelli et al., Traumatic life experiences during critical periods lead to diverse developmental trajectories, Cell Reports Medicine (2026), https://doi.org/10.1016/j.xcrm.2026.102798

CellPress
OPEN ACCESS

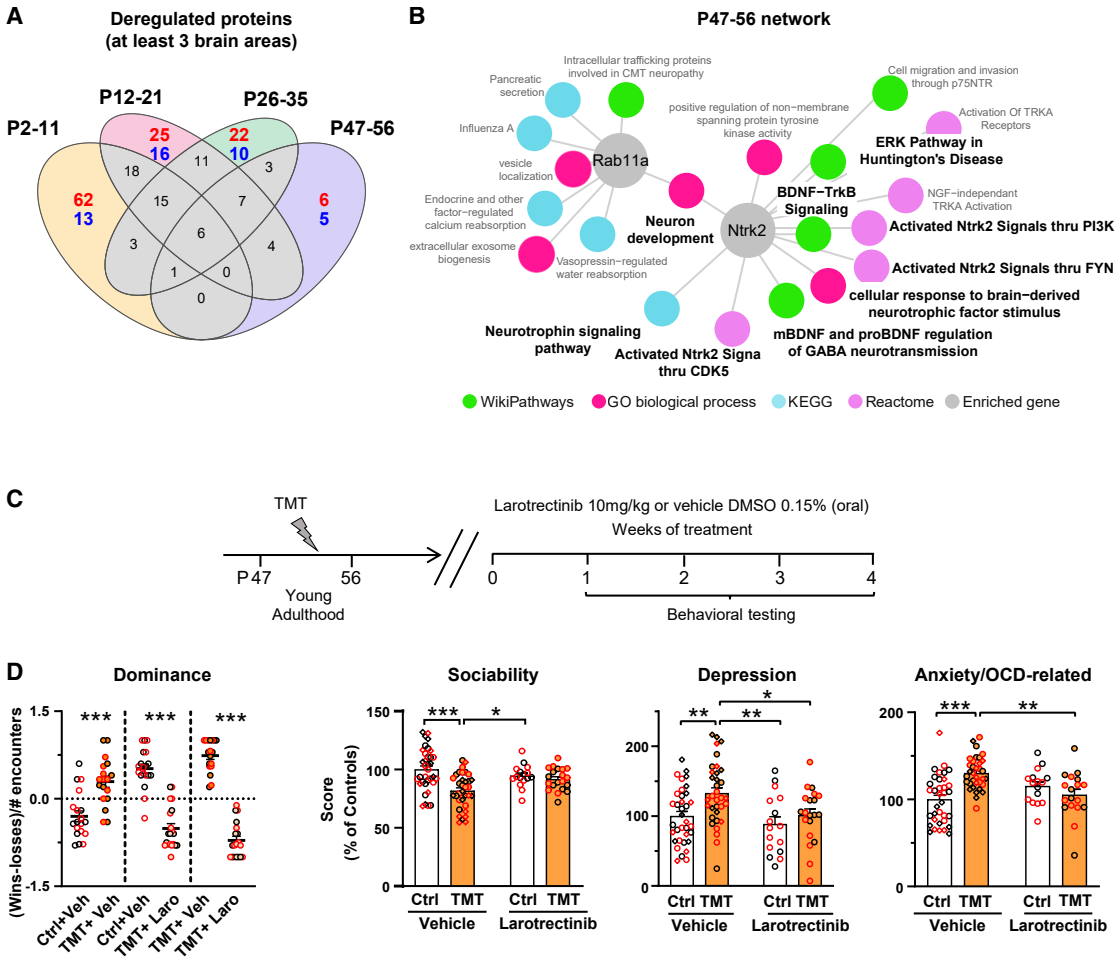

Figure 3. The BDNF pathway is a potential drug target for adult animals exposed to stress during young adulthood

(A) Venn diagram showing all common (gray) and age-specific (bold, color-coded as in Figure 1) up (red) and downregulated (blue) proteins at FDR < 0.05 in at least 3 brain areas in each group of stress age analyzed from Figure 2.

(B) Network plot by diverse databases (bottom) showing pathway enrichment analysis on the six proteins specifically upregulated in adult animals exposed to stress at P47–56 reported in (A). Bold indicates pathways belonging to the neurotrophin and BDNF-related signaling.

(C) Experimental protocol.

(D) Dominance, sociability, depression, and anxiety/OCD scores following larotrectinib or vehicle treatment as in (C). Scores were based on tests from Figures S7B and S7J. Bars represent average (percentage over vehicle controls) scores of analyzed animals + SEM. Symbols: single animal points (black males, red females).

Data were derived from 3 independent experiments for 16–20 animals per experimental group. For sociability, depression, and anxiety/OCD scores, single data points in diamond shape represent data from the experiments in Figures S3C, S3F, S3G, and S3I–S3L, respectively (Dominance: Controls vehicle vs. TMT vehicle: unpaired *t* test; Controls vehicle vs. TMT larotrectinib and TMT vehicle vs. TMT larotrectinib: Mann-Whitney test. Sociability: two-way ANOVA, $F_{interaction(1,101)} = 6.533$ $p = 0.0121$, followed by Tukey's multiple comparisons test. Depression: two-way ANOVA, $F_{treatment(1,101)} = 6.217$, $p = 0.0143$, followed by Tukey's multiple comparisons test. Anxiety/OCD: two-way ANOVA, $F_{interaction(1,99)} = 16.10$, $p = 0.0001$, followed by Tukey's multiple comparisons test). $^{*}p < 0.05$, $^{**}p < 0.01$, $^{***}p < 0.001$).

See also Table S7.

These results suggest that TrkB inhibition by the FDA-approved drug larotrectinib is a potential treatment for maladaptive behaviors due to a history of trauma specifically during young adulthood.

Human PFCs reveal protein alterations that depend on the age of trauma

Next, we expanded our investigation to humans. First, we studied samples from adult people who had experienced trauma earlier in life and unaffected, age-matched controls. The PFC was the only available brain region for this study to perform proteomic analysis.[45] We analyzed 12 samples from individuals noted to have been exposed to a first traumatic event before the age of 12 (before adolescence; Before12 group) and 11 samples from individuals exposed to trauma after 12 years of age (from adolescence onward; After12 group). The results were compared to PFC brain samples from 12 control individuals who had not reported any traumatic experiences ([Ctrl]; all

Please cite this article in press as: Morelli et al., Traumatic life experiences during critical periods lead to diverse developmental trajectories, Cell Reports Medicine (2026), https://doi.org/10.1016/j.xcrm.2026.102798

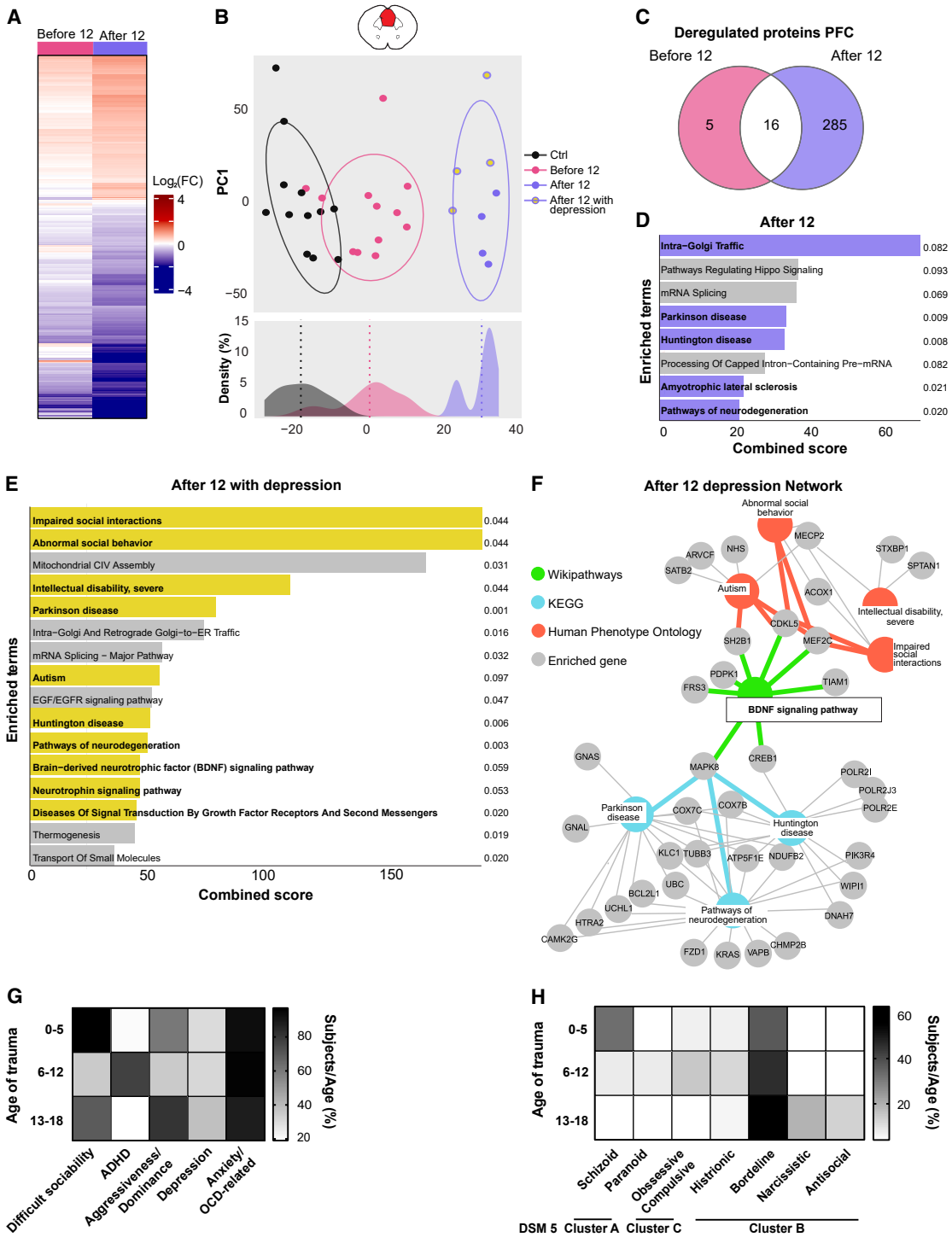

Figure 4. The age of trauma exposure influences specific cellular processes and induces distinct neuropsychiatric profiles in patients

(A) Heatmap of the protein expression (log_2FC [scale bar, right] vs. controls) for the PFC of postmortem brain samples from adult people exposed to trauma before adolescence (before 12) or from adolescence onward (after 12; color-coded on top). Proteins significantly deregulated (Bonferroni adjusted *p* value, [p.adj.], < 0.05 and log2FC < −1 or >1) in at least one group of stress age are plotted. Up- and downregulated proteins are represented in red and blue, respectively.

(B) Top: PCA visualization of the first two components of proteomic expression in PFC (color-coded in red) for each age of trauma. Dots indicate individual subjects; colored circles define clusters at the 80th percentile of multivariate *t* distribution of individuals exposed to stress at a specific age; black circle represents

(legend continued on next page)

Please cite this article in press as: Morelli et al., Traumatic life experiences during critical periods lead to diverse developmental trajectories, Cell Reports Medicine (2026), https://doi.org/10.1016/j.xcrm.2026.102798

reported information about the individuals is summarized in Tables S8–S10). Among the "After12" individuals, we omitted 3 samples identified as outliers by PCA of the global proteomic data (Figure S10A, dots with dashed lines). Examining significantly deregulated proteins (both up- and downregulated) vs. controls, we detected greater protein deregulation in the PFCs of the "Before12" group than in individuals of the After12 group (Figure 4A; Table S11). This finding closely mirrored our findings in mice. Moreover, PCA of the proteomics data revealed clear separation between the controls and people exposed to stressors earlier in life (Figure 4B), and clustering of individuals according to the age of stress exposure, with stronger segregation, and therefore a greater impact on protein expression, in the After12 group (Figure 4B). This finding was also closely analogous to our findings in mice, which showed greater deregulation of cortical genes in animals stressed after adolescence.

By protein enrichment analysis in our PFC human samples, we detected 21 deregulated proteins in the Before12 group and 301 in the After12 group, compared with the Ctrl group (16 in common), which is consistent with the much greater effects at later ages of stress in the PFC observed in mice (Figure 4C). Due to the low number of deregulated proteins in the Before12 group, we could focus only on the biological context of the targets present in the After12 dataset. Among the top enriched ontologies in this dataset, we found Golgi-related processes and diverse neurodegenerative biological processes related to pathophysiology (i.e., Parkinson's disease, Huntington's disease, and amyotrophic lateral sclerosis; Figures 4D and S10B), which was strongly consistent with the pathways deregulated in mouse samples from P26–35 and P47–56 (see Figure 2E for comparison).

Next, we narrowed our bioinformatic analysis of protein expression to the After12 group and to individuals who presented depression as a major reported symptom (yellow dots in Figure 4B). We based this decision on (1) the presence of depression as a behavioral trait exclusive to mice exposed to trauma during young adulthood; (2) the amelioration via larotrectinib of depressive-like behaviors in our mouse models; (3) previous literature showing that TrkB inhibition ameliorates inflammation-induced depressive traits in mice,[46] and (4) the association of trauma-related depression with drug unresponsiveness in individuals.[47] In our subgroup of brain samples, we identified 269 deregulated proteins compared with those in the controls (Table S12). The major processes highlighted in the GO analyses consisted of behavioral alterations, including impaired social interactions and behavior, autism, and (as we found for the entire cohort of After12 samples) several neurodegeneration pathways, including Parkinson's and Huntington's disease (Figure 4E). Interestingly, impaired sociability in mice (as we found in animals stressed in early adulthood) recapitulates the social withdrawal characteristic of individuals with depression,[48] and impaired sociability in people has been linked to suicide attempts.[49] In line with this evidence, half of the After12 individuals with depression whom we analyzed died by suicide (Table S8). Notably, the EnrichR-KG pathway analysis in the After12 subdataset of individuals with depression revealed enrichment in the BDNF pathway, whose proteins represented a pivotal hub in our analysis by linking impaired social behavior with neurodegeneration (Figure 4F).

These results in human samples are consistent with the findings obtained in our mouse models and suggest the BDNF/TrkB pathway as a potential pharmaceutical target for psychopathological traits derived from trauma exposure specifically during young adulthood.

Early-life trauma in people induces specific neuropsychiatric profiles later in life, according to the timing of exposure to aversive events

Finally, to validate our findings in a clinical cohort (72 individuals), we gained access to patients who entered the child and adolescent psychiatric ward of a pediatric tertiary care center in Italy in 2021 and had experienced trauma earlier in life (infancy: 0–5 years old, childhood: 6–12 years old, or adolescence: 13–18 years old; Table S13). Notably, an initial PCA of the behavioral traits, personality traits, and clinical scores of the patients in this cohort revealed clustering according to the age of stress exposure (Figure S10C). Moreover, we found a significant (chi-square, $p < 0.05$) dependency between their behavioral abnormality traits and the age of their stress exposure, with their behavioral traits mostly in line with the effects observed in

the group of controls. Yellow dots: individuals with comorbid depression (i.e., major depressive disorder or depressive disorder). Bottom: PC2 density for PFC color-coded for age as in top. Dotted lines: mean distribution curves.

(C) Venn diagram of commonly (white) and age-specific (pink, purple) deregulated proteins (log2FC threshold = 1) in the PFC in proteomic experiments in (A).

(D) EnrichR-KG pathway enrichment analysis on proteins deregulated in After12 individuals from (C) (white, purple); all significantly enriched terms are shown in the bar plot. *q* value (FDR-corrected *p* value) < 0.1 was set as threshold, and specific values for each term are indicated on the right of each bar. Purple: pathways of interest.

(E) EnrichR-KG pathway enrichment analysis on proteins deregulated in the subgroup of After12 individuals with a diagnosis of depression in (B) (yellow dots); all significantly enriched terms are shown in the bar plot. FC = 1 and q value (FDR-corrected *p* value) < 0.05 were set as thresholds, and specific values for each term are indicated on the right of each bar. Yellow indicates pathways of interest.

(F) Network plot by diverse databases (left) showing pathway enrichment analysis on proteins deregulated in the same adult individuals as in (B) (yellow dots). Square highlights BDNF signaling.

(G) Heatmap of percentage of patients presenting maladaptive behavioral phenotypes among all individuals who had experienced trauma at that specific age. Scale bar on the right. Chi-square: difficult sociability $p < 0.0001$, ADHD $p < 0.0001$, aggressiveness/dominance $p < 0.0001$, depression $p = 0.4234$, anxiety/OCD $p = 0.0995$.

(H) Heatmap of percentage of patients presenting maladaptive personality traits among all individuals who had experienced trauma at that specific age. Scale bar on the right. Lines below the heatmap indicate the cluster of each maladaptive personality trait according to the Diagnostic and Statistical Manual of Mental Disorders (DSM)-5 classification. Chi-square: schizoid $p < 0.0001$, paranoid $p = 0.0098$, obsessive-compulsive $p = 0.0003$, histrionic $p = 0.2585$, borderline $p = 0.0009$, narcissistic $p < 0.0001$, antisocial $p = 0.0076$.

See also Tables S11, S12, and S13.

Please cite this article in press as: Morelli et al., Traumatic life experiences during critical periods lead to diverse developmental trajectories, Cell Reports Medicine (2026), https://doi.org/10.1016/j.xcrm.2026.102798

mice (Figure 4G). In particular, we found that individuals who had experienced trauma during infancy primarily exhibited difficulties in sociability, with a secondary effect on aggressiveness/dominance. Individuals who had experienced trauma during childhood frequently showed symptoms of attention-deficit hyperactivity disorder (ADHD), whereas individuals who had experienced trauma during adolescence mainly presented with aggressiveness/dominance, accompanied by secondary difficulties in sociability. We also found that anxiety/OCD-related traits were highly present across all ages of trauma exposure.

Next, we analyzed maladaptive personality traits typical of human participants. We found a significant (chi-square $p < 0.05$) dependency on the age of trauma for these traits, with schizoid traits predominantly observed in individuals who experienced trauma during infancy; milder paranoid, obsessive-compulsive, and histrionic traits mostly present in individuals who experienced trauma during childhood; and narcissistic and antisocial traits mostly observed in individuals who experienced trauma during adolescence (Figure 4H). Notably, borderline personality traits were highly represented in all the analyzed groups but increased with increasing age of trauma exposure. Consistent with our mouse data, the type of trauma did not strongly influence the determination of any specific maladaptive behavioral trait (Figure S10D).

These findings reveal specific maladaptive behavioral phenotypes and personality traits arising from earlier life stress experienced at diverse postnatal ages in patients and parallel the behavioral results that we obtained in mice.

DISCUSSION

In this study, we found evidence that the timing of trauma during development is a key regulator of the ultimate adult maladaptive behavioral outcome, shaping long-term consequences at the molecular/cellular level in mice. These findings demonstrate the existence of precise and timely biological mechanisms underlying the early observations and theories of developmental psychologists of the early 20th century, who argued that child development occurs in distinct stages, each with significant implications for adult personality. Our study also extends the experimental evidence of a critical period for sensory system plasticity gathered over the past century to complex behavioral outcomes. Moreover, our proteomic studies provide insights into specific biological processes that could be targeted by future therapeutic approaches, which we exemplified in our proof-of-concept study. Finally, our human data provide a significant clinical relevance to our results.

We developed experimental models of the negative sequelae of trauma exposure by subjecting mice to stress paradigms specifically designed to be perceived as traumatic across developmental stages. These paradigms were also selected to have potentially meaningful translational value for humans. Indeed, innate fear triggered by predators or unforeseen dangers (i.e., TMT) and acquired fear of new life-threatening situations (i.e., IMM) represent unescapable, unpredictable, and significant traumatic experiences for both animals and humans. We employed MS to mimic child neglect in humans, serving as a translatable preweaning stress protocol.[26,50] Our findings indicate that all stressors were effective at inducing a significant increase in corticosterone levels (also in the infancy period, notwithstanding the stress hyporesponsive period[51]). Most importantly, all stressors induced similar behavioral outcomes in adult mice for each specific age of stress. This highlights the importance of the timing of stress exposure rather than the type of stress in determining later behavioral outcomes, with only subtle differences in specific subdomains of maladaptive behavior (e.g., sociability vs. social novelty of the social interaction domain) driven by TMT, IMM, or MS.

Stress-related disorders in humans manifest through various maladaptive behaviors,[52,53] such as disinhibition, social withdrawal, avoidance, impulsivity, negative thoughts, helplessness, anxiety, hypervigilance, intrusive memories, and an exaggerated sense of self.[54] Although some of these maladaptive behaviors may seem specific to humans, we focused on prevalent psychiatric traits that can be effectively mirrored in rodents. These included dominance, social interaction, attention, depression-related behaviors, and anxiety/OCD-related behaviors (comprising both the generalized and the repetitive components of anxiety, thereby allowing a comprehensive evaluation). We found that adult animals exposed to stress during infancy showed social deficits and submissive/passive behaviors, irrespective of the nature of the trauma (innate vs. acquired). These behaviors resemble those of very young, vulnerable individuals who are unable to protect themselves (and can only socially withdraw from a dangerous world) and are characteristic of cluster A personality disorders classified according to the Diagnostic and Statistical Manual of Mental Disorders (DSM)-5 (e.g., schizoid personality disorder) or children with PTSD.[54] Thus, our data provide experimental support for early systematic observation in psychology, suggesting that maladaptive behaviors in adulthood are projections of coping mechanisms developed during particular stages of childhood development.[55]

In further agreement, we found that mice exposed to stress during adolescence presented aggressiveness/dominance, mirroring the typical coping strategies of adolescents and some aspects of DSM cluster B PDs (e.g., borderline, narcissistic, and antisocial personality) or adolescents with PTSD.[54] These maladaptive behaviors were accompanied by reduced attention and asocial, inattentive, and depressive-like behaviors that could parallel the coping mode of an adult exposed to a life-threatening event, also independent of the type of stressor. On the other hand, exposure to traumatic events during childhood led to a milder phenotype across stressors, with adult animals presenting only attention deficits, a characteristic feature of people with ADHD,[54,56] which has also been associated with childhood trauma exposure.[57] Accordingly, in the PCA of behavioral data from mice exposed to TMT or IMM at different ages, we observed the greatest overlap between the control group and the P12–21 group. These findings align with those of previous reports indicating that students who experienced parental separation after the age of 7 years exhibited fewer anxiety and depression symptoms than those whose parents left earlier in their lives did.[58] Moreover, all the animals, irrespective of the nature of the stressor and the age at which it was experienced, exhibited anxiety/OCD-related behaviors in line with the anxiety associated with trauma uncontrollability in both humans and rodents.[59,60]

Please cite this article in press as: Morelli et al., Traumatic life experiences during critical periods lead to diverse developmental trajectories, Cell Reports Medicine (2026), https://doi.org/10.1016/j.xcrm.2026.102798

We paralleled our mouse findings with a cohort of patients, not only showing that the timing, rather than the type, of trauma plays a key role in shaping long-term behavioral consequences, but also (1) associating trauma in infancy mainly with difficulties in sociability (and schizoid PD traits), (2) indicating that childhood as a period is associated with milder maladaptive behavioral phenotypes yet characterized by ADHD (and mild paranoid, obsessive-compulsive, and histrionic PD traits), and (3) associating trauma in adolescence with aggressiveness/dominance (and narcissistic and antisocial PD traits), in close agreement with our mouse data. The fact that borderline personality traits were highly represented across all ages of trauma is in line with the prevalence of this disorder.[61] Moreover, borderline personality traits were most represented in the adolescence group of trauma exposure, in agreement with the high aggressiveness/dominance described in individuals with borderline PD.[62] Therefore, our results suggest a continuum across maladaptive personality traits according to the age of trauma exposure, with traits typical of DMS cluster A and C PDs (characterized by submission, isolation, and fearfulness) particularly represented during early ages of trauma exposure (infancy and childhood) and traits typical of cluster B (characterized by aggressiveness/dominance) particularly represented during the adolescence period of trauma exposure. In addition, the most represented phenotype in our subjects was anxiety/OCD-related behaviors, present irrespective of the age of trauma, again in agreement with our mouse data. As we did not have access to data from subjects who experienced trauma during young adulthood, we could not assess whether the level of depression would be greater in these groups, as we observed in mice.

Some previous studies have already reported correlations between the age of traumatic exposure and the onset of specific types of neuropsychiatric disorders in both humans and mice.[63–75] Although all the previous evidence is in complete agreement with our own results when considering specific ages of stress, to our knowledge, no study in the literature has compared the same stressor paradigms covering all the main developmental stages, thus missing the overall picture and message of a time-dependent and type-of-stress-independent outcome of adult behavioral consequences of earlier stress.

Building on proteomic analysis in mice, we confirmed an overall significant alteration in metabolic processes, as in other studies.[76,77] We also found distinct effects of trauma on subcortical vs. cortical brain regions. This opposite pattern provides a significant experimental basis for what had been merely hypothesized in previous studies on the existence of periods of sensitivity to trauma specific to particular brain areas (infancy/childhood for the limbic system and adolescence/young adulthood for the PFC), which depend on the maturation state of a specific brain region at the time of the trauma.[13,78–83]

In the context of our proteomic analysis in mice, we identified biological pathways that were enriched in an age-specific manner. For example, we found that apoptotic processes were specifically altered in adult animals exposed to a stressor during infancy, in line with previous studies on stressed mice and humans.[75,84] Although these studies did not focus specifically on trauma during infancy, apoptosis predominantly occurs in early development.[85] Moreover, our results on the association between stress exposure during childhood and alterations in biological processes related to oxidative stress/mitochondrial function in adulthood also align with previous studies in stressed animal models and humans.[86] Furthermore, we found that ontologies related to the biogenesis of vesicles were enriched in adult mice exposed to stress during adolescence, in line with evidence that diseases characterized by impaired lysosome function are frequently linked to neuropsychiatric disturbances, including increased aggressiveness/dominance and anxiety.[87] Finally, we found that traumatic events during young adulthood were specifically associated with aging-related pathways, which is consistent with the increased vulnerability to neurodegenerative disorders in individuals with stress-related diseases.[88] At the level of protein-network analysis, we found that most of the proteins differentially expressed during infancy and childhood were linked to general synaptic processes, in line with the previously observed relevant impact of traumatic events exerted on synapses in rodents and humans.[89] Analogously, pathways linked to circadian entrainment and morphine addiction were altered specifically upon stress during adolescence, in line with the important changes in circadian rhythm occurring after puberty[90] and the association between trauma during adolescence and the subsequent risk of drug abuse.[91] Interestingly, among the proteins commonly upregulated in the young adulthood group of stress exposure, we detected proteins related to BDNF signaling, also previously involved in stress-induced alterations.[92]

As in mice, we found that the PFC was particularly affected in humans who experienced stress after adolescence, which is in line with continuous prefrontal maturation until the late 20s.[80] In parallel with our mouse findings, we detected alterations in Golgi-related pathways upon trauma exposure in adulthood, as reported in people with neurodegenerative disorders.[93] We found enrichment of the BDNF pathway in people with depression who were exposed to trauma after 12 years of age, as observed in our mice exposed to trauma during young adulthood, which also exhibited depressive-like behavior. The association between trauma and aging-related pathways that we found in mice and humans is in line with the known link between chronic stress/trauma and accelerated aging or increased susceptibility to neurodegenerative diseases (e.g., Alzheimer's and Parkinson's diseases[88,94]).

There are only a few types of medications currently available for stress-related disorders, and they are not specific. They are indeed commonly prescribed for a diversity of stress-related conditions and even other brain disorders (e.g., antidepressants, mood stabilizers, and antipsychotics.[95,96] Possibly, it is the absence of valid animal models that has hindered the development and testing of new specific drugs for stress-related disorders.[97] Here, we generated potential mouse models for stress-related disorders that provided us with a working hypothesis for our proof-of-concept study on the use of modulators of the BDNF pathway for treating stress-related behaviors due to exposure specifically during young adulthood. Our working hypothesis was reinforced by the enrichment of the BDNF pathway in people with depression who were exposed to trauma after 12 years of age. Interestingly, BDNF signaling has already been established as a key player in social anxiety and depression,[98,99] which can be ameliorated by TrkB inhibition.[46,100,101] In line

with these works and our own study, TrkB methylation has been associated with a reduced risk of developing PTSD.[102] On the other hand, reduced BDNF levels have been detected in people with stress-related disorders, and treatment with antidepressants has reversed this phenotype.[103] Beyond depression, the role of BDNF signaling in aggressiveness/dominance has been controversial, with aggressiveness linked to both the administration[104] and the disruption of BDNF signaling in mice,[105] indicating that further research in the field of BDNF and stress is still needed. Anyhow, our findings offer preclinical evidence in support of the potential repurposing of the FDA-approved anticancer drug larotrectinib[106] in people with depressive disorder related to young-adulthood trauma. This could be highly relevant considering that treatment-resistant depression occurs mainly in trauma-related depression.[47] Indeed, it is possible that people with stress-related disorders should be treated differently from those with depression due to other causes, such as strong genetic vulnerability.[47] We should also consider the only partial reduction of social deficits upon larotrectinib treatment, which indicates the possible need for combination therapies to fully ameliorate all complex stress-related behaviors in future translational approaches in patients. Since exposure of fully adult animals to trauma resulted in a different phenotype than exposure of young adults and the maladaptive behaviors induced by trauma exposure are maintained over time, larotrectinib effects specific to stress experienced during young adulthood are likely not related to transient gene expression modifications induced by trauma. Finally, on the basis of our mouse models, patient stratification for the selection of effective treatments could also be driven by the timing of the reported traumatic event in future clinical trials, in line with "transdiagnostic" approaches, better representing the complexity and dimensionality of PDs and PTSD.[107]

Limitations of the study

In mice, the specific type of trauma did not differentially influence behavioral outcomes in adulthood, a finding mirrored in the human data. Nevertheless, the limited range of the types of trauma included in the study may have constrained the identification of different clusters of outcomes, especially in humans, which show a much more complex repertoire of potential behaviors.

All human postmortem brains analyzed in this study were derived from individuals of Caucasian ethnicity; the number of female participants was limited (3–6/group), and information on socioeconomic status was not available. Thus, the lack of sufficient diversity and sample size limited the generalizability of our findings to other populations and precluded the assessment of potential effects of gender, ancestry, or other related factors. Analogously, the participants in the human clinical study were mainly Caucasians, with only a 20% Hispanic and 5% African minorities, and socioeconomic status was not collected.

RESOURCE AVAILABILITY

Lead contact

Further information and requests for resources and reagents should be directed to and will be fulfilled by the lead contact, Laura Cancedda (laura.cancedda@iit.it).

Materials availability

This study did not generate new unique reagents.

Data and code availability

Proteomics data are available via ProteomeXchange with identifier PXD054552. This study did not generate any code. Any additional information required to reanalyze the data reported in this article is available from the lead contact upon request.

ACKNOWLEDGMENTS

We thank M. Mangano for help importing human samples, E. Hill for discussions, and IIT animal facility staff. This work sets within the Brain and Machines Flagship of IIT.

This work has been funded by the Ministero dell'Università e della ricerca–BANDO FIS 2 (#FIS-2023-02972 to L.C.).

This work was partially funded by the European Research Council (ERC) (grant agreement no.725563 to L.C.) and #NEXTGENERATIONEU (NGEU), the Ministry of University and Research (MUR), National Recovery and Resilience Plan (NRRP), project MNESYS (PE0000006) (DN. 1553, 11.10.2022 to S.U.).

AUTHOR CONTRIBUTIONS

L.C., V.T., G.M., and G.V. designed the experiments. G.M. and G.V. performed most of the experiments. E.G. and A. Serani performed proteomic analyses with contribution from M.R. S.U., M. D'A., and D.P. collected clinical data. A. Scalabrini participated in human data analysis. M.B. and A.P. performed proteomics experiments. M.F., G.M., and G.V. performed the Phenopy test. M.M.C. and A.C. performed experiments for the revision. G.T. collected human samples. G.V., L.C., and V.T. wrote the manuscript. G.M., G.V., and E.G. prepared figures of the manuscript. L.C. and V.T. supervised the project. All authors contributed to manuscript writing.

DECLARATION OF INTERESTS

L.C. is a cofounder, shareholder, and scientific advisor at IAMA Therapeutics and scientific advisor of the Fondazione Pisana per la Scienza.

STAR★METHODS

Detailed methods are provided in the online version of this paper and include the following:

- KEY RESOURCES TABLE
- EXPERIMENTAL MODEL AND STUDY PARTICIPANT DETAILS
  - Animals and stress-induction protocols
  - Postmortem human samples
  - Participants in the human study
- METHOD DETAILS
  - Serum corticosterone detection
  - Behavioral testing and pharmacological treatment
  - Proteomics on mouse and human samples
  - Assessment of symptoms in the human study
- QUANTIFICATION AND STATISTICAL ANALYSIS

SUPPLEMENTAL INFORMATION

Supplemental information can be found online at https://doi.org/10.1016/j.xcrm.2026.102798.

Received: June 18, 2025
Revised: January 5, 2026
Accepted: April 13, 2026

REFERENCES

1. Twardosz, S. (2012). Effects of Experience on the Brain: The Role of Neuroscience in Early Development and Education. Early Educ. Dev. *23*, 96–119.
2. Tau, G.Z., and Peterson, B.S. (2010). Normal Development of Brain Circuits. Neuropsychopharmacology *35*, 147–168.
3. Piaget, J. (1971). The theory of stages in cognitive development. In Measurement and Piaget (McGraw-Hill), pp. 1–11.
4. Piaget J. The Moral Judgment of the Child. 1st Edition. 1932. 428 p.
5. Freud, S. (1905). Three Essays on the Theory of Sexuality, *VII*.
6. Dehorter, N., and Del Pino, I. (2020). Shifting Developmental Trajectories During Critical Periods of Brain Formation. Front. Cell. Neurosci. *14*, 283.
7. Hensch, T.K. (2004). CRITICAL PERIOD REGULATION. Annu. Rev. Neurosci. *27*, 549–579.
8. Fagiolini, M., Jensen, C.L., and Champagne, F.A. (2009). Epigenetic influences on brain development and plasticity. Curr. Opin. Neurobiol. *19*, 207–212.
9. Springer, K.W., Sheridan, J., Kuo, D., and Carnes, M. (2003). The long-term health outcomes of childhood abuse: An overview and a call to action. J. Gen. Intern. Med. *18*, 864–870.
10. Everaerd, D., Klumpers, F., Zwiers, M., Guadalupe, T., Franke, B., van Oostrom, I., Schene, A., Fernández, G., and Tendolkar, I. (2016). Childhood abuse and deprivation are associated with distinct sex-dependent differences in brain morphology. Neuropsychopharmacology *41*, 1716–1723.
11. Lutz, P.E., Tanti, A., Gasecka, A., Barnett-Burns, S., Kim, J.J., Zhou, Y., Chen, G.G., Wakid, M., Shaw, M., Almeida, D., et al. (2017). Association of a History of Child Abuse With Impaired Myelination in the Anterior Cingulate Cortex: Convergent Epigenetic, Transcriptional, and Morphological Evidence. Am. J. Psychiatry *174*, 1185–1194.
12. Catani, C. (2018). Mental health of children living in war zones: a risk and protection perspective. World Psychiatry *17*, 104–105.
13. Alberini, C.M., and Travaglia, A. (2017). Infantile Amnesia: A Critical Period of Learning to Learn and Remember. J. Neurosci. *37*, 5783–5795.
14. Bremne, J.D., and Vermetten, E. (2001). Stress and development: Behavioral and biological consequences. Dev. Psychopathol. *13*, 473–489.
15. Schneiderman, N., Ironson, G., and Siegel, S.D. (2005). Stress and Health: Psychological, Behavioral, and Biological Determinants. Annu. Rev. Clin. Psychol. *1*, 607–628.
16. Connor, D.F., Newcorn, J.H., Saylor, K.E., Amann, B.H., Scahill, L., Robb, A.S., Jensen, P.S., Vitiello, B., Findling, R.L., and Buitelaar, J.K. (2019). Maladaptive Aggression: With a Focus on Impulsive Aggression in Children and Adolescents. J. Child Adolesc. Psychopharmacol. *29*, 576–591.
17. Rojahn, J., and Meier, L.J. (2009). Epidemiology of Mental Illness and Maladaptive Behavior in Intellectual Disabilities. In International Review of Research in Mental Retardation, R.M. Hodapp, ed. (Elsevier), pp. 239–287. https://linkinghub.elsevier.com/retrieve/pii/S0074775008380094.
18. Giourou, E., Skokou, M., Andrew, S.P., Alexopoulou, K., Gourzis, P., and Jelastopulu, E. (2018). Complex posttraumatic stress disorder: The need to consolidate a distinct clinical syndrome or to reevaluate features of psychiatric disorders following interpersonal trauma? World J. Psychiatry *8*, 12–19.
19. Gómez-Beneyto, M., Salazar-Fraile, J., Martí-Sanjuan, V., and Gonzalez-Luján, L. (2006). Posttraumatic stress disorder in primary care with special reference to personality disorder comorbidity. Br J Gen Pract J R Coll Gen Pract *56*, 349–354.
20. Scheiderer, E.M., Wood, P.K., and Trull, T.J. (2015). The comorbidity of borderline personality disorder and posttraumatic stress disorder: revisiting the prevalence and associations in a general population sample. Borderline Personal. Disord. Emot. Dysregul. *2*, 11.
21. Ekselius, L. (2018). Personality disorder: a disease in disguise. Upsala J. Med. Sci. *123*, 194–204.
22. Santiago, P.N., Ursano, R.J., Gray, C.L., Pynoos, R.S., Spiegel, D., Lewis-Fernandez, R., Friedman, M.J., and Fullerton, C.S. (2013). A systematic review of PTSD prevalence and trajectories in DSM-5 defined trauma exposed populations: intentional and non-intentional traumatic events. PLoS One *8*, e59236.
23. Perrin, M., Vandeleur, C.L., Castelao, E., Rothen, S., Glaus, J., Vollenweider, P., and Preisig, M. (2014). Determinants of the development of post-traumatic stress disorder, in the general population. Soc. Psychiatry Psychiatr. Epidemiol. *49*, 447–457.
24. Husarewycz, M.N., El-Gabalawy, R., Logsetty, S., and Sareen, J. (2014). The association between number and type of traumatic life experiences and physical conditions in a nationally representative sample. Gen. Hosp. Psychiatry *36*, 26–32.
25. Daníelsdóttir, H.B., Aspelund, T., Shen, Q., Halldorsdottir, T., Jakobsdóttir, J., Song, H., Lu, D., Kuja-Halkola, R., Larsson, H., Fall, K., et al. (2024). Adverse Childhood Experiences and Adult Mental Health Outcomes. JAMA Psychiatry *81*, e240039.
26. Alves, R.L., Portugal, C.C., Summavielle, T., Barbosa, F., and Magalhães, A. (2020). Maternal separation effects on mother rodents' behaviour: A systematic review. Neurosci. Biobehav. Rev. *117*, 98–109.
27. Balzani, E., Falappa, M., Balci, F., and Tucci, V. (2018). An approach to monitoring home-cage behavior in mice that facilitates data sharing. Nat. Protoc. *13*, 1331–1347.
28. Bosch-Bouju, C., Larrieu, T., Linders, L., Manzoni, O.J., and Layé, S. (2016). Endocannabinoid-Mediated Plasticity in Nucleus Accumbens Controls Vulnerability to Anxiety after Social Defeat Stress. Cell Rep. *16*, 1237–1242.
29. Stein, D.J., Scott, K.M., de Jonge, P., and Kessler, R.C. (2017). Epidemiology of anxiety disorders: from surveys to nosology and back. Dialogues Clin. Neurosci. *19*, 127–136.
30. Yang, X., Fang, Y., Chen, H., Zhang, T., Yin, X., Man, J., Yang, L., and Lu, M. (2021). Global, regional and national burden of anxiety disorders from 1990 to 2019: results from the Global Burden of Disease Study 2019. Epidemiol. Psychiatr. Sci. *30*, e36.
31. Thomas, J.M. (1995). Traumatic stress disorder presents as hyperactivity and disruptive 'behavior: Case presentation, diagnoses, and treatment. Infant Ment. Health J. *16*, 306–317.
32. Philipsen, A., Limberger, M.F., Lieb, K., Feige, B., Kleindienst, N., Ebner-Priemer, U., Barth, J., Schmahl, C., and Bohus, M. (2008). Attention-deficit hyperactivity disorder as a potentially aggravating factor in borderline personality disorder. Br. J. Psychiatry *192*, 118–123.
33. Adamis, D., Kasianenko, D., Usman, M., Saleem, F., Wrigley, M., Gavin, B., and McNicholas, F. (2023). Prevalence of Personality Disorders in Adults With Attention Deficit Hyperactivity Disorder (ADHD). J. Atten. Disord. *27*, 658–668.
34. Caspi, A., Houts, R.M., Belsky, D.W., Goldman-Mellor, S.J., Harrington, H., Israel, S., Meier, M.H., Ramrakha, S., Shalev, I., Poulton, R., and Moffitt, T.E. (2014). The p Factor: One General Psychopathology Factor in the Structure of Psychiatric Disorders? Clin. Psychol. Sci. *2*, 119–137.
35. Marshall, M. (2020). The hidden links between mental disorders. Nature *581*, 19–21.
36. Ehlert, U., Gaab, J., and Heinrichs, M. (2001). Psychoneuroendocrinological contributions to the etiology of depression, posttraumatic stress disorder, and stress-related bodily disorders: the role of the hypothalamus–pituitary–adrenal axis. Biol. Psychol. *57*, 141–152.
37. Chattarji, S., Tomar, A., Suvrathan, A., Ghosh, S., and Rahman, M.M. (2015). Neighborhood matters: divergent patterns of stress-induced plasticity across the brain. Nat. Neurosci. *18*, 1364–1375.
38. Evangelista, J.E., Xie, Z., Marino, G.B., Nguyen, N., Clarke, D.J.B., and Ma'ayan, A. (2023). Enrichr-KG: bridging enrichment analysis across multiple libraries. Nucleic Acids Res. *51*, W168–W179.

39. Moreno-García, A., Kun, A., Calero, O., Medina, M., and Calero, M. (2018). An Overview of the Role of Lipofuscin in Age-Related Neurodegeneration. Front. Neurosci. *12*, 464.

40. Kritsilis, M., V Rizou, S., Koutsoudaki, P.N., Evangelou, K., Gorgoulis, V.G., and Papadopoulos, D. (2018). Ageing, Cellular Senescence and Neurodegenerative Disease. Int. J. Mol. Sci. *19*, 2937.

41. Fariba, K., Gupta, V., and Kass, E. (2021). Personality Disorder. In StatPearls, E. Kass and T.J. Torrico, eds. (StatPearls Publishing). http://www.ncbi.nlm.nih.gov/books/NBK556058/.

42. Javanbakht, A., and Alberini, C.M. (2019). Editorial: Neurobiological Models of Psychotherapy. Front. Behav. Neurosci. *13*, 144.

43. Huang, E.J., and Reichardt, L.F. (2001). Neurotrophins: Roles in Neuronal Development and Function. Annu. Rev. Neurosci. *24*, 677–736.

44. Wang, Y., Sparidans, R.W., Wang, J., Li, W., Lebre, M.C., Beijnen, J.H., and Schinkel, A.H. (2022). Rifampin and ritonavir increase oral availability and elacridar enhances overall exposure and brain accumulation of the NTRK inhibitor larotrectinib. Eur. J. Pharm. Biopharm. *170*, 197–207.

45. Douglas Brain Bank. https://douglasbrainbank.ca.

46. Zhang, J.c., Wu, J., Fujita, Y., Yao, W., Ren, Q., Yang, C., Li, S.x., Shirayama, Y., and Hashimoto, K. (2014). Antidepressant effects of TrkB ligands on depression-like behavior and dendritic changes in mice after inflammation. Int. J. Neuropsychopharmacol. *18*, pyu077.

47. Wang, S.K., Feng, M., Fang, Y., Lv, L., Sun, G.L., Yang, S.L., Guo, P., Cheng, S.F., Qian, M.C., and Chen, H.X. (2023). Psychological trauma, posttraumatic stress disorder and trauma-related depression: A mini-review. World J. Psychiatry *13*, 331–339.

48. Zain, M.A., Pandy, V., Majeed, A.B.A., Wong, W.F., and Mohamed, Z. (2019). Chronic restraint stress impairs sociability but not social recognition and spatial memoryin C57BL/6J mice. Exp. Anim. *68*, 113–124.

49. Jia, H., Min, Z., Yiyun, C., Zhiguo, W., Yousong, S., Feng, J., Na, Z., Yiru, F., and Daihui, P. (2024). Association between social withdrawal and suicidal ideation in patients with major depressive disorder: The mediational role of emotional symptoms. J. Affect. Disord. *347*, 69–76.

50. Carlyle, B.C., Duque, A., Kitchen, R.R., Bordner, K.A., Coman, D., Doolittle, E., Papademetris, X., Hyder, F., Taylor, J.R., and Simen, A.A. (2012). Maternal separation with early weaning: A rodent model providing novel insights into neglect associated developmental deficits. Dev. Psychopathol. *24*, 1401–1416.

51. Schmidt, M.V., Enthoven, L., Van Der Mark, M., Levine, S., De Kloet, E.R., and Oitzl, M.S. (2003). The postnatal development of the hypothalamic–pituitary–adrenal axis in the mouse. Int. J. Dev. Neurosci. *21*, 125–132.

52. Halbreich, U. (2021). Stress-related physical and mental disorders: a new paradigm. BJPsych Adv. *27*, 145–152.

53. Shalev, A.Y. (2009). Posttraumatic stress disorder and stress-related disorders. Psychiatr. Clin. North Am. *32*, 687–704.

54. American Psychiatric Association (2013). Diagnostic and Statistical Manual of Mental Disorders, Fifth Edition (American Psychiatric Association). https://psychiatryonline.org/doi/book/10.1176/appi.books.9780890425596.

55. Wadsworth, M.E. (2015). Development of Maladaptive Coping: A Functional Adaptation to Chronic, Uncontrollable Stress. Child Dev. Perspect. *9*, 96–100.

56. Boodoo, R., Lagman, J.G., Jairath, B., and Baweja, R. (2022). A Review of ADHD and Childhood Trauma: Treatment Challenges and Clinical Guidance. Curr. Dev. Disord. Rep. *9*, 137–145.

57. Vrijsen, J.N., Tendolkar, I., Onnink, M., Hoogman, M., Schene, A.H., Fernández, G., van Oostrom, I., and Franke, B. (2018). ADHD symptoms in healthy adults are associated with stressful life events and negative memory bias. Atten. Defic. Hyperact. Disord. *10*, 151–160.

58. Liu, Z., Li, X., and Ge, X. (2009). Left Too Early: The Effects of Age at Separation From Parents on Chinese Rural Children's Symptoms of Anxiety and Depression. Am. J. Public Health *99*, 2049–2054.

59. Grillon, C., Baas, J.P., Lissek, S., Smith, K., and Milstein, J. (2004). Anxious Responses to Predictable and Unpredictable Aversive Events. Behav. Neurosci. *118*, 916–924.

60. Amat, J., Matus-Amat, P., Watkins, L.R., and Maier, S.F. (1998). Escapable and inescapable stress differentially alter extracellular levels of 5-HT in the basolateral amygdala of the rat. Brain Res. *812*, 113–120.

61. Leichsenring, F., Fonagy, P., Heim, N., Kernberg, O.F., Leweke, F., Luyten, P., Salzer, S., Spitzer, C., and Steinert, C. (2024). Borderline personality disorder: a comprehensive review of diagnosis and clinical presentation, etiology, treatment, and current controversies. World Psychiatry *23*, 4–25.

62. Neukel, C., Bullenkamp, R., Moessner, M., Spiess, K., Schmahl, C., Bertsch, K., and Herpertz, S.C. (2022). Anger instability and aggression in Borderline Personality Disorder – an ecological momentary assessment study. Borderline Personal. Disord. Emot. Dysregul. *9*, 29.

63. Shrira, A., Shmotkin, D., and Litwin, H. (2012). Potentially traumatic events at different points in the life span and mental health: Findings from SHARE-Israel. Am. J. Orthopsychiatry *82*, 251–259.

64. Dulin, P.L., and Passmore, T. (2010). Avoidance of potentially traumatic stimuli mediates the relationship between accumulated lifetime trauma and late-life depression and anxiety. J. Trauma Stress *23*, 296–299.

65. Maercker, A., Michael, T., Fehm, L., Becker, E.S., and Margraf, J. (2004). Age of traumatisation as a predictor of post-traumatic stress disorder or major depression in young women. Br. J. Psychiatry *184*, 482–487.

66. Panter-Brick, C., Eggerman, M., Gonzalez, V., and Safdar, S. (2009). Violence, suffering, and mental health in Afghanistan: a school-based survey. Lancet Lond Engl. *374*, 807–816.

67. Askenazy, F., Bodeau, N., Nachon, O., Gittard, M., Battista, M., Fernandez, A., and Gindt, M. (2023). Analysis of Psychiatric Disorders by Age Among Children Following a Mass Terrorist Attack in Nice, France, on Bastille Day, 2016. JAMA Netw. Open *6*, e2255472.

68. Makino, Y., Hodgson, N.W., Doenier, E., Serbin, A.V., Osada, K., Artoni, P., Dickey, M., Sullivan, B., Potter-Dickey, A., Komanchuk, J., et al. (2024). Sleep-sensitive dopamine receptor expression in male mice underlies attention deficits after a critical period of early adversity. Sci. Transl. Med. *16*, eadh9763.

69. Shin, S., Pribiag, H., Lilascharoen, V., Knowland, D., Wang, X.Y., and Lim, B.K. (2018). Drd3 Signaling in the Lateral Septum Mediates Early Life Stress-Induced Social Dysfunction. Neuron *97*, 195–208.e6.

70. Cuarenta, A., Kigar, S.L., Henion, I.C., Chang, L., Bakshi, V.P., and Auger, A.P. (2021). Early life stress during the neonatal period alters social play and Line1 during the juvenile stage of development. Sci. Rep. *11*, 3549.

71. Sandi, C., and Haller, J. (2015). Stress and the social brain: behavioural effects and neurobiological mechanisms. Nat. Rev. Neurosci. *16*, 290–304.

72. Locci, A., Geoffroy, P., Miesch, M., Mensah-Nyagan, A.G., and Pinna, G. (2017). Social Isolation in Early versus Late Adolescent Mice Is Associated with Persistent Behavioral Deficits That Can Be Improved by Neurosteroid-Based Treatment. Front. Cell. Neurosci. *11*, 208.

73. Yohn, N.L., and Blendy, J.A. (2017). Adolescent Chronic Unpredictable Stress Exposure Is a Sensitive Window for Long-Term Changes in Adult Behavior in Mice. Neuropsychopharmacology *42*, 1670–1678.

74. Walker, S.E., Papilloud, A., Huzard, D., and Sandi, C. (2018). The link between aberrant hypothalamic–pituitary–adrenal axis activity during development and the emergence of aggression—Animal studies. Neurosci. Biobehav. Rev. *91*, 138–152.

75. Parul, M.A., Mishra, A., Singh, S., Singh, S., Tiwari, V., Chaturvedi, S., Wahajuddin, M., Palit, G., and Shukla, S. (2021). Chronic unpredictable stress negatively regulates hippocampal neurogenesis and promote anxious depression-like behavior via upregulating apoptosis and inflammatory signals in adult rats. Brain Res. Bull. *172*, 164–179.

76. van der Kooij, M.A. (2020). The impact of chronic stress on energy metabolism. Mol. Cell. Neurosci. *107*, 103525.

77. Kuo, T., McQueen, A., Chen, T.C., and Wang, J.C. (2015). Regulation of Glucose Homeostasis by Glucocorticoids. In Glucocorticoid Signaling, J.C. Wang and C. Harris, eds. (Springer New York), pp. 99–126. Advances in Experimental Medicine and Biology. http://link.springer.com/10.1007/978-1-4939-2895-8_5.

78. Gogtay, N., Giedd, J.N., Lusk, L., Hayashi, K.M., Greenstein, D., Vaituzis, A.C., Nugent, T.F., 3rd, Herman, D.H., Clasen, L.S., Toga, A.W., et al. (2004). Dynamic mapping of human cortical development during childhood through early adulthood. Proc. Natl. Acad. Sci. *101*, 8174–8179.

79. Gómez, R.L., and Edgin, J.O. (2016). The extended trajectory of hippocampal development: Implications for early memory development and disorder. Dev. Cogn. Neurosci. *18*, 57–69.

80. Kolk, S.M., and Rakic, P. (2022). Development of prefrontal cortex. Neuropsychopharmacology *47*, 41–57.

81. Lupien, S.J., McEwen, B.S., Gunnar, M.R., and Heim, C. (2009). Effects of stress throughout the lifespan on the brain, behaviour and cognition. Nat. Rev. Neurosci. *10*, 434–445.

82. Lockhart, S., Sawa, A., and Niwa, M. (2018). Developmental trajectories of brain maturation and behavior: Relevance to major mental illnesses. J. Pharmacol. Sci. *137*, 1–4.

83. Andersen, S.L., Tomada, A., Vincow, E.S., Valente, E., Polcari, A., and Teicher, M.H. (2008). Preliminary Evidence for Sensitive Periods in the Effect of Childhood Sexual Abuse on Regional Brain Development. J. Neuropsychiatry Clin. Neurosci. *20*, 292–301.

84. Nolan, C.L., Moore, G.J., Madden, R., Farchione, T., Bartoi, M., Lorch, E., Stewart, C.M., and Rosenberg, D.R. (2002). Prefrontal cortical volume in childhood-onset major depression: preliminary findings. Arch. Gen. Psychiatry *59*, 173–179.

85. Ikonomidou, C. (2009). Triggers of apoptosis in the immature brain. Brain Dev. *31*, 488–492.

86. Daniels, T.E., Olsen, E.M., and Tyrka, A.R. (2020). Stress and Psychiatric Disorders: The Role of Mitochondria. Annu. Rev. Clin. Psychol. *16*, 165–186.

87. Staretz-Chacham, O., Choi, J.H., Wakabayashi, K., Lopez, G., and Sidransky, E. (2010). Psychiatric and behavioral manifestations of lysosomal storage disorders. Am J Med Genet B Neuropsychiatr Genet. *153B*, 1253–1265.

88. Song, H., Sieurin, J., Wirdefeldt, K., Pedersen, N.L., Almqvist, C., Larsson, H., Valdimarsdóttir, U.A., and Fang, F. (2020). Association of Stress-Related Disorders With Subsequent Neurodegenerative Diseases. JAMA Neurol. *77*, 700–709.

89. Sanacora, G., Yan, Z., and Popoli, M. (2022). The stressed synapse 2.0: pathophysiological mechanisms in stress-related neuropsychiatric disorders. Nat. Rev. Neurosci. *23*, 86–103.

90. Hagenauer, M.H., Perryman, J.I., Lee, T.M., and Carskadon, M.A. (2009). Adolescent Changes in the Homeostatic and Circadian Regulation of Sleep. Dev. Neurosci. *31*, 276–284.

91. Burke, A.R., and Miczek, K.A. (2014). Stress in adolescence and drugs of abuse in rodent models: Role of dopamine, CRF, and HPA axis. Psychopharmacology *231*, 1557–1580.

92. McEwen, B.S. (1998). Protective and Damaging Effects of Stress Mediators. N. Engl. J. Med. *338*, 171–179.

93. Kim, W.K., Choi, W., Deshar, B., Kang, S., and Kim, J. (2023). Golgi Stress Response: New Insights into the Pathogenesis and Therapeutic Targets of Human Diseases. Mol. Cells *46*, 191–199.

94. Yegorov, Y.E., Poznyak, A.V., Nikiforov, N.G., Sobenin, I.A., and Orekhov, A.N. (2020). The Link between Chronic Stress and Accelerated Aging. Biomedicines *8*, 198.

95. Schrader, C., and Ross, A. (2021). A Review of PTSD and Current Treatment Strategies. Mo. Med. *118*, 546–551.

96. Stoffers-Winterling, J., Völlm, B., and Lieb, K. (2021). Is pharmacotherapy useful for treating personality disorders? Expert Opin. Pharmacother. *22*, 393–395.

97. Corniquel, M.B., Koenigsberg, H.W., and Likhtik, E. (2019). Toward an animal model of borderline personality disorder. Psychopharmacology *236*, 2485–2500.

98. Berton, O., McClung, C.A., DiLeone, R.J., Krishnan, V., Renthal, W., Russo, S.J., Graham, D., Tsankova, N.M., Bolanos, C.A., Rios, M., et al. (2006). Essential Role of BDNF in the Mesolimbic Dopamine Pathway in Social Defeat Stress. Science *311*, 864–868.

99. Eisch, A.J., Bolaños, C.A., de Wit, J., Simonak, R.D., Pudiak, C.M., Barrot, M., Verhaagen, J., and Nestler, E.J. (2003). Brain-derived neurotrophic factor in the ventral midbrain–nucleus accumbens pathway: a role in depression. Biol. Psychiatry *54*, 994–1005.

100. Cazorla, M., Prémont, J., Mann, A., Girard, N., Kellendonk, C., and Rognan, D. (2011). Identification of a low–molecular weight TrkB antagonist with anxiolytic and antidepressant activity in mice. J. Clin. Investig. *121*, 1846–1857.

101. Walsh, J.J., Friedman, A.K., Sun, H., Heller, E.A., Ku, S.M., Juarez, B., Burnham, V.L., Mazei-Robison, M.S., Ferguson, D., Golden, S.A., et al. (2014). Stress and CRF gate neural activation of BDNF in the mesolimbic reward pathway. Nat. Neurosci. *17*, 27–29.

102. Vukojevic, V., Coynel, D., Ghaffari, N.R., Freytag, V., Elbert, T., Kolassa, I.T., Wilker, S., McGaugh, J.L., Papassotiropoulos, A., and de Quervain, D.J.F. (2020). *NTRK2* methylation is related to reduced PTSD risk in two African cohorts of trauma survivors. Proc. Natl. Acad. Sci. *117*, 21667–21672.

103. Lin, C.C., and Huang, T.L. (2020). Brain-derived neurotrophic factor and mental disorders. Biomed. J. *43*, 134–142.

104. Naumenko, V.S., Kondaurova, E.M., Bazovkina, D.V., Tsybko, A.S., Il'chibaeva, T.V., and Popova, N.K. (2014). On the role of 5-HT $_{1A}$ receptor gene in behavioral effect of brain-derived neurotrophic factor. J. Neurosci. Res. *92*, 1035–1043.

105. Lyons, W.E., Mamounas, L.A., Ricaurte, G.A., Coppola, V., Reid, S.W., Bora, S.H., Wihler, C., Koliatsos, V.E., and Tessarollo, L. (1999). Brain-derived neurotrophic factor-deficient mice develop aggressiveness and hyperphagia in conjunction with brain serotonergic abnormalities. Proc. Natl. Acad. Sci. *96*, 15239–15244.

106. Dunn, B., and PharmD, D. (2020). Larotrectinib and Entrectinib: TRK Inhibitors for the Treatment of Pediatric and Adult Patients With NTRK Gene Fusion. J. Adv. Pract. Oncol. *11*, 418.

107. Dalgleish, T., Black, M., Johnston, D., and Bevan, A. (2020). Transdiagnostic approaches to mental health problems: Current status and future directions. J. Consult. Clin. Psychol. *88*, 179–195.

108. Tyanova, S., Temu, T., Sinitcyn, P., Carlson, A., Hein, M.Y., Geiger, T., Mann, M., and Cox, J. (2016). The Perseus computational platform for comprehensive analysis of (prote)omics data. Nat. Methods *13*, 731–740.

109. Takahashi, L.K. (2014). Olfactory systems and neural circuits that modulate predator odor fear. Front. Behav. Neurosci. *8*, 72.

110. Sree, A.B., Hanifa, M., and Bali, A. (2023). Investigations on Rho/ROCK signaling in post-traumatic stress disorder-like behavior in mice. Behav. Brain Res. *443*, 114347.

111. Bifulco, A., Brown, G.W., and Harris, T.O. (1994). Childhood Experience of Care and Abuse (CECA): A Retrospective Interview Measure. J. Child Psychol. Psychiatry *35*, 1419–1435.

112. Bifulco, A., Brown, G.W., Lillie, A., and Jarvis, J. (1997). Memories of Childhood Neglect and Abuse: Corroboration in a Series of Sisters. J. Child Psychol. Psychiatry *38*, 365–374.

113. American Psychiatric Association. Diagnostic and Statistical Manual of Mental Disorders (DSM-5-TR). https://www.psychiatry.org/psychiatrists/practice/dsm.

114. Hughes, K., Bellis, M.A., Hardcastle, K.A., Sethi, D., Butchart, A., Mikton, C., Jones, L., and Dunne, M.P. (2017). The effect of multiple adverse childhood experiences on health: a systematic review and meta-analysis. Lancet Public Health *2*, e356–e366.

115. Felitti, V.J., Anda, R.F., Nordenberg, D., Williamson, D.F., Spitz, A.M., Edwards, V., Koss, M.P., and Marks, J.S. (1998). Relationship of Childhood Abuse and Household Dysfunction to Many of the Leading Causes of Death in Adults. Am. J. Prev. Med. *14*, 245–258.

116. Uccella, S., Mongelli, F., Majno-Hurst, P., Pavan, L.J., Uccella, S., Zoia, C., and Uccella, L. (2022). Psychological Impact of the Very Early Beginning of the COVID-19 Outbreak in Healthcare Workers: A Bayesian Study on the Italian and Swiss Perspectives. Front. Public Health *10*, 768036.

117. Uccella, S., De Grandis, E., De Carli, F., D'Apruzzo, M., Siri, L., Preiti, D., Di Profio, S., Rebora, S., Cimellaro, P., Biolcati Rinaldi, A., et al. (2021). Impact of the COVID-19 Outbreak on the Behavior of Families in Italy: A Focus on Children and Adolescents. Front. Public Health *9*, 608358.

118. Di Profio, S., Uccella, S., Cimellaro, P., Biolcati Rinaldi, A., D'Apruzzo, M., Rebora, S., Primavera, L., Zanetti, A., DE Giuseppe, S., Robotti, S., et al. (2022). The pandemic seen through the eyes of the youngest people: evaluating psychological impact of the early COVID-19 related confinement on children and adolescents through the analysis of drawings and of an e-survey on their parents. Minerva Pediatr. *78*, 104–113. https://www.minervamedica.it/en/journals/minerva-pediatrics/article.php?cod=R15Y2026N01A0104.

119. Giallonardo, M., Uccella, S., De Carli, F., Nobili, L., Bruni, O., De Grandis, E., and Melegari, M.G. (2021). Stress symptoms and Coronavirus disease 2019 (COVID-19): a comparative study between Attention Deficit Hyperactivity Disorder and typically developing children and adolescents. Minerva Pediatr. *77*, 62. https://www.minervamedica.it/index2.php?show=R15Y9999N00A21101406.

120. Wong, S.S., Wong, C.C., Ng, K.W., Bostanudin, M.F., and Tan, S.F. (2023). Depression, anxiety, and stress among university students in Selangor, Malaysia during COVID-19 pandemics and their associated factors. Mahmoud AB. PLoS One *18*, e0280680.

121. Lindzey, G., Winston, H., and Manosevitz, M. (1961). Social Dominance in Inbred Mouse Strains. Nature *191*, 474–476.

122. Potenzieri, A., Uccella, S., Preiti, D., Pisoni, M., Rosati, S., Lavarello, C., Bartolucci, M., Debellis, D., Catalano, F., Petretto, A., et al. (2024). Early IGF-1 receptor inhibition in mice mimics preterm human brain disorders and reveals a therapeutic target. Sci. Adv. *10*, eadk8123.

123. Savardi, A., Borgogno, M., Narducci, R., La Sala, G., Ortega, J.A., Summa, M., Armirotti, A., Bertorelli, R., Contestabile, A., De Vivo, M., and Cancedda, L. (2020). Discovery of a Small Molecule Drug Candidate for Selective NKCC1 Inhibition in Brain Disorders. Chem *6*, 2073–2096.

124. Can, A., Dao, D.T., Terrillion, C.E., Piantadosi, S.C., Bhat, S., and Gould, T.D. (2012). The tail suspension test. J. Vis. Exp. *59*, e3769.

125. Can, A., Dao, D.T., Arad, M., Terrillion, C.E., Piantadosi, S.C., and Gould, T.D. (2012). The mouse forced swim test. J. Vis. Exp. *59*, e3638.

126. Colombi, I., Rastogi, M., Parrini, M., Alberti, M., Potenzieri, A., Chellali, M.M., Rosati, S., Chiappalone, M., Nanni, M., Contestabile, A., and Cancedda, L. (2024). Heterogeneous subpopulations of GABAAR-responding neurons coexist across neuronal network scales and developmental stages in health and disease. iScience *27*, 109438.

127. Rogers, D.C., Fisher, E.M., Brown, S.D., Peters, J., Hunter, A.J., and Martin, J.E. (1997). Behavioral and functional analysis of mouse phenotype: SHIRPA, a proposed protocol for comprehensive phenotype assessment. Mamm. Genome *8*, 711–713.

128. Mandillo, S., Tucci, V., Hölter, S.M., Meziane, H., Banchaabouchi, M.A., Kallnik, M., Lad, H.V., Nolan, P.M., Ouagazzal, A.M., Coghill, E.L., et al. (2008). Reliability, robustness, and reproducibility in mouse behavioral phenotyping: a cross-laboratory study. Physiol. Genomics *34*, 243–255.

129. Dumais, A., Lesage, A.D., Alda, M., Rouleau, G., Dumont, M., Chawky, N., Roy, M., Mann, J.J., Benkelfat, C., and Turecki, G. (2005). Risk Factors for Suicide Completion in Major Depression: A Case-Control Study of Impulsive and Aggressive Behaviors in Men. Am. J. Psychiatry *162*, 2116–2124.

130. Batth, T.S., Tollenaere, M.A.X., Rüther, P., Gonzalez-Franquesa, A., Prabhakar, B.S., Bekker-Jensen, S., Deshmukh, A.S., and Olsen, J.V. (2019). Protein Aggregation Capture on Microparticles Enables Multipurpose Proteomics Sample Preparation. Mol. Cell. Proteomics *18*, 1027–1035.

131. Kulak, N.A., Pichler, G., Paron, I., Nagaraj, N., and Mann, M. (2014). Minimal, encapsulated proteomic-sample processing applied to copy-number estimation in eukaryotic cells. Nat. Methods *11*, 319–324.

132. Bruderer, R., Bernhardt, O.M., Gandhi, T., Miladinović, S.M., Cheng, L.Y., Messner, S., Ehrenberger, T., Zanotelli, V., Butscheid, Y., Escher, C., et al. (2015). Extending the Limits of Quantitative Proteome Profiling with Data-Independent Acquisition and Application to Acetaminophen-Treated Three-Dimensional Liver Microtissues. Mol. Cell. Proteomics *14*, 1400–1410.

133. Zhu, Y., Orre, L.M., Zhou Tran, Y., Mermelekas, G., Johansson, H.J., Malyutina, A., Anders, S., and Lehtiö, J. (2020). DEqMS: A Method for Accurate Variance Estimation in Differential Protein Expression Analysis. Mol. Cell. Proteomics *19*, 1047–1057.

134. R Core Team (2021). R: A Language and Environment for Statistical Computing. https://www.R-project.org/.

135. Lê, S., Josse, J., and Husson, F. (2008). FactoMineR: An *R* Package for Multivariate Analysis. J Stat Softw *25*, 1. http://www.jstatsoft.org/v25/i01/.

136. Evangelista J.E., Xie Z., Marino G.B., Nguyen N., Clarke D.J.B., Ma'ayan A. Enrichr-KG: bridging enrichment analysis across multiple libraries. Nucleic Acids Res. 2023:gkad393. https://maayanlab.cloud/enrichr-kg.

137. Achenbach, T.M., and Rescorla, L.A. (2000). Manual for the ASEBA Preschool Forms & Profiles: An Integrated System of Multi-Informant Assessment. [Italian Version] (ASEBA).

138. Achenbach, T.M., and Rescorla, L.A. (2001). Manual for the ASEBA School-Age Forms & Profiles: Child Behavior Checklist for Ages 6-18. [Italian Version] (ASEBA).

139. March, J.S. (2013). Multidimensional Anxiety Scale for Children. [Italian version], 2nd Edition (Giunti Psychometrics). (MASC-2).

140. Kovacs, M. (2011). Children's Depression Inventory. [Italian version], 2nd Edition (Giunti Psychometrics). (CDI-2).

Please cite this article in press as: Morelli et al., Traumatic life experiences during critical periods lead to diverse developmental trajectories, Cell Reports Medicine (2026), https://doi.org/10.1016/j.xcrm.2026.102798

STAR★METHODS

KEY RESOURCES TABLE

REAGENT or RESOURCE	SOURCE	IDENTIFIER
Biological samples		
Adult PFC brain tissue from controls	Douglas-Bell Canada Brain Bank	N/A
Adult PFC brain tissue from people who experienced a trauma before 12 years of age	Douglas-Bell Canada Brain Bank	N/A
Adult PFC brain tissue from people who experienced a trauma after 12 years of age	Douglas-Bell Canada Brain Bank	N/A
Chemicals, peptides, and recombinant proteins		
Phosphatase Inhibitor Cocktail 2	Sigma-Aldrich	P5726
Phosphatase Inhibitor Cocktail 3	Sigma-Aldrich	P0044
PMSF	Sigma-Aldrich	329-98-6
Complete mini EDTA-free protease inhibitor cocktail	Roche	11836170001
2,4,5-Trimethylthiazole, 98%	Sigma-Aldrich	219185
BCA Assay	Thermo Fisher	23225
Larotrectinib	BioSynth	FD145150
DMSO	Sigma-Aldrich	276855
Critical commercial assays		
Corticosterone Enzyme Immunoassay Kit	Arbor Assay	K014-H1/H5
Deposited data		
Proteomic data	This paper	ProteomeXchange
Experimental models: Organisms/strains		
Male and female C57BL/6J mice	Charles River	632C57BL/6J
Software and algorithms		
Phenopy software platform	Balzani et al.[27]	N/A
Any-maze software	Stoelting Co.	Version 7.51
GraphPad (Prism) software	Dotmatics	Version 9
Perseus software	Tyanova et al.[108]	Version 1.6.15.0
Tube dominance apparatus	2biological instruments S.N.C.	LE899M
Open field apparatus	Ugo Basile	47432

EXPERIMENTAL MODEL AND STUDY PARTICIPANT DETAILS

Animals and stress-induction protocols

All care of animals and experimental procedures were conducted in accordance with Istituto Italiano di Tecnologia (IIT) licensing as well as the Italian Ministry of Health (D.Lgs 26/2014) and EU guidelines (Directive 2010/63/EU). A veterinarian was employed to maintain the health and comfort of the mice. All animals were housed in filtered cages in a climate-controlled animal facility (22 ± 2°C) and maintained on a 12-h light/dark cycle with *ad libitum* access to food and water. All efforts were made to minimize animal suffering and use the lowest possible number of animals required to produce statistical relevant results, according to the "3Rs concept." We used male and female C57BL/6J (Charles River) mice. We allowed dams used in the study to produce a maximum of two litters with one or two different males. The pups were obtained through harem breeding (i.e., one male mouse housed with two or three female mice). The litter size ranged from 5 to 9 pups. Offsprings were weaned around P24 and then group-housed according to gender (maximum 5 animals/cage). Control groups were distinct from stressed litters and housed separately, to avoid potential influence of stress among control and stressed mates within a same litter or cage. Groups were defined based on trauma exposure (10 consecutive mornings, between 7 and 10 a.m.) which was performed at different developmental periods in mice: (infancy: from postnatal day (P)2 to P11, P2-11; childhood: P12-21; adolescence: P26-35; young-adulthood: P47-56). *Exposure to TMT* (2,4,5-Trimethylthiazole, Sigma Aldrich, 98%), consisted of 10 μL of the predator scent applied on a filter paper in a 30.5 cm × 19.5 cm x 12.0 cm cage[109] and it was performed once a day for 10 min a day during one of the above-mentioned developmental time windows (TMT group). For *underwater immersion* (IMM; 30 ± 2°C) animals were exposed to a daily forced immersion sequence (2 s of underwater immersion every minute during 2 min of floating in water (IMM group,[110]). For *maternal separation* (MS; only P2-11 or P12-21 groups) we selected a paradigm of a duration

comparable with other stressors: all pups were removed at the same time from their cage for 15 min daily (MS group). For each experiment of stress, we run experiments in parallel between stress and control groups in litters born at the same time (age-matched). Control groups were distinct from the stressed litters, to avoid the potential influence of stress among control and stressed mates within a same litter. Control litters entailed three diverse paradigms: naive animals not subjected to any manipulation, and handled animals (2 min every day of operator handling) were used as overall controls for all type of stress; as controls specific for the TMT group, age-matched mice were exposed to a saline solution for 10 min daily following the exact procedures for TMT exposure. For each behavioral test performed at any age, we included all three groups of controls. Since we did not detect any significant difference among the three diverse groups of controls (three-chamber, tail suspension, forced swim, marble burying, grooming, dark/light, and open field tests), we pooled them together as "controls" in the figures. Male and female mice were considered together unless otherwise stated.

Postmortem human samples

Postmortem PFC brain tissues (Local Ethical Committee 573/2021 - DB id 11849) were obtained from the Douglas-Bell Canada Brain Bank (http://douglasbrainbank.ca/) and were the only available region among the those we collected in mice. Characterization of early-life histories was based on an adapted version of the Childhood Experience of Care and Abuse interview, assessing several dimensions of childhood experience, including neglect, sexual and physical abuse.[111,112] We considered as severe adversity, reports of non-random major physical and/or sexual abuse during infancy/childhood (before 12 years of age) or during adolescence/young-adulthood (after 12 years of age). Only cases with the maximum severity ratings of 1 and 2 (out of 6, with 6 being absence) were included. Histories of abuse were validated with reports from medical charts, coroner files, or reports from youth protection services when available. The groups were matched for age, postmortem interval, and brain pH. Detailed sample characteristics are presented in Tables S8–S10.

Participants in the human study

Clinical informative data from a cohort of pediatric subjects (collected between 0 and 18 years of age) who entered the Child and Adolescent psychiatric ward of a Tertiary Care center in Italy between the 1st of January 2021 and the 31st of December 2021 were retrospectively analyzed (Local Ethical Committee 542/2021 - DB id 12712). All subjects who experienced or witnessed either a traumatic experience or a complex trauma (according to DSM 5-TR criteria[113]) or had multiple Adverse Childhood Events (ACE), defined as described in[114] were enrolled. Considering the multiplicity and the cumulative effect of ACE lifelong during human life,[115] the traumatic effects of COVID-19 pandemic and related measures of social restriction for contagion containment were accounted as ACE[116–120]

The following information were collected for all enrolled subjects: gender, family positive history of ACE, age at first episode, type of episode, age at time of the data collection and assessment, clinical dimensional outcome (categorized as difficult sociability, ADHD, aggressiveness/dominance, depression with irritability, anxiety), and predominant personality trait.

METHOD DETAILS

Serum corticosterone detection

Animals at different ages (P2, P12, P26 or P47) were exposed to the diverse stress-induction protocols described above for 10 consecutive days and sacrificed 30 min after the last stress exposure (P11, P21, P35 or P56, respectively). The blood was collected, allowed to clot at RT and centrifuged at 5000 rcf for 20 min at 4°C. Corticosterone was detected in the supernatant by the Corticosterone Kit immunoassay DetectX (Arbor Assay K014-H1), following the manufacturer instructions.

Behavioral testing and pharmacological treatment

All behavioral tests were performed in 3-month-old mice. Adult control and previously stressed mice were tested over a total period of 45 days. The behavioral tests were performed from the least to the most stressful test, with order and modalities detailed in Table S1. The tasks were video-recorded and then analyzed manually by a blind operator, unless otherwise indicated. After each trial or experiment, the diverse apparatuses and objects were cleaned with 70% ethanol. Mice were habituated to the room 45 min before testing. For larotrectinib experiments, mice were tested after 1 week of oral treatment with vehicle (DMSO, 0.15%) or larotrectinib 10 mg/Kg constantly present in the drinking water until the end of tests. The route of administration and the concentration of the drug were determined as in.[44]

Tube dominance test

The test evaluates dominance and it was adapted from.[121] We used a transparent Plexigas tube with 30 cm length and 3 cm inside diameter (76–0930 (LE899M), Harvard Apparatus). On the habituation day, each mouse was released at alternating ends of the tube and let ran through it. Each animal was given 5 training trials. Matches were organized among same gender, but different groups of mice (control vs. stressed mice; for larotrectinib experiments: vehicle-treated control vs. vehicle-treated stressed mice, vehicle-treated control vs. larotrectinib-treated stressed mice, and vehicle-treated stressed vs. larotrectinib-treated stressed mice). Each mouse was tested against 3–5 different mice in 5 matches of maximum 2 min each. The mouse that first retreated from the tube was designated as the loser of the trial. From trial to trial, mice were released at alternate ends of the tube. In cases when no mice retreated within 2 min, the test was repeated and if there was still no winner, the match ended as draw (<5% of total encounters).

Please cite this article in press as: Morelli et al., Traumatic life experiences during critical periods lead to diverse developmental trajectories, Cell Reports Medicine (2026), https://doi.org/10.1016/j.xcrm.2026.102798

Between each trial, tube was cleaned with 30% ethanol. Dominance score was calculated as [the number of won encounters – the number of lost encounters] divided by the total number of encounters.

Three-chamber test

The test evaluates the social approach of the mouse vs. a never-met intruder in comparison to an object (sociability) or vs. a novel never-met intruder in comparison to the already-met intruder (social novelty). The three-chamber apparatus comprises a rectangle, three-chambered box of gray acrylic (20 × 40.5 × 22 cm), evenly illuminated by overhead dim lighting (12–14 lux). The chambers are accessible by rectangle openings with sliding doors. Firstly, the tested mouse was habituated to the empty apparatus for 10 min. Then, the tested mouse was briefly confined in the center chamber, while two inverted stainless-steel wire pencil cups (10 cm L x 10 cm H, pencil box, Spectrum Diversified) were placed, one in each of the two side chambers. These cups have holes that allow nose contacts between mice but prevent them to fight. A weighted plastic cup was placed on top of each cup to prevent the mouse climbing. An unfamiliar stranger mouse (stranger 1, previously habituated to the wire cups) was placed in the cup in one of the external compartments of the apparatus. For the following 10 min (sociability test), the tested mouse was allowed to explore all three chambers. Then, the tested mouse was again briefly confined in the center chamber, while a novel unfamiliar stranger mouse (stranger 2, previously habituated to the wire cups) was placed in the other side chamber under the pencil cup. Measures of the amount of time spent in the compartments was automatically calculated by the Any-maze software (Stoelting Co.). *Sociability and Social Novelty scores* were calculated as [the percent time spent in the target zone/field minus the percent time in the non-target zone/field] divided by [the percent time spent in the target zone/field plus the percent time in the non-target zone/field], as previously described in.[122,123] The *social interaction score* consisted in the sum of the sociability and social novelty scores.

Phenopy attention test

The attention test was conducted using 12 automated devices, operated in remote via the Phenopy software platform.[27] Each device was individually housed in a cage placed in sound-attenuating boxes. The cage consisted of a waiting area containing the housing litter, and an area containing the Chora feeder (AM Microsystems, pre-order code PCHFEA01) consisting of 3 nose pokes two of which (left and right) with both light-emitting diodes (LED) and small speakers. Mice were individually isolated after 3 days of habituation in the boxes. The training phase consisted of 9 days in which mice were trained to retrieve pellets, after a central nose-poke activation, either in the left or right nose-poke prior the signal of a target light. Target light turned on after 1 s of the central nose-poke activation and lasted for 10 s (5 days) followed by 5 (2 days) and 2 s (2 days). Afterward, a cue (white noise of 50 dB) was added to the test in to identify no cue (30% probability) and cued (70% probability) trials. Of the cued trials, 70% were congruent (sound and light from the same nose-poke) and 30% were incongruent (sound and light from opposite nose-pokes). Errors were considered as the lack of the nose-poke under the target light. Two types of errors were scored: commissions - when animal approached the nose-poke opposite to the target light, and omissions when the animal did not approach any nose-poke. Percentages of error rate, accuracy and omission were plotted using Phenopy. The *attention score* was calculated as percentage of correct trials over total number of performed trials (considering all congruent, incongruent, and no-cue trials).

Tail suspension test

The test evaluates the depressive-related behavior, and it was performed as in.[124] Briefly, mice were suspended by their tail to a horizontal suspension platform (25 cm height) for 6 min. Mouse tails were taped 1 cm from the tip of the tail, such that the mouse head was about 20 cm above the apparatus floor. Recordings were performed using Any-maze software and the time spent immobile by the animals was scored.

Forced swim test

The test evaluates the depressive-related behavior, and it was performed as in.[125] Briefly, mice were place on a 2 L glass beaker filled with 20 cm of water (28 ± 1°C) for 6 min. Recordings were performed using Any-maze software and the time spent immobile by the animals was scored.

Depression score calculation

The depression score was calculated based on,[28] as an algebraic sum of standardized indexes of the time spent immobile in the tail suspension and forced swim tests. The standardized indexes for each test were obtained applying the following calculation: [x – min value] divided by [max value - min value], where the minimum and the maximum values referred to the whole population for each age of stress exposure. This procedure created standardized indexes ranging from 0 to 1 and their algebraic sum corresponded to the depression score, which was distributed along a scale from 0 (no depression) to 2 (maximum level of depression).

Marble burying

The test evaluates the repetitive (anxiety/OCD-related) behavior as the tendency to dig and bury marbles in a novel environment. It was performed as in.[113] Briefly, mice were place into a cage of the same dimensions of their home-cage (26 × 48 × 20 cm) filled with 4 cm deep fresh bedding material evenly distributed into a flat surface across the cage, and evenly illuminated by overhead dim lighting (12–14 lux). After 30 min of habituation, the mouse was briefly removed, bedding surface was leveled, and 15 marbles (1.4 cm diameter) were evenly spaced in a 3 × 5 grid on the surface of the bedding. At the end of the test, the mouse was returned to the home-cage and the number of marbles buried up to 2/3 in depth was counted. A picture post-testing was taken.

Grooming

The test evaluates repetitive (anxiety/OCD-related) behavior in mouse grooming of all body parts. It was performed as in.[122,123] Briefly, mice were placed individually into a clear plexiglass cylinder (30 cm high, 10 cm wide) illuminated at ∼ 40 lux. After

10 min of habituation, the mouse was manually scored for 5 min for the time spent self-grooming in all body regions. Self-grooming was defined as licking or scratching the head or body parts with any of the forelimbs.

Open field

The test evaluates the general anxiety-like behaviors and general locomotor activity, and it was performed as in.[126] Mice were individually placed in the central area (16 × 16 cm) of a gray acrylic arena (40 × 40 cm), evenly illuminated by overhead dim lighting (12–14 lux) and their behavior was recorded for 30 min. Mice were allowed to freely explore the apparatus for the entire duration of the test session. Recordings and automatic analysis were performed with Any-maze software, which can track both the exploratory activity of the animals between the different parts of the open field (i.e., center and border) and the time they spent immobile.

Dark/light test

The test evaluates the general anxiety-like behaviors, and it was performed based on.[126] Mice were placed in the lit compartment of a box (21 × 42 × 25 cm) divided into two equivalent parts: a dark compartment (5 lux) and an illuminated one (300 lux). Mice were allowed to freely move between the two compartments for 5 min. Recordings and automatic analysis were performed by Any-maze software, detecting the time spent in each of the two differently enlightened areas of the behavioral apparatus.

Anxiety/OCD-related score calculation

The anxiety/OCD-related score was calculated based on,[28] as an algebraic sum of standardized indexes of the analyzed parameters of the four anxiety/OCD-related behavioral tests above. Specifically, the analyzed parameters were the number of buried marbles in the marble burying test, the time spent grooming in the grooming test, the time spent in the dark compartment of the dark/light apparatus, and the time spent outside the center of the open field box. The standardized indexes for each test were obtained applying the following calculation: [x – min value] divided by [max value - min value], where the minimum and the maximum values refer to the whole population for each age of stress exposure. This procedure created standardized indexes ranging from 0 to 1 and their algebraic sum corresponded to the anxiety/OCD-related score, which was distributed along a scale from 0 (no anxiety/OCD) to 4 (maximum level of anxiety/OCD). In Figures S8C–S8M and S9C–S9J data were normalized to experiment-specific controls and animals treated with DMSO or larotrectinib were normalized to DMSO controls.

Modified SHIRPA

The SHIRPA battery consists of a comprehensive observational phenotypic analysis based on a systematic assessment of behavioral and neurological parameters. A modified version of the protocol was used to reduce the potential for ambiguity and subjectivity within the experiments.[127] The apparatus included: a cylindrical viewing jar (diameter ~15 cm, height ~35 cm) on a raised platform, a Perspex arena (55 × 33 × 18 cm), whose floor was divided into 15 clearly marked squares. A wire grid was secured across the top (middle section) of the arena. In the modified procedure, each mouse was placed into a viewing jar (5 min) and assessed for unprovoked behaviors (i.e., spontaneous activity, respiratory rate, and tremor), after which mice were transferred to a test arena for a series of observations and manipulations (i.e., transfer arousal, palpebral closure, piloerection, gait, pelvic elevation, tail elevation, startle response, touch escape, trunk curl, limb grasping, visual placing, grip strength, toe pinch, wire maneuver, lacrimation, salivation, provoked biting, righting reflex, contact righting reflex, negative geotaxis, fear and aggression). Score sheets were used to record data assessing semi-quantitatively abnormal phenotypes as shown in[128] and detailed in Table S4.

Proteomics on mouse and human samples

Mouse samples

Amygdala, hypothalamus, hippocampus and prefrontal cortex (PFC) were dissected from adult mice previously exposed to TMT during infancy, childhood, adolescence or young-adulthood (see "animals and stress-induction protocols" section), and naive adult mice (as common controls). For mouse proteomics, all cohorts were naive to any behavioral testing, to avoid confounding effects. After collections, samples were frozen in dry ice.

Human subjects details

Dissections and freezing of brain tissue were performed as previously described in.[11,129] Briefly, PFC samples were dissected from each subject from 0.5 cm-thick coronal brain sections by expert brain bank staff following standard dissection procedures and kept frozen at −80°C.

Sample preparation

Human and mouse brain samples were first lysed in ice-cold RIPA buffer (1% NP40, 0.5% sodium deoxycholate, 0.1% SDS, 150 mM NaCl, 1 mM EDTA, pH 8, 50 mM Tris, pH 7.4) supplemented with protease (complete mini EDTA-free protease inhibitor cocktail, Roche) and phosphatase inhibitors (1mM phenylmethylsulfonyl fluoride, 10 mM NaF and 2 mM sodium orthovanadate). Lysates were incubated for 30 min at 4°C and clarified by centrifugation at 20,000 rcf for 20 min at 4°C. Protein concentration was determined by performing the BCA assay (Pierce). 50mg of each sample lysate were then reduced and alkylated with 10 mM TCEP and 40 mM Chloroacetamide for 10 min at RT. Then, proteins were isolated by the protein aggregation capture method.[130] Briefly, proteins aggregation was induced by addition of 70% acetonitrile, and 200 mg of magnetic beads were used to capture aggregated proteins. Magnetic beads were retained by a magnet and the supernatant was discarded. Beads were washed one time with 1 mL of acetonitrile, followed by one wash with 1 mL of 70% ethanol and one wash with 1 mL isopropanol. Washed beads were resuspended in 100 mL of resuspension solution (25 mM Tris pH 8), and captured proteins were digested overnight at 37°C with Trypsin and LysC at a 1:50 and 1:100 ratio of enzyme to sample protein mg, respectively.

Please cite this article in press as: Morelli et al., Traumatic life experiences during critical periods lead to diverse developmental trajectories, Cell Reports Medicine (2026), https://doi.org/10.1016/j.xcrm.2026.102798

Nano-LC and mass spectrometer (MS) setup

Elution of mouse peptides was performed using a PharmaFluidics separation columns (200 cm uPAC C18 column) mounted in the thermostated column compartment maintained at 50°C. Initially, a concentration gradient from 5% to 7% buffer B (80% ACN and 20% H_2O, 5% DMSO, 0.1% FA) coupled with a flow gradient from 750 nL/min to 350 nL/min was applied for 12 min. Then, peptides were eluted with a 78 min non-linear gradient from 7% to 22.5% of buffer B in 56 min and then to 45% of buffer B in 22 min, at a constant flow rate of 350 nL/min. MS analysis was performed in data-independent acquisition (DIA) mode. Orbitrap detection was used for MS1 measurements at a resolving power of 120 K in a range between 375 and 1500 m/z with an AGC target of $12E^5$, maximum injection time 50 ms. Advanced Peack Determination was enabled for MS1 measurements. Double FAIMS CV was set to −40 and −50 at standard resolution and with a total carrier gas flow of 1.5 L/min. Precursors were selected for data-independent fragmentation with an isolation window width of 10 m/z in 60 windows ranging from 380 to 980 m/z, 2 m/z overlap. HCD collision energy was set to 30% and MS2 scans were acquired at a resolution of 15 K, 22 ms max. IT, and $5E^5$ AGC target.

Mouse peptides were desalted in Stage-Tips[131] and analyzed by a nano-UHPLC-MS/MS system using an Ultimate 3000 RSLC coupled to an Orbitrap Fusion Tribrid mass spectrometer (Thermo Scientific Instrument) with FAIMS Pro interface. *For human samples*, obtained peptides were analyzed by the Evosep One system coupled to an Orbitrap Exploris 480 mass spectrometer (Thermo Scientific) with FAIMS Pro Duo Interface (Thermo Scientific).*Human peptides* were analyzed on the Evosep One system using an EASY spray column (150 μm × 15 cm, 2 μm particle size, Thermo Scientific) and the pre-programmed extended gradient of 15 sample per day, with a flow rate of 220 nL/min. The column temperature was maintained at 50°C and interfaced online with the Orbitrap Exploris 480 MS (Thermo Scientific) with FAIMS Pro Duo Interface (Thermo Scientific). MS analysis was performed in DIA mode. Double FAIMS CV was set to −40 and −65 at standard resolution. Full MS resolution was set to 120000 in a range between 375 and 1500 m/z and with a normalized AGC target of 300%, with a maximum IT set to Auto. Normalized AGC target for fragment spectra was set at 1000%. 40 windows of 15 m/z were used with an overlap of 1 m/z. Resolution was set to 30000 and IT to Auto. Normalized collision energy was set at 30%. All data were acquired in profile mode, using positive polarity.

Data analysis and statistics

Mouse and human DIA raw files were processed with Spectronaut[132] version 15 and 17 respectively, using a library-free approach (directDIA) under default settings. Enzymes/Cleavage Rules was set to Trypsin/P for mice data and to Trypsin/P, LysC for human data. Library was generated against Uniprot Mouse database (UP000000589, 63656 entries) for mice data and against Uniprot Human database (UP000005640_9606, 102572 entries) for human data. Carbamidomethylation was selected as a fixed modification for both mouse and human data, methionine oxidation and N-terminal acetylation were selected as variable modifications for both mouse and human data and Deamidation (NQ) as variable modifications for human data only. FDRs of PSMs and peptide/protein groups were set to 0.01. For quantification, Precursor Filtering was set to Identified (Qvalue), Imputation Strategy was set to Global Imputing for mouse data and to Run Wise Imputing for human data, and MS2 was chosen as quantity MS-level. The Protein Quant Pivot Report generated by Spectronaut was statistically evaluated using Perseus software[108] version 1.6.15.0. After Quantile normalization, differences in protein expression between different stress ages and controls were evaluated with the ANOVA test. To reduce the probability of false positive findings deriving from multiple hypothesis testing a permutation-based false discovery rate (FDR) p-value lower than 0.05 was applied, and the artificial within groups variance (S0) was set to 0.1.

Differentially expressed proteins between groups were determined using the Limma-based methods DEqMS in the R environment.[133,134] Proteins with a log2(fold change) of ±0.3 and a Bonferroni adjusted p-value $\leq$0.05 were considered as differentially expressed compared to the respective controls and used in further analysis.

Principal component analysis (PCA)

Multivariate exploratory data analysis and sample clustering were performed on normalized proteomic data and behavioral tests (i.e., dominance, sociability and social novelty scores, time spent immobile in the tail suspension and forced swim tests, number of buried marbles, time spent grooming, time spent in the dark of the dark/light apparatus and time spent outside the center of the open field apparatus), using the FactoMineR tool in the R environment.[135] The group segregations were measured according to the most representative components and the centroid distance, and the group distributions were represented as density plots of the projected data on the axes. Based on these parameters, for human samples, three outliers (centroid distance ±3 SD from group mean) were identified and removed; a second round of PCA was performed and showed that all samples correctly clustered within their own group. No further samples were therefore removed after the second round of PCA.

Pathways enrichment analysis

Protein list enrichments were performed with EnrichR-KG.[38,136] Specific libraries were selected for each type of data. The mouse brain area analyses included Gene Ontology Biological Process, Reactome, DisGeneT, MGI (mammalian phenotype 2021), and Jensen Disease databases, and the terms related to the same macro-pathways were grouped as unique entities. Age-specific analyses in mouse data were performed using Human_Phenotype_Ontology, KEGG, MGI_Mammalian_Phenotype, Reactome, WikiPathways datasets. Human data enrichment was analyzed using WikiPathways, Human Phenotype Ontology, KEGG, Gene Ontology Biological Process, and Reactome libraries. Enrichments were analyzed and graphically represented in R environment.

Proteomics data are available via ProteomeXchange with identifier PXD054552. Reviewer account details: Username: reviewer_pxd054552@ebi.ac.uk Password: KPPCqOm50kyP.

Please cite this article in press as: Morelli et al., Traumatic life experiences during critical periods lead to diverse developmental trajectories, Cell Reports Medicine (2026), https://doi.org/10.1016/j.xcrm.2026.102798

Assessment of symptoms in the human study

Anxiety/OCD

For infants and children aged <8 years, we used the Child Behavior Checklist (CBCL) scales.[137,138] The CBCL scales are questionnaires in the form of caregiver reports distinct in 2 age groups (i.e., 1.5–5.11 and 6–18.11 years). Those are widely used for assessing behavioral issues in infancy.[137,138] Information regarding the scale Somatic Complaints were extracted for children aged 1.5–5.11, while information regarding the scale Somatic Complaints DSM-Oriented Anxiety Problems Scale data were extracted for children aged 6–7.11 years.[137,138] For children and adolescents aged >8 years, we used the Multidimensional Anxiety Scale for Children 2 (MASC 2).[139] This is a self-report tool constructed with fifty questions rated on a four-point Likert scale, commonly used to assess anxiety levels in children and adolescents aged 8–19 years. The MASC 2 provides scores regarding anxiety symptoms in general (Total score) and across six specific domains: Separation Anxiety/Phobias, Generalized Anxiety, Social Anxiety, Obsessions and Compulsions, Physical Symptoms, and Harm Avoidance.

Depression

For infants and children aged <7 years, we used the Child Behavior Checklist (CBCL) scales.[137,138] Information regarding the scale Withdrawn were extracted for children aged 1.5–5.11, while information regarding the scale Withdrawn/Depressed DSM-Oriented Depressive Problems Scale data were extracted for children aged 6–7.11 years. For children and adolescents aged >7 years, we used the Children's Depression Inventory 2 (CDI 2,[140]). This is a self-report tool (with 28 Likert questions) widely used for assessing depressive symptoms in children and adolescents aged 7–17 years. The CDI 2 provides insights into emotional, cognitive, and behavioral aspects of depression. The CDI 2 provides a global index (Total Score) of depressive symptoms, and information on five specific areas: Emotional Problems, Negative Mood/Physical Symptoms, Negative Self-Esteem, Functional Problems, and Interpersonal Problems. Responses are rated on a three-point scale (0–2) to indicate symptom severity. From raw scores calculated using CBCL, MASC2 and CDI2, T scores are calculated depending on age and gender and clinical significance is considered for T scores >60.

Principal component analysis (clinical data)

Clinical informative data from the cohort of pediatric subjects were used in multivariate exploratory data analysis and sample clustering using the FAMD function from FactoMineR tool in the R environment,[128] allowing the integration of both dicotomic and numeric variables. Behavioral traits (ADHD, Anxiety/OCD, Depression, Aggressiveness, Eating Disorder, Obesity, Difficult Hyper sociability) and personality traits (Antisocial, Borderline, Histrionic, Narcissistic, Obsessive-Compulsive, Paranoid, Schizoid) were indicated as dicotomic variables (0 = assence, 1 = presence), while clinical assigned scores (MASC_tot_Tscore, A_Separation_Phobias_Tscore, B_Generalized_Anxiety_Disorder_Tscore, C_Social Anxiety_Tscore, D Obsessive_Compulsive_Tscore, E_MASC2_SomaticSymptomsTOT_Tscore, F_Harm Avoidance_Tscore, self_CDI2_TOT_Tscore, self_CDI2_EmotionalProblems_Tscore, self_CDI2_Negativemood and Somatic Sympoms_Tscore, self_CDI2_NegativeSelfEsteem_Tscore, self_CDI2_FuncionalProblems_Tscore, self_-CDI2_Inefficency_Tscore, self_CDI2_InterpersonalProblems_Tscore) were indicated as continuous variables. Clustering was performed by the age of the occurrence of the stress episode. Patients with missing information on the anxiety/OCD and depressive symptoms were excluded from the PCA analysis (see Table S13).

QUANTIFICATION AND STATISTICAL ANALYSIS

For behavioral experiments, all litters of stressed animals were normalized to all age-specific controls represented in Figure 3, except where otherwise indicated. For each experiment, when we indicate in figure legends the number of independent experiments run, we refer to the number of different cohorts of animals that we assessed, whose data were combined for the analysis of the effect induced by each single stressor at each specific developmental window. Animals stressed with different stressors were never averaged together. The results were presented as the means ± standard error of the mean (SEM). The statistical analysis was performed using GraphPad (Prism) software, except where otherwise indicated. The statistical significance was evaluated using two-way ANOVA followed by Tukey's *post hoc* test (when comparing every mean with every other mean or when comparing every mean for each stress age against their own controls), Dunnett's *post hoc* test (when comparing all four ages of stress against their own controls) or Šídák's *post hoc* test (for MS, when comparing 2 ages of stress). Since maternal separation was not performed in all selected developmental time windows, this stressor had to be excluded from the comparative analysis among all ages and all types of stress assessed through two-way ANOVA in Figures 1B–1G, S3A–S3L, S4A–S4I, S4K, and S5B. Repeated measure ANOVA analysis followed by Dunnett's multiple comparison test was performed for comparing the percentage of correct trials among different stressors at the same age during 9 days of Phenopy test. p-values <0.05 were considered significant. For comparisons in corticosterone levels and in the tube dominance test (two groups only), we performed unpaired parametric t test (normal data distribution) or Mann-Whitney (non-normal data distribution) tests with Welch's correction in case of non-equal SDs. The normality of the data was assessed with the Shapiro-Wilk normality test, with 95% confidence. For comparisons among subjects in the pediatric cohort, we performed a chi-square test. For all statistical analysis, outliers were excluded only from the final pool of data by a Grubb's test ($\alpha = 0.05$).

Cell Reports Medicine, Volume *7*

Supplemental information

Traumatic life experiences during critical periods lead to diverse developmental trajectories

Giovanni Morelli, Greta Visintin, Elisa Gelli, Angelo Serani, Martina Bartolucci, Sara Uccella, Maria D'Apruzzo, Deborah Preiti, Mariam Marie Chellali, Alessandra Cucinelli, Mohit Rastogi, Matteo Falappa, Andrea Scalabrini, Gustavo Turecki, Andrea Petretto, Valter Tucci, and Laura Cancedda

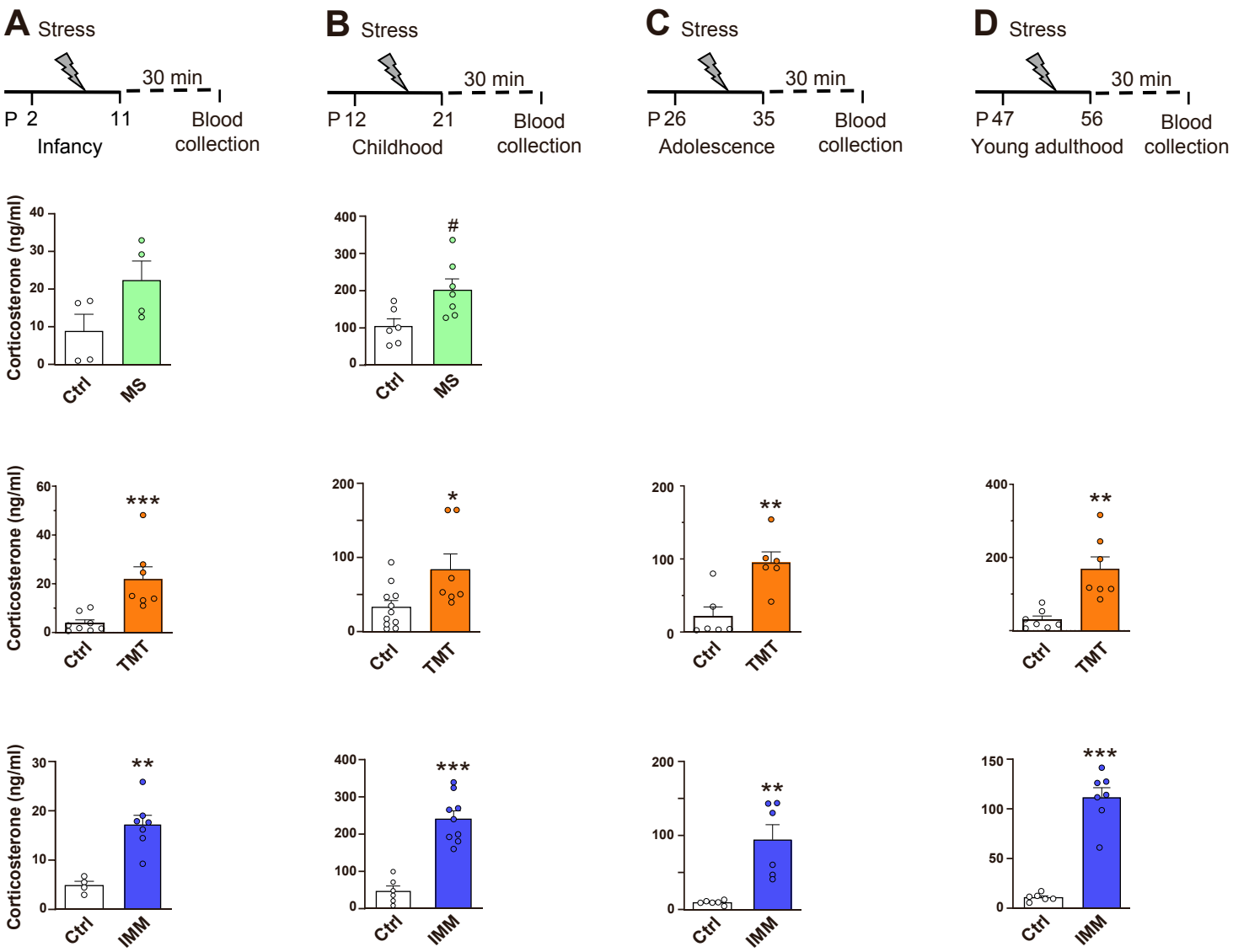
A Stress
30 min
P 2
11
Infancy
Blood collection
B Stress
30 min
P 12
21
Childhood
Blood collection
C Stress
30 min
P 26
35
Adolescence
Blood collection
D Stress
30 min
P 47
56
Young adulthood
Blood collection
Corticosterone (ng/ml)
Ctrl
MS
TMT
IMM
#
*
**
***

Figure S1. Stress paradigms performed at diverse ages in mice increase serum corticosterone levels. Related to Figure 1.

(A-D) *Top*. Schematic cartoon of the experimental protocol of serum collection for assessing corticosterone levels in mice exposed to our diverse stress paradigms at the indicated ages and age-matched naïve controls. *Bottom*. Concentration of mouse serum corticosterone collected after 10 days of maternal separation (MS), predator odor exposure (TMT), or underwater immersion (IMM) and in their age-matched naïve control mice at the end of each experimental protocol indicated by the cartoon on top. Bars indicate the average concentration of serum corticosterone + SEM, dots indicate values for each individual animal. Data derived from 1 experiment for a total of 4-9 animals per experimental group (MS *vs* controls: Two-sided Mann-Whitney U test (P2-11) or unpaired t test (P12-21); TMT *vs* controls: Two-sided Mann-Whitney U test, or unpaired t test with Welch's correction (P47-56); IMM *vs* controls: Unpaired t test or unpaired t test with Welch's correction (P26-35)). #$p<0.05$; *$p<0.05$, **$p<0.01$, ***$p<0.001$). The same data represented as percentage over controls are presented in Figure 1G for clearer comparison across ages.

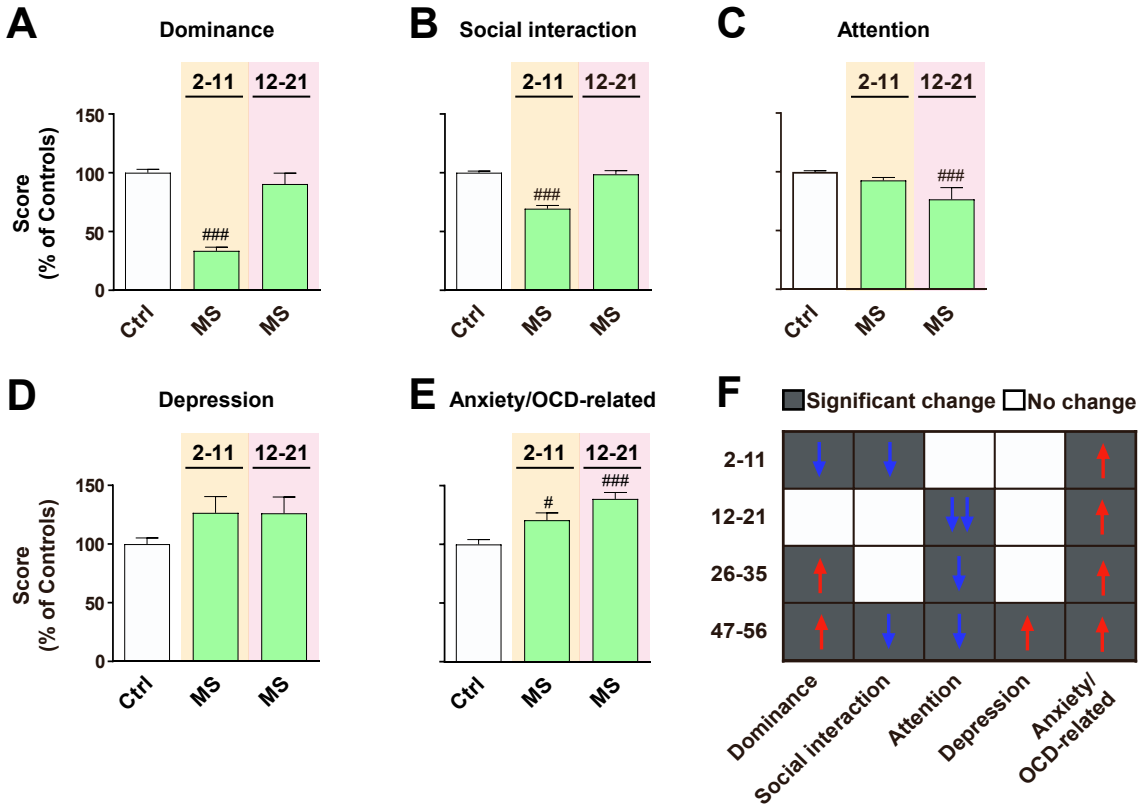
A
Dominance
2-11
12-21
Score
(% of Controls)
150
100
50
0
###
Ctrl
MS
MS
B
Social interaction
2-11
12-21
###
Ctrl
MS
MS
C
Attention
2-11
12-21
###
Ctrl
MS
MS
D
Depression
2-11
12-21
Score
(% of Controls)
150
100
50
0
Ctrl
MS
MS
E
Anxiety/OCD-related
2-11
12-21
#
###
Ctrl
MS
MS
F
Significant change
No change
2-11
12-21
26-35
47-56
Dominance
Social interaction
Attention
Depression
Anxiety/
OCD-related

Figure S2. The timing of maternal separation determines the presence of specific neuropsychiatric-like traits in adult mice, and behavioral scores in general reflect dependency on the timing of trauma exposure. Related to Figure 1.

(**A-E**) Average percentage (+ SEM) of the dominance (A), social interaction (B), attention (C), depression (D) and anxiety/OCD (E) scores of adult animals exposed to 15 minutes of MS at the indicated ages and age-matched controls. The percentages were calculated on the scores created based on the experiments on the tube dominance (dominance), three-chamber test (social interaction), Phenopy (attention), tail suspension and forced swim tests (depression), marble burying, grooming, open field, and dark/light tests (anxiety/OCD), presented in Figure S3A-S3L. Data derived from at least 2 independent experiments for a total of 12-13 animals per experimental group. Exclusively for attention, data derived from 1 or 2 experiments for a total of 6-9 animals per experimental group. Each score is represented as percentage over controls (each age is normalized to its own control) for clearer comparison across ages (Two-way ANOVA, (A) $F_{stress(1,67)}=48.84$, $p<0.0001$; (B) $F_{stress(1,67)}=41.56$, $p<0.0001$; (C) $F_{stress(1,46)}=14.15$, $p=0.0005$; (D) $F_{stress(1,66)}=6.778$, $p=0.0114$; (E) $F_{stress(1,67)}=21.23$, $p<0.0001$, followed by Šidák's multiple comparisons test). #$p<0.05$, ###$p<0.001$. These data are also represented in Figure 1B-1F for comparison across types of stress. (**F**) Heatmap showing significant changes (gray; increase and decrease, red and blue arrows, respectively), and no-changes (white) in the behavioral scores (dominance, social interaction, attention, depression, and anxiety/OCD) of adult mice previously exposed to MS, TMT or IMM at the indicated ages compared to their age-related controls, as in Figure 1B-1F.

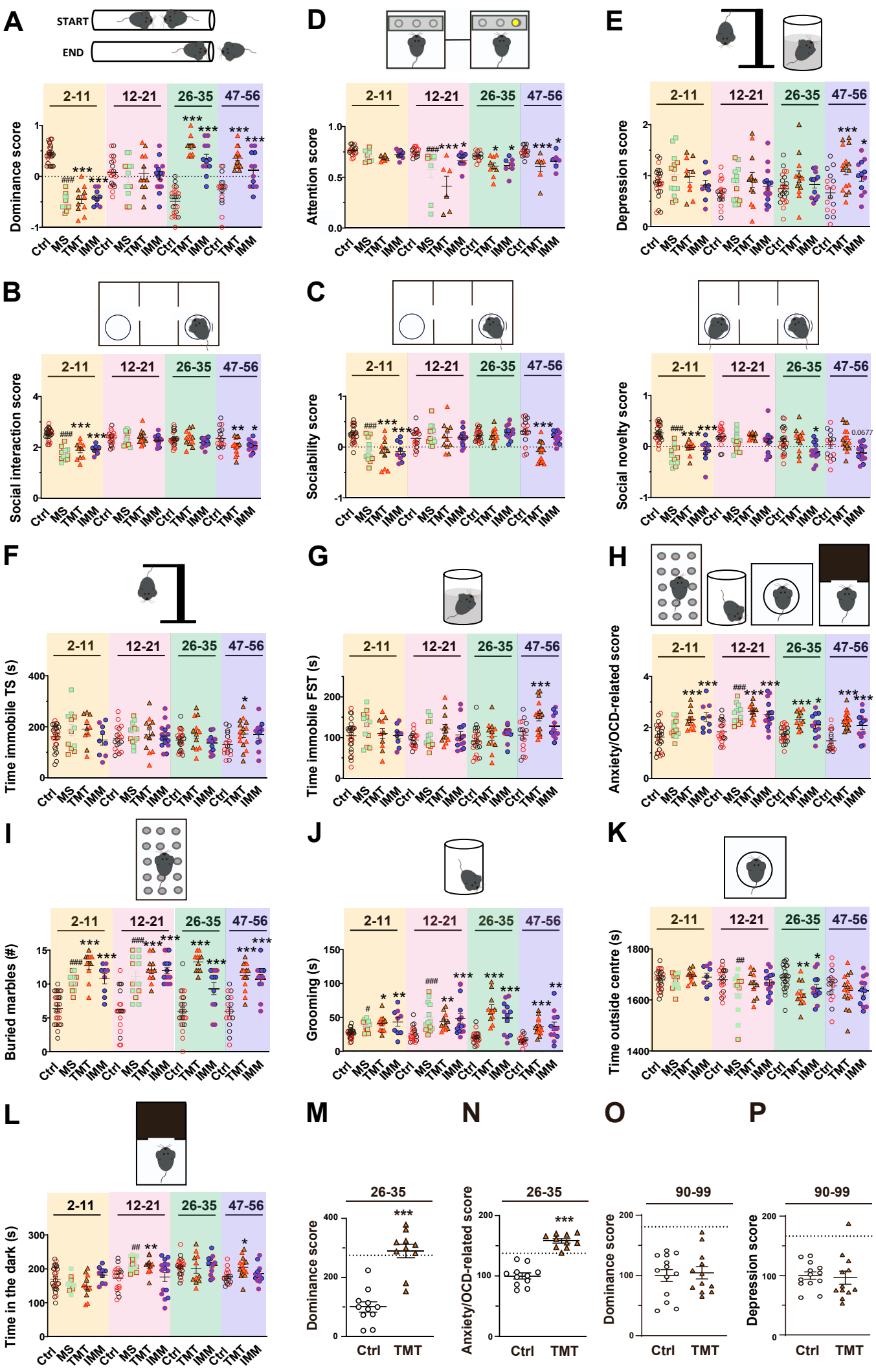
A
START
END
Dominance score
2-11
12-21
26-35
47-56
Ctrl
MS
TMT
IMM
D
Attention score
E
Depression score
B
Social interaction score
C
Sociability score
Social novelty score
0.0677
F
Time immobile TS (s)
G
Time immobile FST (s)
H
Anxiety/OCD-related score
I
Buried marbles (#)
J
Grooming (s)
K
Time outside centre (s)
L
Time in the dark (s)
M
N
O
P
90-99

Figure S3. The timing of trauma determines the presence of specific neuropsychiatric-like traits that are maintained over time in adult mice. Related to Figure 1 and Tables S1-S3.

(**A**-**E**) *Top*. Schematic representation of the tube dominance (A), three-chamber (B,C), Phenopy (D), tail suspension and forced swim tests (E) for dominance, social interaction, attention, and depression assessment, respectively. *Bottom.* Dominance (A), social interaction (B), sociability and social novelty (C), attention (D) and depression (E) scores of adult mice previously exposed to MS, TMT or IMM at the indicated ages and their age-related controls (represented in Figure 1B-1E and S2A-S2D). Central horizontal lines indicate the average score of all analyzed animals ± SEM. ((A) MS *vs* controls: two-way ANOVA, $F_{stress(1,67)}$=72.27, p<0.0001, followed by Šidák's multiple comparisons test; TMT and IMM *vs* controls: two-way ANOVA, $F_{stress(2,171)}$=8.045, p=0.0005, followed by Dunnett's multiple comparisons test; (B) MS *vs* controls: two-way ANOVA, $F_{stress(1,67)}$=44.31, p<0.0001, followed by Šidák's multiple comparisons test; TMT and IMM *vs* controls: two-way ANOVA, $F_{stress(2,169)}$=19.51, p<0.0001, followed by Dunnett's multiple comparisons test. (C) Sociability: MS *vs* controls: two-way ANOVA, $F_{stress(1,67)}$=8.581, p=0.0046, followed by Šidák's multiple comparisons test; TMT and IMM *vs* controls: two-way ANOVA, $F_{stress(2,172)}$=16.15, p<0.0001, followed by Dunnett's multiple comparisons test. Social Novelty: MS *vs* controls: two-way ANOVA, $F_{stress(1,67)}$=41.62, p<0.0001, followed by Šidák's multiple comparisons test; TMT and IMM *vs* controls: two-way ANOVA, $F_{stress(2,170)}$=15.40, p<0.0001, followed by Dunnett's multiple comparisons test. (D) MS *vs* controls: two-way ANOVA, $F_{stress(1,46)}$=14.23, p=0.0005, followed by Šidák's multiple comparisons test; TMT and IMM *vs* controls: two-way ANOVA, $F_{stress(2,107)}$=40.17, p<0.0001, followed by Dunnett's multiple comparisons test. (E) MS *vs* controls: two-way ANOVA, $F_{stress(1,68)}$=5.23, p=0.0253, followed by Šidák's multiple comparisons test; TMT and IMM *vs* controls: two-way ANOVA, $F_{stress(2,170)}$=9.14, p=0.0002, followed by Dunnett's multiple comparisons test). (**F, G**) *Top.* Schematic representation of the tail suspension (F) and forced swim (G) tests for depression assessment in E. *Bottom.* Time spent immobile in the tail suspension (TS; F) and forced swim tests (FST; G) by adult mice previously exposed to MS, TMT or IMM at the indicated ages and their age-related controls represented in E. Central horizontal lines indicate the average time spent immobile by all analyzed animals ± SEM ((F) MS *vs* controls: two-way ANOVA, $F_{stress(1,66)}$=3.286, p=0.0744, followed by Šidák's multiple comparisons test; TMT and IMM *vs* controls: two-way ANOVA, $F_{stress(2,170)}$=4.631, p=0.011, followed by Dunnett's multiple comparisons test. (G) MS *vs* controls: two-way ANOVA, $F_{stress(1,66)}$=4.239, p=0.0435, followed by Šidák's multiple comparisons test; TMT and IMM *vs* controls: two-way ANOVA, $F_{stress(2,170)}$=7.26, p=0.0009, followed by Dunnett's multiple comparisons test). (**H**) *Top.* Schematic representation of the marble burying, grooming, open field, and dark/light tests for anxiety/OCD assessment. *Bottom.* Anxiety/OCD-related score of adult mice previously exposed to MS, TMT or IMM at the indicated ages and their age-related controls represented in Figures 1F and S2E. Central horizontal lines indicate the average anxiety/OCD score of all analyzed animals ± SEM (MS *vs* controls: two-way ANOVA, $F_{stress(1,67)}$=22.82, p<0.0001, followed by Šidák's multiple comparisons test; TMT and IMM *vs* controls: two-way ANOVA, $F_{stress(2,170)}$=54.36, p<0.0001, followed by Dunnett's multiple comparisons test). (**I**-**L**) *Top.* Schematic representation of the marble burying (I), grooming (J), open field (K) and dark/light (L) tests for anxiety/OCD assessment in H. *Bottom.* Number of buried marbles (I), time spent grooming (J), time spent outside the center (K) and time spent in the dark compartment (L) by adult mice previously exposed to MS, TMT or IMM at the indicated ages and their age-related controls represented in H. Central horizonal lines indicate the average numbers by all analyzed animals ± SEM. ((I) MS *vs* controls: two-way ANOVA, $F_{stress(1,67)}$=50.02, p<0.0001, followed by Šidák's multiple comparisons test; TMT and IMM *vs* controls: two-way ANOVA, $F_{stress(2,170)}$=118.7, p<0.0001, followed by Dunnett's multiple comparisons test. (J) MS *vs* controls: two-way ANOVA, $F_{stress(1,67)}$=37.3, p<0.0001, followed by Šidák's multiple comparisons test; TMT and IMM *vs* controls: two-way ANOVA, $F_{stress(2,170)}$=49.80, p<0.0001, followed by Dunnett's multiple comparisons test. (K) MS *vs* controls: two-way ANOVA, $F_{interaction(1,67)}$=13.10, p=0.0006, followed by Šidák's multiple comparisons test; TMT and IMM *vs* controls: two-way ANOVA, $F_{interaction(6,170)}$=3.103, p=0.0066, followed by Dunnett's multiple comparisons test. (L) MS *vs* controls: two-way ANOVA, $F_{stress(1,67)}$=6.174, p=0.0155, followed by Šidák's multiple comparisons test; TMT and IMM *vs* controls: two-way ANOVA, $F_{stress(2,170)}$=3.115, p=0.0469, followed by Dunnett's multiple comparisons test). For all panels, symbols represent the single data points for each animal; black/gray and red symbol lines represent males and females, respectively. For A-C,E-L, data derived from at least 2 independent experiments for a total of 9-16 animals per experimental group. Exclusively for D, data derived from 1 or 2 experiments for a total of 6-9 animals per experimental group. #p<0.05, ##p<0.01, ###p<0.001; *p<0.05, **p<0.01, ***p <0.001. (**M,N)** Average percentage of the dominance and anxiety/OCD scores ± SEM in mice exposed to TMT during adolescence (P26-35) and behaviorally tested 105 days after (P140). The percentages were calculated based on the scores created on the experiments on the tube dominance (dominance), marble burying, grooming, open field, and dark/light tests (anxiety/OCD) reported in Table S3. Each score is represented as percentage over controls (normalized to its own control). Tests were analyzed with unpaired t-test with Welch's correction, ***p<0.001. Data derived from 1 experiment included 10-11 animals per group. Dotted lines represent mean values of mice exposed to

TMT during adolescence and behaviorally tested starting at P90 (Figure 1B,1F), following our standard protocol, and reported for direct comparison. (**O,P**) Average percentage of the dominance and depressive-like scores ± SEM in mice exposed to TMT during full adulthood (P90-99) and behaviorally tested 4 weeks after (P130). The percentages were calculated based on the scores created on the experiments on the tube dominance (dominance), forced swim and tail suspension tests, as reported in Table S3. Each score is represented as percentage over controls (normalized to its own control). Tests were analyzed with unpaired t-test with Welch's correction. Data derived from 1 experiment included 12-13 animals per group. Dotted lines represent mean values of mice exposed to TMT during young adulthood and behaviorally tested at P90 (Figure 1B,1E), following our standard protocol, and reported for direct comparison.

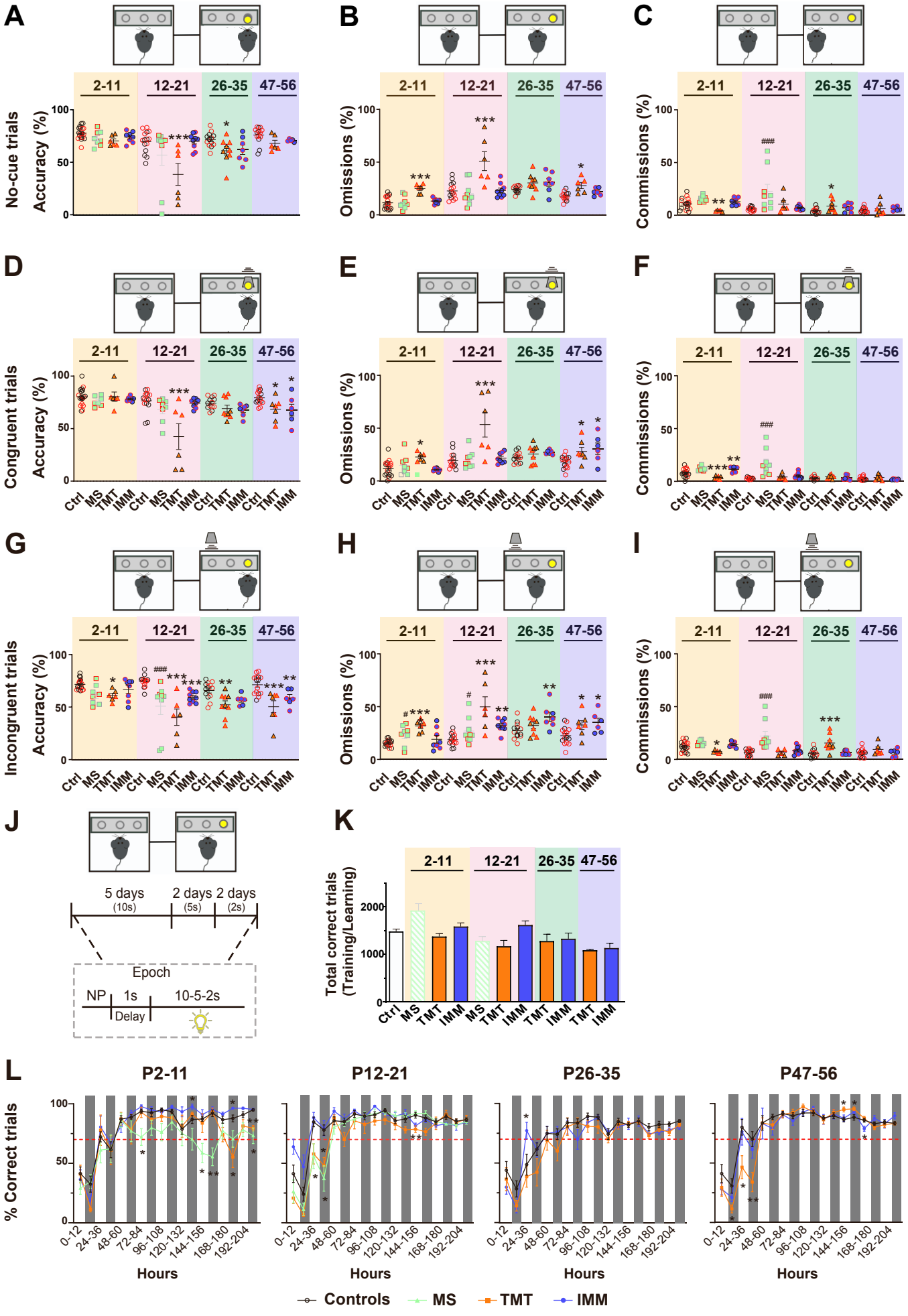
A
B
C
D
E
F
G
H
I
J
K
L
No-cue trials
Congruent trials
Incongruent trials
Accuracy (%)
Omissions (%)
Commissions (%)
2-11
12-21
26-35
47-56
Ctrl
MS
TMT
IMM
5 days
(10s)
2 days
(5s)
2 days
(2s)
Epoch
NP
1s
Delay
10-5-2s
Total correct trials
(Training/Learning)
% Correct trials
P2-11
P12-21
P26-35
P47-56
0-12
24-36
48-60
72-84
96-108
120-132
144-156
168-180
192-204
Hours
Controls
MS
TMT
IMM

Figure S4. The timing of trauma exposure impacts on the performance and on the learning velocity, but not on the learning efficacy in the Phenopy test for attention assessment. Related to Figure 1 and Table S2.

(**A-I**) *Top.* Schematic representation of nose-poke choices in no-cue (A-C), congruent (D-F), and incongruent (G-I) trials in the Phenopy test. *Bottom*. Average percentage (± SEM) of correct nose-poke choices (accuracy), no nose-poke choices (omissions), wrong nose-poke choices (commissions), during the Phenopy test of animals exposed to MS, TMT or IMM at the indicated ages and their age-related controls represented in Figures 1D, S2C and S3D. Data were derived from 1 or 2 experiments for a total of 6-9 animals per group. (MS *vs* controls: two-way ANOVA, (A) $F_{stress(1,46)}$=4.417, p=0.0411, (B) $F_{stress(1,46)}$=0.2503, p=0.6192, (C) $F_{stress(1,44)}$=15.27, p=0.0003, (D) $F_{stress(1,44)}$=5.122, p=0.0286, (E) $F_{stress(1,46)}$=0.7303, p=0.3972, (F) $F_{stress(1,42)}$=23.6, p<0.0001, (G) $F_{stress(1,46)}$=24.34, p<0.0001, (H) $F_{stress(1,45)}$=12.62, p=0.0009, (I) $F_{stress(1,46)}$=23.84, p<0.0001, followed by Šidák's multiple comparisons test; TMT and IMM *vs* controls: two-way ANOVA, (A) $F_{stress(2,104)}$=19.6, p<0.0001, (B) $F_{stress(2,103)}$=32.24, p<0.0001, (C) $F_{interaction(6,102)}$ =3.866, p=0.00016, (D) $F_{stress(2,105)}$=13.97, p<0.0001, (E) $F_{stress(2,104)}$=22.9, p<0.0001, (F) $F_{stress(2,102)}$=3.422, p=0.0364, (G) $F_{stress(2,106)}$=47.82, p<0.0001, (H) $F_{stress(2,106)}$=31.53, p<0.0001, (I) $F_{interaction(6,104)}$=6.544, p<0.0001, followed by Dunnett's multiple comparisons test). #p<0.05, ###p<0.001; *p<0.05, **p<0.01, ***p<0.001. For all panels, black/gray and red symbol lines represent males and females, respectively. **(J)** Schematic representation of the Phenopy training-phase with 5 days of 10 second (s) trial duration, followed by 2 days of 5s trial duration and 2 days of 2s trial duration. *Inset*. In all phases, upon nose-poke (NP) activation, there is 1s of delay before the trial starts. (**K**) Average (+ SEM) total correct trials performed during the Phenopy training-phase by adult mice previously exposed to MS, TMT or IMM at the indicated ages, and their age-related controls represented in Figures 1D, S2C, S3D and S4A-S4I. Data were derived from 1 or 2 experiments for a total 6-9 animals per experimental group (MS *vs* controls: two-way ANOVA, $F_{stress(1,46)}$=0.4625, p=0.4999, followed by Šidák's multiple comparisons test; TMT and IMM *vs* controls: two-way ANOVA, $F_{stress(2,107)}$=4.888, p=0.0093, followed by Dunnett's multiple comparisons test). (**L**) Average percentage (± SEM) of correct trials during the Phenopy test performed by adult mice previously exposed to MS, TMT or IMM and their age-related controls as in B. The grey shadow indicates the 12 hours of dark, the white indicates the 12 hours of light, and the dotted red line indicates the 70% of correct trials (learning threshold). Data were derived from 1 or 2 experiments for a total of 6-9 animals per experimental group (Mixed-effects analysis following Dunnett's multiple comparison (P2-11) $F_{stress(3,36)}$=8.247, p=0.0003; (P12-21) $F_{stress(2.785,350.8)}$=24.37, p<0.0001; (P26-35); $F_{timexstress(34,442)}$=1.703, p=0.0094; (P47-56) $F_{timexstress(34,425)}$=2.669, p<0.001). *p<0.05, **p<0.01).

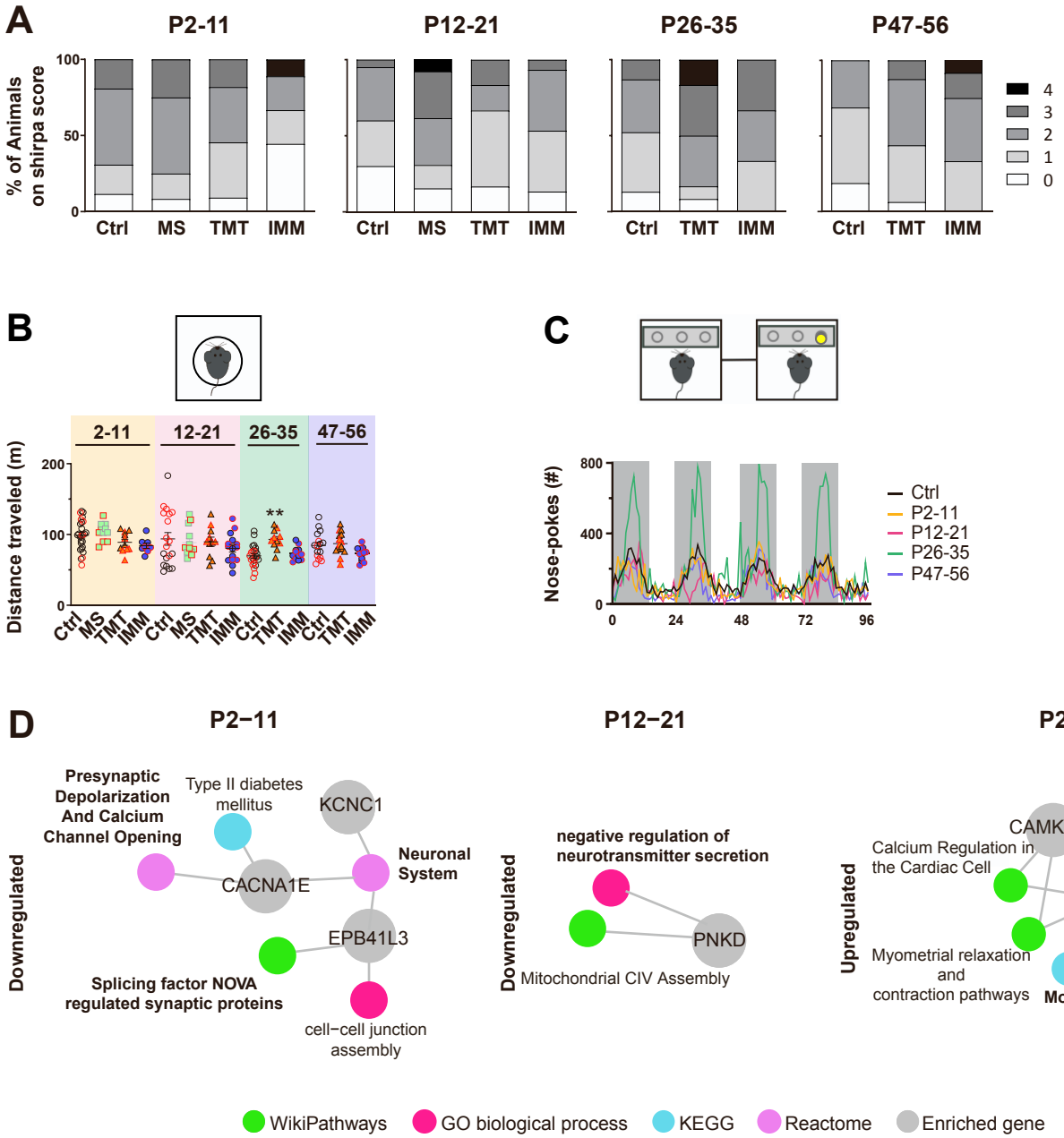
A
P2-11
P12-21
P26-35
P47-56
% of Animals on shirpa score
100
50
0
Ctrl
MS
TMT
IMM
4
3
2
1
0
B
Distance traveled (m)
200
100
0
2-11
12-21
26-35
47-56
**
C
Nose-pokes (#)
800
400
0
0
24
48
72
96
Ctrl
P2-11
P12-21
P26-35
P47-56
D
P2−11
P12−21
P26−35
Downregulated
Presynaptic Depolarization And Calcium Channel Opening
Type II diabetes mellitus
KCNC1
Neuronal System
CACNA1E
EPB41L3
Splicing factor NOVA regulated synaptic proteins
cell−cell junction assembly
Downregulated
negative regulation of neurotransmitter secretion
PNKD
Mitochondrial CIV Assembly
Upregulated
CAMK2G
Calcium Regulation in the Cardiac Cell
Circadian entrainment
GNB2
GABAergic synapse
GABRA5
Myometrial relaxation and contraction pathways
Morphine addiction
WikiPathways
GO biological process
KEGG
Reactome
Enriched gene

Figure S5. Trauma does not affect general health across ages of exposure, but trauma during adolescence specifically impacts adult motor activity, and trauma timing determines the dysregulation of specific biological pathways in adult animals. Related to Figures 1,2 and Table S4.

(**A**) Percentage of all animals with no abnormality and 1, 2 or 3 abnormalities (color-coded on the right) out of 25 analyzed parameters in the SHIRPA test among adult mice previously exposed to MS, TMT or IMM at the indicated ages, and their age-related controls. Data were derived from the same animals utilized for the experiments detailed in Figures 1B,1C,1E,1F,S2A,S2B,S2D,S2E and S3A-S3C,S3E-S3L; at least 2 independent experiments for a total of 9-16 animals per experimental group. (**B**) Average (±SEM) total distance traveled in the open field test by adult mice exposed to MS, TMT or IMM at the indicated ages represented in Figure S3K. Data were derived from at least 2 independent experiments for a total of 9-16 animals per experimental group. (MS *vs* controls: two-way ANOVA, $F_{stress}(1,66)=4.409$, p=0.08301, followed by Šidák's multiple comparisons test; TMT and IMM *vs* controls: two-way ANOVA, $F_{stress}(2,168)=4.409$, p=0.0136, followed by Dunnett's multiple comparisons test). **p<0.01. Black/gray and red symbol lines represent males and females, respectively. (**C**) Average nose-poke activity during the Phenopy training-phase (4 consecutive days starting from the 2nd day of training) of adult mice previously exposed to TMT at the indicated ages represented in Figures 1D, S2C, S3D, and S4. The grey shadow indicates the 12 hours of dark, the white indicates the 12 hours of light. Data were derived from 1 or 2 experiments for a total 6-9 animals per experimental group. (**D**) Network plot by diverse databases (*bottom*) showing pathway-enrichment analysis on the proteins specifically deregulated (up or down) in adult animals exposed to stress at each reported age taken from bold, color-coded backgrounds of Figure 3A. Bold highlights pathways of special interest.

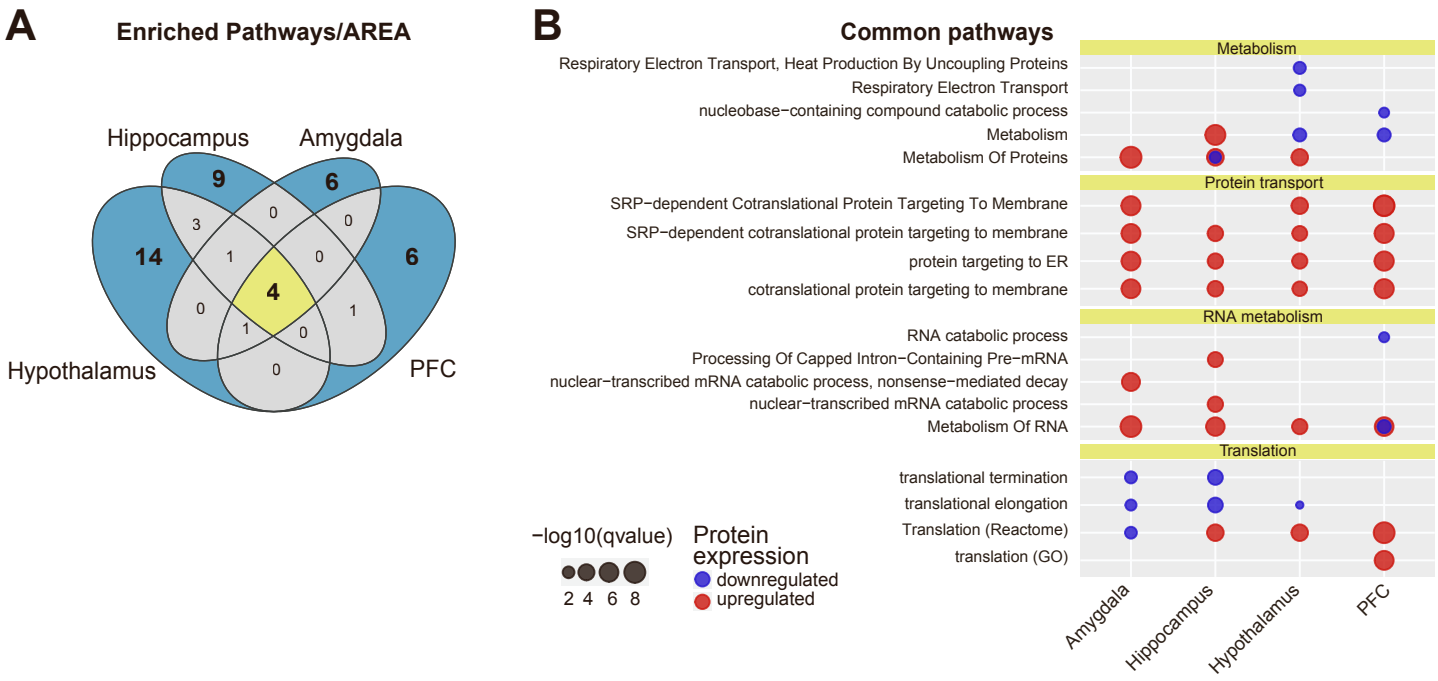
A
Enriched Pathways/AREA
Hippocampus
Amygdala
Hypothalamus
PFC
9
6
14
6
4
3
0
0
1
0
0
1
1
0
0
B
Common pathways
Respiratory Electron Transport, Heat Production By Uncoupling Proteins
Respiratory Electron Transport
nucleobase−containing compound catabolic process
Metabolism
Metabolism Of Proteins
SRP−dependent Cotranslational Protein Targeting To Membrane
SRP−dependent cotranslational protein targeting to membrane
protein targeting to ER
cotranslational protein targeting to membrane
RNA catabolic process
Processing Of Capped Intron−Containing Pre−mRNA
nuclear−transcribed mRNA catabolic process, nonsense−mediated decay
nuclear−transcribed mRNA catabolic process
Metabolism Of RNA
translational termination
translational elongation
Translation (Reactome)
translation (GO)
Metabolism
Protein transport
RNA metabolism
Translation
Amygdala
Hippocampus
Hypothalamus
PFC
−log10(qvalue)
2 4 6 8
Protein expression
downregulated
upregulated

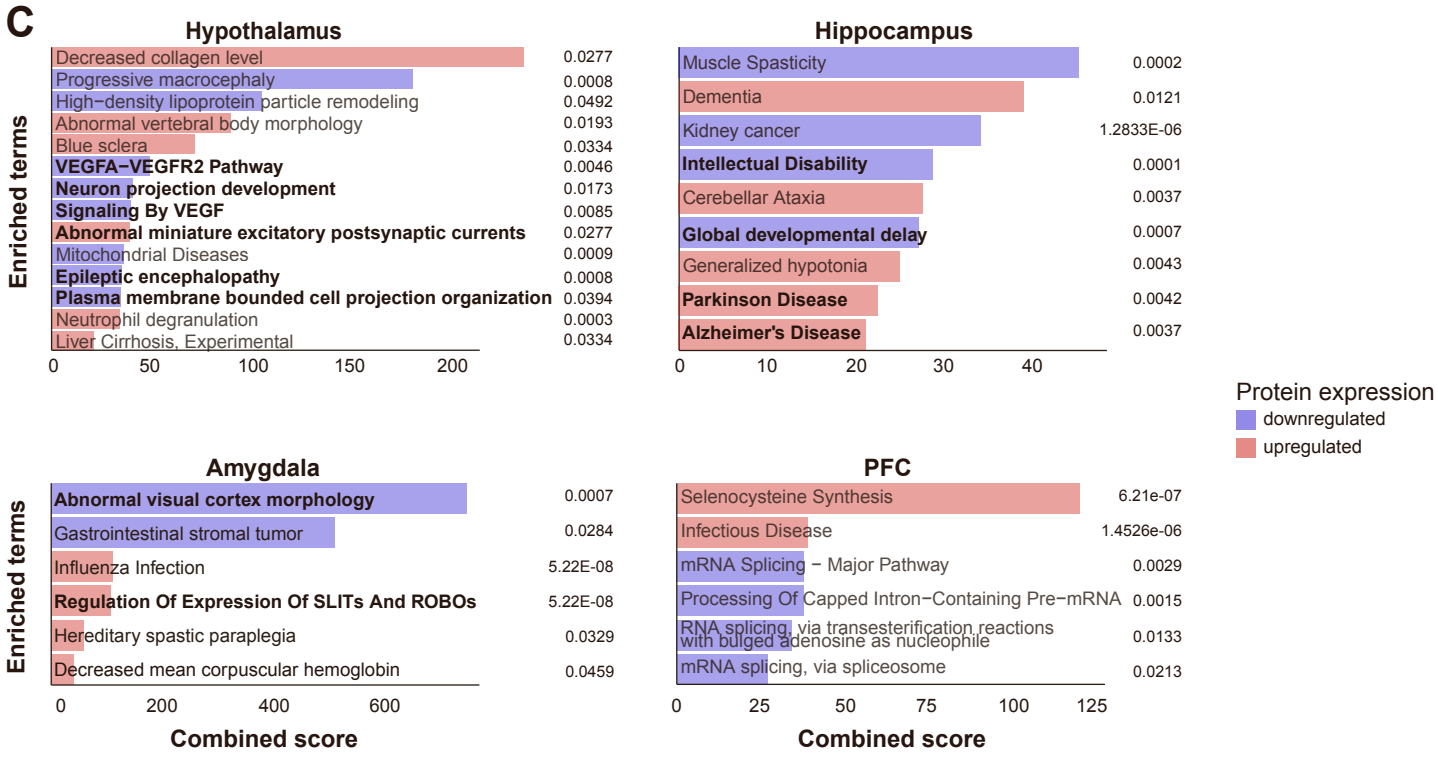
C
Hypothalamus
Enriched terms
Decreased collagen level 0.0277
Progressive macrocephaly 0.0008
High−density lipoprotein particle remodeling 0.0492
Abnormal vertebral body morphology 0.0193
Blue sclera 0.0334
VEGFA−VEGFR2 Pathway 0.0046
Neuron projection development 0.0173
Signaling By VEGF 0.0085
Abnormal miniature excitatory postsynaptic currents 0.0277
Mitochondrial Diseases 0.0009
Epileptic encephalopathy 0.0008
Plasma membrane bounded cell projection organization 0.0394
Neutrophil degranulation 0.0003
Liver Cirrhosis, Experimental 0.0334
0 50 100 150 200
Hippocampus
Muscle Spasticity 0.0002
Dementia 0.0121
Kidney cancer 1.2833E-06
Intellectual Disability 0.0001
Cerebellar Ataxia 0.0037
Global developmental delay 0.0007
Generalized hypotonia 0.0043
Parkinson Disease 0.0042
Alzheimer's Disease 0.0037
0 10 20 30 40
Protein expression
downregulated
upregulated
Amygdala
Enriched terms
Abnormal visual cortex morphology 0.0007
Gastrointestinal stromal tumor 0.0284
Influenza Infection 5.22E-08
Regulation Of Expression Of SLITs And ROBOs 5.22E-08
Hereditary spastic paraplegia 0.0329
Decreased mean corpuscular hemoglobin 0.0459
0 200 400 600
Combined score
PFC
Selenocysteine Synthesis 6.21e-07
Infectious Disease 1.4526e-06
mRNA Splicing − Major Pathway 0.0029
Processing Of Capped Intron−Containing Pre−mRNA 0.0015
RNA splicing, via transesterification reactions with bulged adenosine as nucleophile 0.0133
mRNA splicing, via spliceosome 0.0213
0 25 50 75 100 125
Combined score

Figure S6. Trauma exposure impacts on adult metabolism and other general processes in all brain areas, regardless of the age of occurrence. Related to Figure 2 and Table S5.

(**A**) Venn diagram showing commonly (gray and yellow) and brain area-specific (blue) enriched pathways (Bonferroni adjusted p-value, *p.adj*., <0.05 and log2FC<-0.3 or >0.3) in each brain areas in all groups of stress age analyzed in proteomic experiments from Figure 2 performed on adult animals stressed at diverse ages with TMT. Bold numbers in blue background represent brain-specific enriched pathways; bold number in yellow background represents pathways enriched in all four analyzed brain areas. (**B**) Bubbleplot highlighting biological pathways enriched (q-value<0.05) in all the brain areas as in A (yellow background), upon interrogation of EnrichR-KG geneset libraries (GO biological process, Reactome, MGI mammalian phenotype, DisGenEt, Jensen Disease). Red and blue dots indicate up- and downregulated processes, respectively. The magnitude of the bubble is correlated to q-value (scalebar on the bottom left). (**C**) EnrichR-KG pathway-enrichment analysis of specific up- and downregulated (pink and purple, respectively) proteins for each brain area as in A (blue background). q-value<0.05 was set as threshold, and the specific values for each term are indicated on the right of each bar. Bold highlights pathways of special interest.

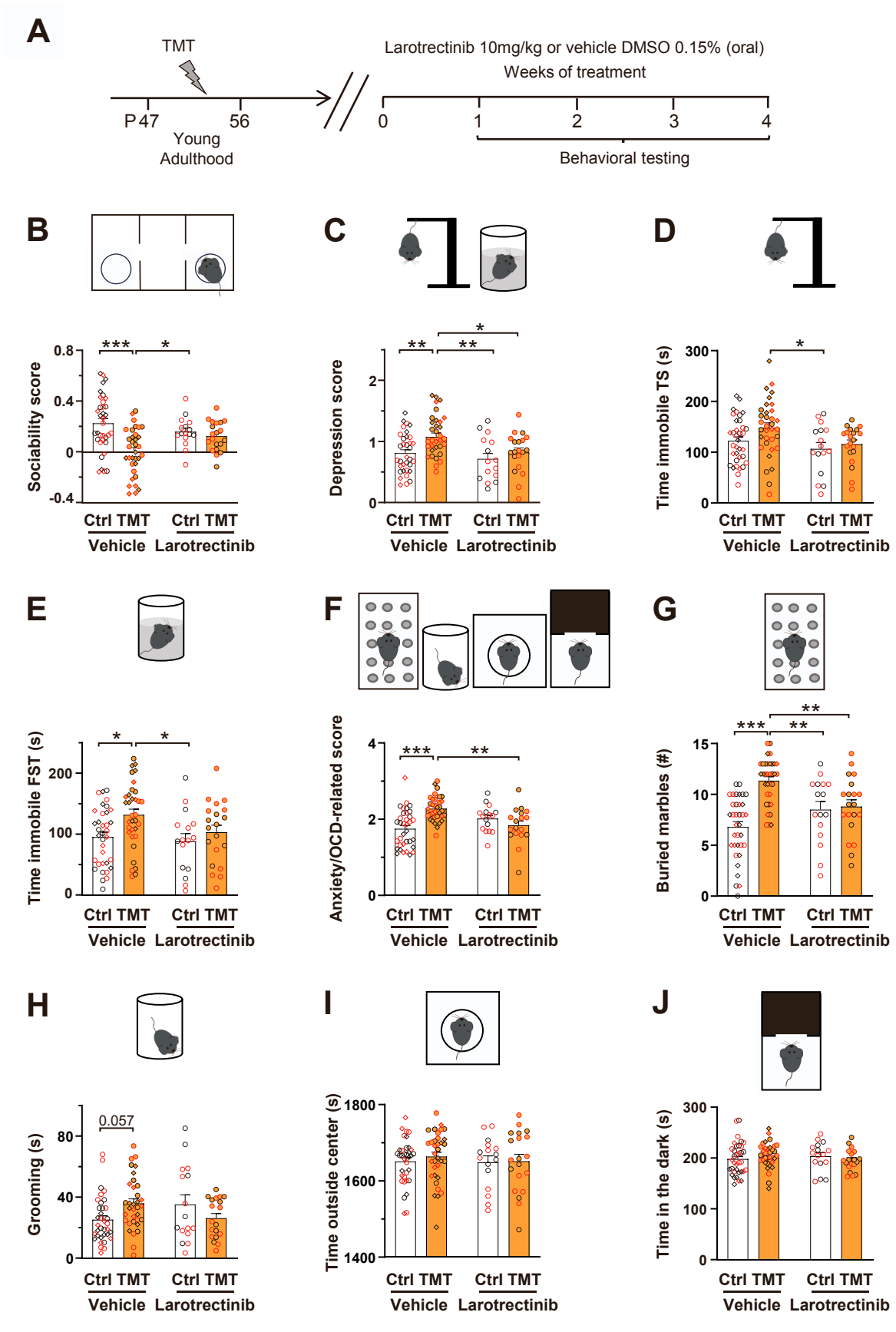
A
TMT
P 47
56
Young
Adulthood
Larotrectinib 10mg/kg or vehicle DMSO 0.15% (oral)
Weeks of treatment
0
1
2
3
4
Behavioral testing
B
Sociability score
0.8
0.4
0
-0.4
***
*
C
Depression score
2
1
0
**
**
*
D
Time immobile TS (s)
300
200
100
0
*
E
Time immobile FST (s)
200
100
0
*
*
F
Anxiety/OCD-related score
4
2
0
***
**
G
Buried marbles (#)
15
10
5
0
***
**
**
H
Grooming (s)
80
40
0
0.057
I
Time outside center (s)
1800
1600
1400
J
Time in the dark (s)
300
200
100
0
Ctrl TMT
Ctrl TMT
Vehicle
Larotrectinib

Figure S7. Treatment with the FDA-approved drug larotrectinib rescues behavioral abnormalities in adult mice exposed to predator odor during young adulthood. Related to Figure 3.

(**A**) Schematic cartoon of the experimental protocol for the treatment with the FDA-approved drug larotrectinib or vehicle of fully adult mice exposed to TMT during young adulthood and controls. (**B,C**) *Top*. Schematic representation of the three-chamber test (B), tail suspension and forced swim tests (C) for sociability and depression assessment, respectively. *Bottom.* Sociability (B) and depression (C) scores following larotrectinib or vehicle treatment in controls and adult mice exposed to TMT at P47-56 represented in Figure 3D. Bars indicate the average sociability and depression scores of all analyzed animals + SEM, and symbols represent the single data points for each animal; single data points in diamond shape represent data from the experiment in Figure S3C,S3F,S3G (Two-way ANOVA, (B) $F_{interaction(1,101)}$=6.533, p=0.0121, (C) $F_{stress(1,101)}$=6.217, p=0.0143, followed by Tukey's multiple comparisons test). (**D**,**E**) *Top*. Schematic representation of tests for depression assessment. *Bottom.* Time spent immobile in the tail suspension (TS; D) and forced swim (FST; E) tests following larotrectinib or vehicle treatment in controls and adult mice exposed to TMT at P47-56 represented in C. Bars indicate the average time spent immobile by all analyzed animals + SEM, and symbols represent the single data points for each animal; single data points in diamond shape represent data from the experiment in Figure S3F,S3G (Two-way ANOVA, (D) $F_{stress(1,100,)}$=6.71, p=0.011, (E) $F_{stress(1,101)}$=6.076, p=0.0154, followed by Tukey's multiple comparisons test). (**F**) *Top*. Schematic representation of the marble burying, grooming, open field, and dark/light tests for anxiety/OCD assessment. *Bottom*. Anxiety/OCD score following larotrectinib or vehicle treatment in controls and adult mice exposed to TMT at P47-56 represented in Figure 3D. Bars indicate the average anxiety/OCD score of all analyzed animals + SEM, and symbols represent the single data points for each animal; single data points in diamond shape represent data from the experiment in Figure S3I-S3L (two-way ANOVA, $F_{interaction(1,99)}$=16.10, p=0.0001, followed by Tukey's multiple comparisons test). (**G-J**) *Top*. Schematic representation of tests for anxiety/OCD assessment. *Bottom.* Number of buried marbles (G), time spent grooming (H), time spent outside the center in the open field test (I) and time spent in the dark compartment in the dark/light test (J) following larotrectinib or vehicle treatment in controls and adult mice exposed to TMT at P47-56 represented in F. Bars indicate the average numbers of all analyzed animals + SEM, and symbols represent the single data points for each animal; single data points in diamond shape represent data from the experiments in Figure S3I-S3L (Two-way ANOVA, (G) $F_{interaction(1,101)}$=13.42, p=0.0004, (H) $F_{interaction(1,100)}$=7.443, p=0.0075, (I) $F_{interaction(1,100)}$=1.725, p=0.1921, (J) $F_{interaction(1,101,)}$=0.1307, p=0.7184, followed by Tukey's multiple comparisons test). For all graphs, data were derived from 3 independent experiments for a total 16-20 animals per experimental group. *p<0.05, **p<0.01, ***p<0.001. For all panels, black/gray and red symbol lines represent males and females, respectively.

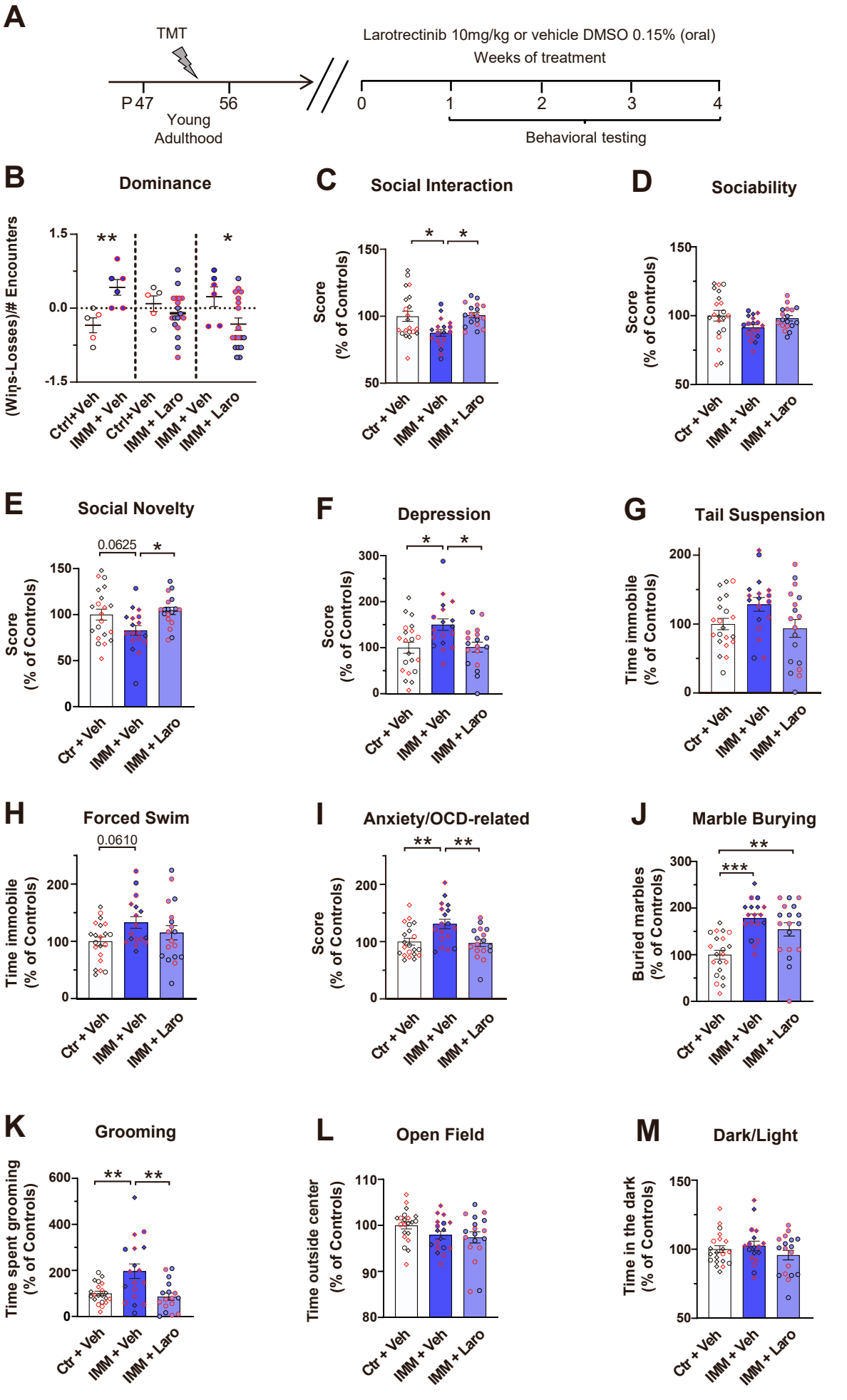
A
TMT
P 47
56
Young Adulthood
Larotrectinib 10mg/kg or vehicle DMSO 0.15% (oral)
Weeks of treatment
0
1
2
3
4
Behavioral testing
B
Dominance
(Wins-Losses)/# Encounters
Ctrl+Veh
IMM + Veh
Ctrl+Veh
IMM + Laro
IMM + Veh
IMM + Laro
C
Social Interaction
Score (% of Controls)
Ctr + Veh
IMM + Veh
IMM + Laro
D
Sociability
Score (% of Controls)
Ctr + Veh
IMM + Veh
IMM + Laro
E
Social Novelty
0.0625
Score (% of Controls)
Ctr + Veh
IMM + Veh
IMM + Laro
F
Depression
Score (% of Controls)
Ctr + Veh
IMM + Veh
IMM + Laro
G
Tail Suspension
Time immobile (% of Controls)
Ctr + Veh
IMM + Veh
IMM + Laro
H
Forced Swim
0.0610
Time immobile (% of Controls)
Ctr + Veh
IMM + Veh
IMM + Laro
I
Anxiety/OCD-related
Score (% of Controls)
Ctr + Veh
IMM + Veh
IMM + Laro
J
Marble Burying
Buried marbles (% of Controls)
Ctr + Veh
IMM + Veh
IMM + Laro
K
Grooming
Time spent grooming (% of Controls)
Ctr + Veh
IMM + Veh
IMM + Laro
L
Open Field
Time outside center (% of Controls)
Ctr + Veh
IMM + Veh
IMM + Laro
M
Dark/Light
Time in the dark (% of Controls)
Ctr + Veh
IMM + Veh
IMM + Laro

Figure S8. Treatment with the FDA-approved drug larotrectinib rescues specific behavioral abnormalities in adult mice exposed to underwater immersion during young adulthood. Related to Figure 3.

(**A**) Schematic cartoon of the experimental protocol for the treatment with the FDA-approved drug larotrectinib or vehicle of fully adult mice exposed to IMM during young adulthood and controls. (**B-F**) Dominance (B), social interaction (C), sociability (D), social novelty (E), and depression (F) scores following larotrectinib or vehicle treatment in controls and adult mice exposed to IMM at P47-56. Scores were based on the experiments on the tube dominance, on the three-chamber, on the tail suspension and forced swim tests. Bars indicate the average (percentage normalized to age-specific controls for social interaction, sociability, social novelty, and depression) scores of all analyzed animals + SEM, and symbols represent the single data points for each animal. For social interaction, sociability, social novelty, and depression scores single data points in diamond shape represent data from the experiment in Figure S3B,S3C,S3E ((B): Controls vehicle *vs* TMT vehicle & Controls vehicle *vs* TMT Larotrectinib: unpaired t-test; TMT vehicle *vs* TMT Larotrectinib: Mann-Whitney test. (C) One-way ANOVA $F_{(2,54)}$=5.852, p=0.0050, (D) $F_{(2,54)}$=2.399, p=0.1005, (E) $F_{(2,54)}$=4.321, p=0.0182, (F) $F_{(2,54)}$=5.666, p=0.0058 followed by Tukey's multiple comparisons test). (**G,H**) Percentage time spent immobile in the tail suspension (G) and forced swim tests (H) following larotrectinib or vehicle treatment in controls and adult mice exposed to IMM at P47-56. Bars indicate the average percentage of time spent immobile by all analyzed animals normalized to age-specific controls + SEM, and symbols represent the single data points for each animal; single data points in diamond shape represent data from the experiment in Figure S3F,S3G. (G) One-way ANOVA, $F_{(2,54)}$=3.076, p=0.0543, (H) $F_{(2,53)}$=2.702, p=0.0763, followed by Tukey's multiple comparisons test). (**I**) Anxiety/OCD score following larotrectinib or vehicle treatment in controls and adult mice exposed to IMM at P47-56. The score was based on the experiments on marble burying, grooming, open field, and dark/light tests. Bars indicate the average percentage normalized to age-specific controls for anxiety/OCD score of all analyzed animals + SEM, and symbols represent the single data points for each animal. Single data points in diamond shape represent data from the experiment in Figure S3H (One-way ANOVA, $F_{(2,53)}$=6.909, p=0.0022, followed by Tukey's multiple comparisons test). (**J-M**) Percentage of the number of buried marbles (J), time spent grooming (K), time spent outside the center (L) and time spent in the dark compartment (M) following larotrectinib or vehicle treatment in controls and adult mice exposed to IMM at P47-56. Bars indicate the average percentages of all analyzed animals normalized to age-specific controls + SEM, and symbols represent the single data points for each animal; single data points in diamond shape represent data from the experiment in Figure S3I-S3L. ((J) One-way ANOVA, $F_{(2,54)}$=13.43, p<0.0001, (K), $F_{(2,53)}$=8.408, p=0.0007, (L) $F_{(2,54)}$=2.192, p=0.1215, (M) $F_{(2,54)}$=1.159, p=0.3214, followed by Tukey's multiple comparisons test). For all graphs, data were derived from 2 independent experiments for a total 5-21 animals per experimental group. *p<0.05, **p<0.01, ***p<0.001. For all panels, black/gray and red symbol lines represent males and females, respectively.

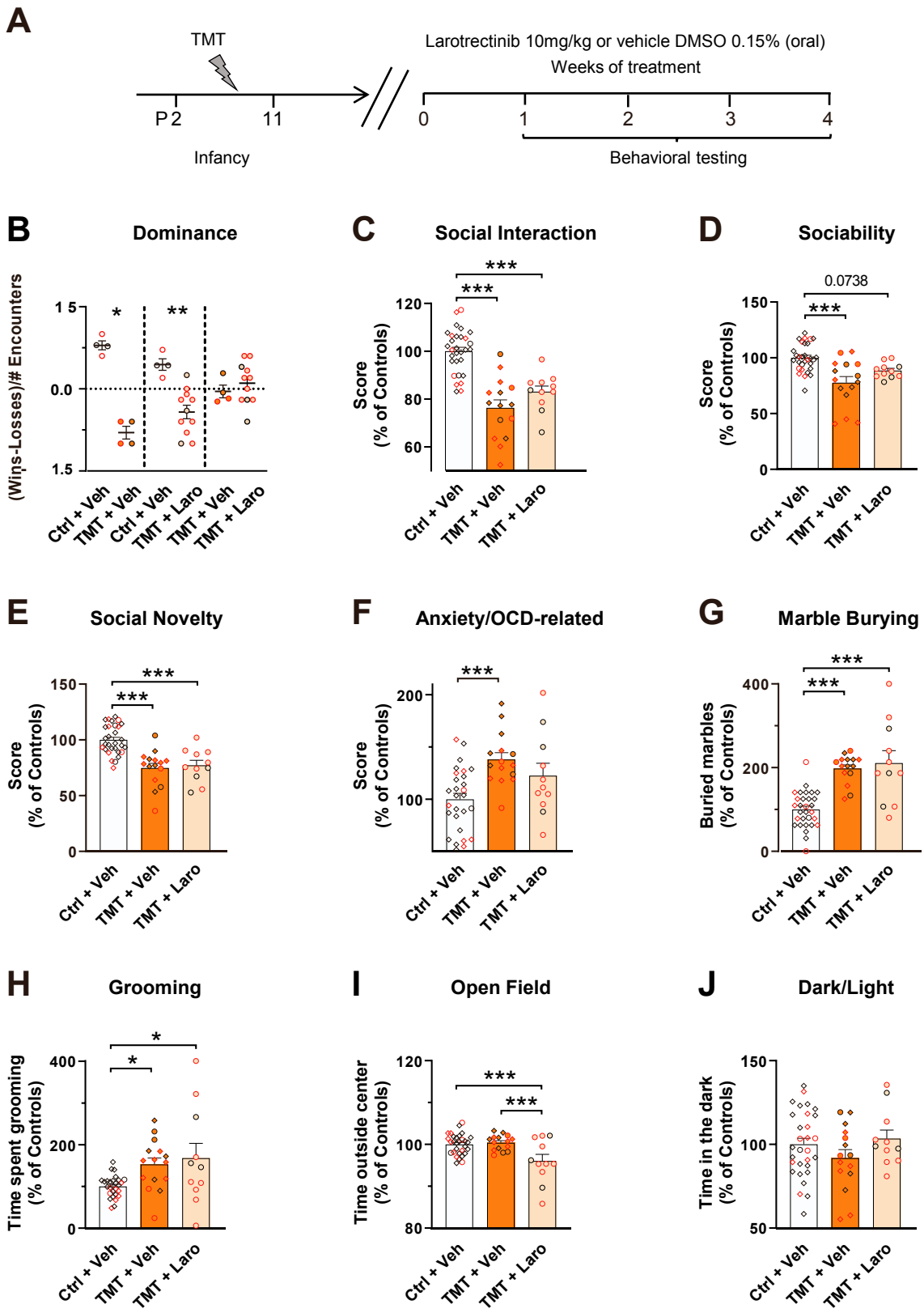
A
TMT
P 2
11
Infancy
Larotrectinib 10mg/kg or vehicle DMSO 0.15% (oral)
Weeks of treatment
0
1
2
3
4
Behavioral testing
B
Dominance
(Wins-Losses)/# Encounters
1 5
0.0
1.5
Ctrl + Veh
TMT + Veh
Ctrl + Veh
TMT + Laro
TMT + Veh
TMT + Laro
C
Social Interaction
Score (% of Controls)
120
100
80
60
Ctrl + Veh
TMT + Veh
TMT + Laro
D
Sociability
Score (% of Controls)
150
100
50
0
0.0738
Ctrl + Veh
TMT + Veh
TMT + Laro
E
Social Novelty
Score (% of Controls)
150
100
50
0
Ctrl + Veh
TMT + Veh
TMT + Laro
F
Anxiety/OCD-related
Score (% of Controls)
200
100
Ctrl + Veh
TMT + Veh
TMT + Laro
G
Marble Burying
Buried marbles (% of Controls)
400
200
0
Ctrl + Veh
TMT + Veh
TMT + Laro
H
Grooming
Time spent grooming (% of Controls)
400
200
0
Ctrl + Veh
TMT + Veh
TMT + Laro
I
Open Field
Time outside center (% of Controls)
120
100
80
Ctrl + Veh
TMT + Veh
TMT + Laro
J
Dark/Light
Time in the dark (% of Controls)
150
100
50
Ctrl + Veh
TMT + Veh
TMT + Laro

Figure S9. Treatment with the FDA-approved drug larotrectinib does not rescue specific behavioral abnormalities of adult mice exposed to predator odor during infancy. Related to Figure 3.

(**A**) Schematic cartoon of the experimental protocol for the treatment with the FDA-approved drug larotrectinib or vehicle of fully adult mice exposed to TMT during infancy and controls. (**B-F**) Dominance (B), social interaction (C), sociability (D), social novelty (E), and anxiety/OCD (F) scores following larotrectinib or vehicle treatment in controls and adult mice exposed to TMT at P2-11. Scores were based on the experiments on the tube dominance, on the three-chamber, and on the marble burying, grooming, open field and dark/light tests. Bars indicate the average (percentage normalized to age-specific controls for social interaction, sociability, social novelty, and anxiety/OCD) scores of all analyzed animals + SEM, and symbols represent the single data points for each animal. For social interaction, sociability, social novelty, and anxiety/OCD scores, single data points in diamond shape represent data from the experiment in Figure S3B,S3C,S3H ((B): Control vehicle *vs* TMT vehicle, Control vehicle *vs* TMT Larotrectinib & TMT vehicle *vs* TMT Larotrectinib: unpaired t-test. (C) One-way ANOVA $F_{(2,53)}=31.75$, $p<0.0001$, (D) $F_{(2,53)}=12.15$, $p<0.0001$, (E) $F_{(2,53)}=20.08$, $p<0.0001$, (F) $F_{(2,51)}=7.787$, $p=0.0011$, followed by Tukey's multiple comparisons test). (**G-J**) Percentage of the number of buried marbles (G), time spent grooming (H), time spent outside the center (I) and time spent in the dark compartment (J) following larotrectinib or vehicle treatment in controls and adult mice exposed to IMM at P2-11. Bars indicate the average percentages by all analyzed animals normalized to age-specific controls + SEM, and symbols represent the single data points for each animal; single data points in diamond shape represent data from the experiment in Figure S3I-S3L. ((G) One-way ANOVA, $F_{(2,53)}=23.86$, $p<0.0001$, (H) $F_{(2,51)}=6.034$, $p=0.0044$, (I) $F_{(2,53)}=8.025$, $p=0.0009$, (J) $F_{(2,53)}=1.380$, $p=0.2604$, followed by Tukey's multiple comparisons test). For all graphs, data were derived from 2 independent experiments for a total 4-28 animals per experimental group. *$p<0.05$, ***$p<0.001$. For all panels, black/gray and red symbol lines represent males and females, respectively.

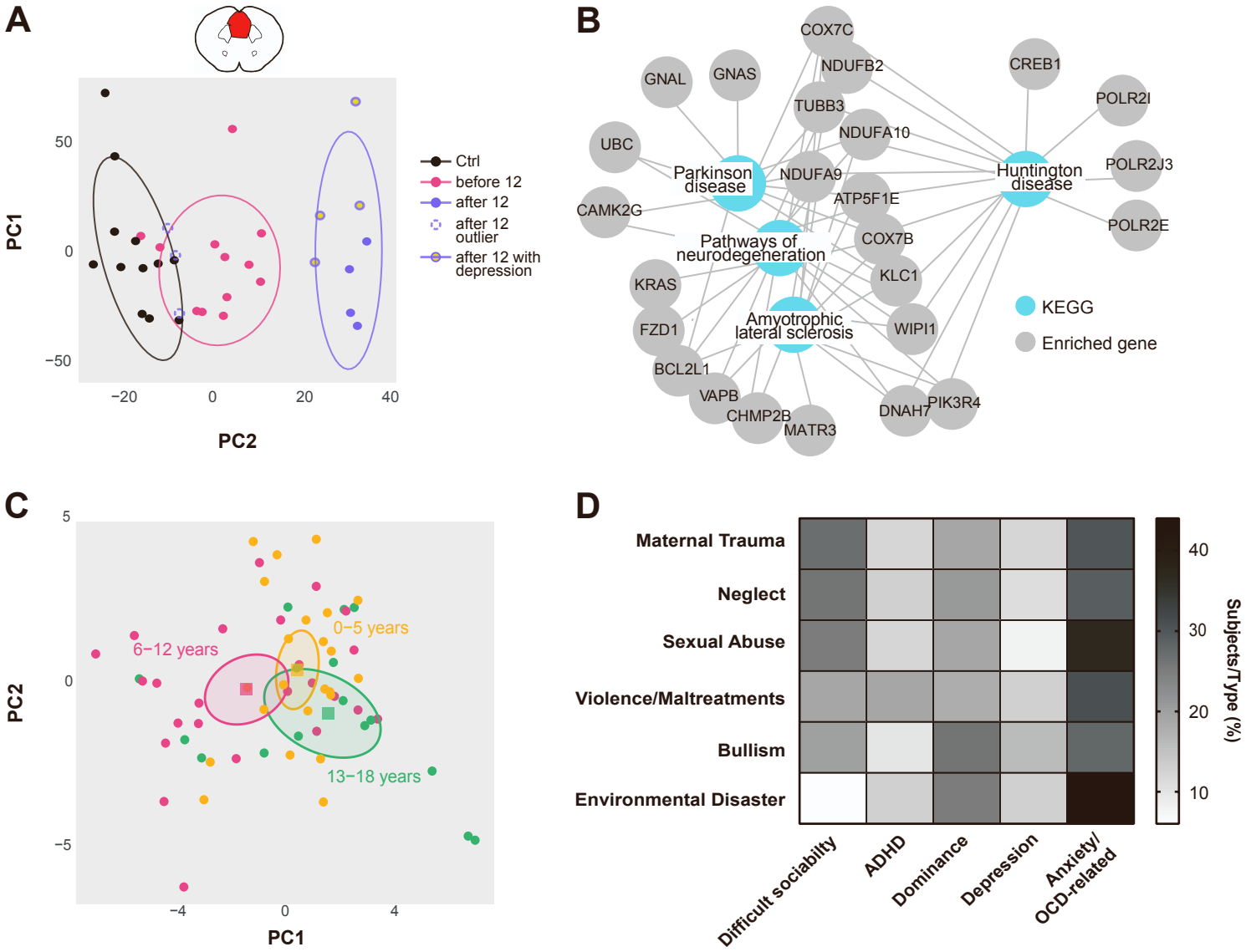
A
PC1
PC2
50
0
−50
−20
0
20
40
Ctrl
before 12
after 12
after 12 outlier
after 12 with depression
B
COX7C
NDUFB2
GNAL
GNAS
TUBB3
CREB1
POLR2I
NDUFA10
UBC
Parkinson disease
NDUFA9
Huntington disease
POLR2J3
ATP5F1E
CAMK2G
POLR2E
Pathways of neurodegeneration
COX7B
KLC1
KRAS
Amyotrophic lateral sclerosis
WIPI1
FZD1
KEGG
Enriched gene
BCL2L1
VAPB
CHMP2B
MATR3
DNAH7
PIK3R4
C
PC2
PC1
5
0
−5
−4
0
4
6−12 years
0−5 years
13−18 years
D
Maternal Trauma
Neglect
Sexual Abuse
Violence/Maltreatments
Bullism
Environmental Disaster
Difficult sociability
ADHD
Dominance
Depression
Anxiety/ OCD-related
Subjects/Type (%)
40
30
20
10

Figure S10. Trauma experienced after 12 years of age modifies PFC protein expression toward neurodegeneration, and type of trauma does not impact on the specificity of patients' maladaptive behaviors. Related to Figure 4 and Tables S8-S13.

(**A**) PCA visualization of the first two components of proteomic expression in PFC (red in the brain cartoon on top) for each age of trauma exposure as in Figure 4D, but with outliers highlighted with dashed lines. Outliers were defined based on group segregations according to the most representative components and the centroid distance. (**B**) Network plot by KEGG database showing pathway-enrichment analysis on proteins deregulated in adult people exposed to stress after 12 years of age in the same dataset as in Figure 4D (no outliers). (**C**) PCA visualization of the first two components of clinical data based on behavioral traits, personality traits and clinical scores). (**D**) Heatmap showing percentage of patients presenting maladaptive personality traits among all individuals who had experienced that specific trauma. Scale bar on the right.

Cohort #	Test 1	Test 2	Test 3	Test 4	Test 5	Test 6	Test 7	Test 8	Test 9
1	Open Field	Grooming	Marble Burying	Three-chamber	Light/dark	Shirpa	Forced Swim	Tail Suspension	Tube Dominance
2	Grooming	Marble Burying	Open Field	Light/dark	Three-Chamber	Shirpa	Tail Suspension	Forced Swim	Tube Dominance
3	Marble Burying	Grooming	Light/dark	Open Field	Shirpa	Three-chamber	Forced Swim	Tail Suspension	Tube Dominance
4	Open Field	Marble Burying	Shirpa	Light/dark	Three-chamber	Grooming	Tail Suspension	Forced Swim	Tube Dominance
5	Open Field	Shirpa	Light/dark	Grooming	Marble Burying	Three-chamber	Forced Swim	Tail Suspension	Tube Dominance
6	Light/dark	Marble Burying	Open Field	Shirpa	Three-chamber	Grooming	Tail Suspension	Forced Swim	Tube Dominance
7	Open Field	Marble Burying	Shirpa	Light/dark	Three-chamber	Grooming	Tail Suspension	Forced Swim	Tube Dominance
8	Marble Burying	Open Field	Shirpa	Three-chamber	Grooming	Light/dark	Tail Suspension	Forced Swim	Tube Dominance
9	Phenopy								

Table S1. Mouse cohorts subjected to behavioral testing. Related to Figure 1.

P26 35 TMT Assessed at P140		
Score/Test	**Controls (mean ± SEM)**	**TMT (mean ± SEM)**
Dominance score	100.0 ± 17.45	289.7 ± 22.72
Anxiety/OCD-related score	100.0 ± 5.018	158.0 ± 3.572
Marble Burying	10 ± 0.9723	12.10 ± 0.6574
Grooming	16.07 ± 1.029	59.82 ± 3.189
Time outside center (OF)	1622 ± 22.05	1642 ± 23.48
Time in the dark (dark/light)	168.8 ± 16.13	224.5 ± 9.503

P90 99 TMT Assessed at P130		
Score/Test	**Controls (mean ± SEM)**	**TMT (mean ± SEM)**
Dominance score	100.0 ± 10.03	104.4 ± 10.13
Depression score	100.0 ± 6.169	96.45 ± 11.03
Tail suspension	106.1 ± 6.906	96.28 ± 8.094
Forced swim test	77.66 ± 4.968	83.12 ± 6.119
Social Interaction score	100.0 ± 2.510	71.67 ± 1.781
Sociability score	0.4605 ± 0.03971	0.08088 ± 0.04067
Social Novelty score	0.4099 ± 0.03864	-0.02359±0.05748
Anxiety/OCD-related score	100 ± 5.168	128.5 ±7.421
Marble Burying	8.923 ± 0.6930	7 ± 0.8528
Grooming	17.89 ± 0.7103	21.68 ± 1.145
Time outside center (OF)	1377 ± 34.05	1475 ± 32.50
Time in the dark (dark/light)	173.6 ± 6.410	202.4 ± 6.674

Table S3. Behavioral tests and scores of P26-35 TMT-exposed mice assessed at P140, and P90-99 TMT-exposed mice assessed at P130. Related to Figure 1.

P2-11					
Term	**Library**	**pvalue**	**qvalue**	**z-score**	**combined score**
Caspase-mediated Cleavage Of Cytoskeletal Proteins R-HSA-264870	Reactome_2022	0.000002811	0.0004947	147.7	1888
arteriovenous malformation MP:0006093	MGI_Mammalian_Phenotype_Level_4_2021	0.0004326	0.1153	78.82	610.5
Deregulation of Rab and Rab Effector Genes in Bladder Cancer WP2291	WikiPathway_2021_Human	0.0006624	0.02319	61.92	453.2
Apoptotic Cleavage Of Cellular Proteins R-HSA-111465	Reactome_2022	0.0001032	0.009079	37.94	348.2
Apoptotic Execution Phase R-HSA-75153	Reactome_2022	0.000264	0.01549	27.08	223.1
Morphological abnormality of the pyramidal tract (HP:0002062)	Human_Phenotype_Ontology	0.002049	0.1418	33.32	206.3
abnormal neuromuscular synapse morphology MP:0001053	MGI_Mammalian_Phenotype_Level_4_2021	0.0008378	0.1153	17.91	126.9
mRNA Splicing - Minor Pathway R-HSA-72165	Reactome_2022	0.006173	0.2173	18.41	93.68
persistence of hyaloid vascular system MP:0001289	MGI_Mammalian_Phenotype_Level_4_2021	0.001585	0.1153	14.24	91.78
abnormal miniature excitatory postsynaptic currents MP:0004753	MGI_Mammalian_Phenotype_Level_4_2021	0.001585	0.1153	14.24	91.78
Teleangiectasia of the skin (HP:0100585)	Human_Phenotype_Ontology	0.006672	0.1418	17.66	88.47
Copper homeostasis WP3286	WikiPathway_2021_Human	0.006929	0.1212	17.31	86.05
Anonychia (HP:0001798)	Human_Phenotype_Ontology	0.009432	0.1418	14.66	68.37
small spleen MP:0000692	MGI_Mammalian_Phenotype_Level_4_2021	0.005283	0.2055	9.17	48.08
Osteoporosis (HP:0000939)	Human_Phenotype_Ontology	0.01508	0.1418	11.37	47.69

P12-21					
Term	**Library**	**pvalue**	**qvalue**	**z-score**	**combined score**
Mitochondrial complex III assembly WP4921	WikiPathway_2021_Human	0.001695	0.09679	37.92	241.9
Airway smooth muscle cell contraction WP4962	WikiPathway_2021_Human	0.001917	0.09679	35.39	221.5
abnormal response of heart to induced stress MP:0004484	MGI_Mammalian_Phenotype_Level_4_2021	0.002398	0.2648	31.23	188.4
Vibrio cholerae infection	KEGG_2021_Human	0.0009442	0.0982	17.14	119.4
Respiratory Electron Transport R-HSA-611105	Reactome_2022	0.0004038	0.05196	12.64	98.77
increased interleukin-1 beta secretion MP:0008657	MGI_Mammalian_Phenotype_Level_4_2021	0.00715	0.2648	17.11	84.54
Respiratory Electron Transport, ATP Synthesis By Chemiosmotic Coupling, Heat Production By Uncoupling Proteins R-HSA-163200	Reactome_2022	0.0009208	0.06122	10.05	70.27
abnormal embryonic epiblast morphology MP:0003886	MGI_Mammalian_Phenotype_Level_4_2021	0.009887	0.2648	14.33	66.17
abnormal coat/ hair morphology MP:0000367	MGI_Mammalian_Phenotype_Level_4_2021	0.002923	0.2648	11.34	66.14
SARS-CoV-2 Infection R-HSA-9694516	Reactome_2022	0.0001089	0.02101	7.118	64.96
abnormal vitreous body morphology MP:0002699	MGI_Mammalian_Phenotype_Level_4_2021	0.01038	0.2648	13.95	63.74
Oxidative Damage WP3941	WikiPathway_2021_Human	0.01038	0.2923	13.95	63.74
Oxidative phosphorylation	KEGG_2021_Human	0.001738	0.0982	8.408	53.43
Cardiac muscle contraction	KEGG_2021_Human	0.004612	0.1616	9.575	51.5
TGF-beta signaling pathway	KEGG_2021_Human	0.005721	0.1616	8.835	45.62

P26-35					
Term	**Library**	**pvalue**	**qvalue**	**z-score**	**combined_score**
Lysosome Vesicle Biogenesis R-HSA-432720	Reactome_2022	0.0002905	0.01888	95.93	781.2
decreased basophil cell number MP:0002607	MGI_Mammalian_Phenotype_Level_4_2021	0.001129	0.0711	47.15	320
trans-Golgi Network Vesicle Budding R-HSA-199992	Reactome_2022	0.001266	0.04115	44.41	296.3
Cargo Recognition For Clathrin-Mediated Endocytosis R-HSA-8856825	Reactome_2022	0.00269	0.05829	29.99	177.5
Lysosome	KEGG_2021_Human	0.004041	0.02829	24.25	133.6
Clathrin-mediated Endocytosis R-HSA-8856828	Reactome_2022	0.004947	0.08039	21.81	115.8

P47-56					
Term	**Library**	**pvalue**	**qvalue**	**z-score**	**combined score**
Increased neuronal autofluorescent lipopigment (HP:0002074)	Human_Phenotype_Ontology	0.0006265	0.03858	70.56	520.4
Increased cerebral lipofuscin (HP:0011813)	Human_Phenotype_Ontology	0.000803	0.03858	60.48	431
increased heart ventricle size MP:0008772	MGI_Mammalian_Phenotype_Level_4_2021	0.002619	0.2787	30.23	179.7
Formation Of A Pool Of Free 40S Subunits R-HSA-72689	Reactome_2022	0.0001095	0.01818	11.7	106.7
Mitochondrial inheritance (HP:0001427)	Human_Phenotype_Ontology	0.001314	0.04747	15.25	101.2
abnormal Purkinje cell dendrite morphology MP:0008572	MGI_Mammalian_Phenotype_Level_4_2021	0.001585	0.2787	14.24	91.78
L13a-mediated Translational Silencing Of Ceruloplasmin Expression R-HSA-156827	Reactome_2022	0.0001731	0.01818	10.56	91.49
GTP Hydrolysis And Joining Of 60S Ribosomal Subunit R-HSA-72706	Reactome_2022	0.0001807	0.01818	10.46	90.16
Translation R-HSA-72766	Reactome_2022	8.3684E-06	0.004209	7.467	87.29
Influenza Infection R-HSA-168255	Reactome_2022	0.0001101	0.01818	8.721	79.48
Endocrine and other factor-regulated calcium reabsorption	KEGG_2021_Human	0.00211	0.08862	12.81	78.92
abnormal nervous system electrophysiology MP:0002272	MGI_Mammalian_Phenotype_Level_4_2021	0.001136	0.2787	9.466	64.18
Developmental regression (HP:0002376)	Human_Phenotype_Ontology	0.000808	0.03858	7.436	52.95
Dysarthria (HP:0001260)	Human_Phenotype_Ontology	0.0004766	0.03858	6.568	50.24
abnormal cerebral cortex morphology MP:0000788	MGI_Mammalian_Phenotype_Level_4_2021	0.0009901	0.2787	7.093	49.07

Table S6. Enriched pathways identified for proteins deregulated in brain areas specific for each TMT-exposure time window. Related to Figure 2.

Trauma <12 years	Code	Gender	Age	Race	Cause of death	PMI (h)	Refr Delay (h)	pH
	1C (<12 years)	F	45	Caucasian	Suicide	96	49.28	6.5
	2C (<12 years)	M	55	Caucasian	Suicide	57.5	8.43	6.1
	3C (<12 years)	M	56	Caucasian	Suicide	77.85	7.18	6.26
	4C (<12 years)	M	39	Caucasian	Undetermined	50.45	9.67	5.44
	5C (<12 years)	M	55	Caucasian	Accidental	51	10.65	6.48
	6C (<12 years)	M	34	Caucasian	Natural	43.5	8.49	6.36
	7C (<12 years)	F	60	Caucasian	Suicide	52	9.9	6.27
	8C (<12 years)	M	48	Caucasian	Suicide	41.5	11.48	6.38
	9C (<12 years)	F	46	Caucasian	Suicide	54	26.87	6.29
	10C (<12 years)	M	58	Caucasian	Suicide	90.25	8.99	5.8
	11C (<12 years)	M	39	Caucasian	Suicide	52	18.39	6.3
	12C (<12 years)	M	45	Caucasian	Natural	55.5	11.98	5.7

Trauma >12 years	Code	Gender	Age	Race	Cause of death	PMI (h)	Refr Delay (h)	pH
	1D (>12 years)	F	27	Caucasian	Accidental	79.5	2	5.98
	2D (>12 years)	M	57	Caucasian	Natural	115.3	24.75	6.34
	3D (>12 years)	F	21	Caucasian	Accidental	69.98	9.42	6.56
	4D (>12 years)	F	22	Caucasian	Suicide	81.33	18.92	6.35
	5D (>12 years)	F	61	Caucasian	Accidental	51.5	10.48	6.02
	6D (>12 years)	M	59	Caucasian	Suicide	47.5	5.99	5.65
	7D (>12 years)	M	58	Caucasian	Suicide	47	14.23	6.03
	8D (>12 years)	M	68	Caucasian	undetermined	43.5	4.99	5.87
	9D (>12 years)	M	53	Caucasian	undetermined	N/A	N/A	6.04
	10D (>12 years)	F	44	Caucasian	Suicide	56.1	8.49	6.01
	11D (>12 years)	F	40	Caucasian	Natural	41.75	6.41	6.46

Controls	Code	Gender	Age	Race	Cause of death	PMI (h)	Refr Delay (h)	pH
	1 Ctr (Controls)	M	61	Caucasian	Accidental	76.5	2	6.37
	2 Ctr (Controls)	M	45	Caucasian	Natural	97.52	11.97	6.36
	3 Ctr (Controls)	F	54	Caucasian	Natural	85.25	50.17	6.19
	4 Ctr (Controls)	M	25	Caucasian	Natural	44.5	6.49	5.9
	5 Ctr (Controls)	M	36	Caucasian	Accidental	49	5.24	6.32
	6 Ctr (Controls)	M	59	Caucasian	Natural	66	31.78	6.21
	7 Ctr (Controls)	F	28	Caucasian	undetermined	80	9.23	6.45
	8 Ctr (Controls)	M	45	Caucasian	Natural	35.5	3	6.19
	9 Ctr (Controls)	F	62	Caucasian	Natural	48.25	12.56	5.91
	10 Ctr (Controls)	M	59	Caucasian	Natural	42	4.99	6.4
	11 Ctr (Controls)	F	58	Caucasian	Natural	42.75	11.23	N/A
	12 Ctr (Controls)	M	67	Caucasian	Accidental	51.08	14.01	6.39

Table S8. General information on human samples whose PFC were subjected to proteomic analysis.

Trauma <12 years	Code	Simplified Axis 1	Axis 1 Dependence
	1C (<12 years)	Nil	Nil
	2C (<12 years)	MDD	Nil
	3C (<12 years)	MDD	Alcohol and Cocaine dependence
	4C (<12 years)	MDD	Cannabis dependence
	5C (<12 years)	Nil	Cocaine
	6C (<12 years)	Bipolar disorder II depression	Cocaine dependence
	7C (<12 years)	Bipolar disorder I mania	Nil
	8C (<12 years)	MDD	Nil
	9C (<12 years)	Substance induced psychotic disorder	Hallucinogens/PCP dependance
	10C (<12 years)	Nil	Polydrug
	11C (<12 years)	Depressive disorder NOS	Nil
	12C (<12 years)	Nil	Nil

Trauma >12 years	Code	Simplified Axis 1	Axis 1 Dependence
	1D (>12 years)	Bipolar disorder I	Nil
	2D (>12 years)	MDD	Substance dependence
	3D (>12 years)	Depressive disorder NOS	Opioid dependence
	4D (>12 years)	Depressive disorder NOS	Nil
	5D (>12 years)	PTSD	Nil
	6D (>12 years)	MDD	Nil
	7D (>12 years)	MDD	Alcohol dependence
	8D (>12 years)	N/A	N/A
	9D (>12 years)	Nil	Alcohol
	10D (>12 years)	MDD	Stimulants dependence
	11D (>12 years)	N/A	N/A

Controls	Code	Simplified Axis 1	Axis 1 Dependence
	1 Ctr (Controls)	Nil	Nil
	2 Ctr (Controls)	Nil	Nil
	3 Ctr (Controls)	Nil	Nil
	4 Ctr (Controls)	Nil	Nil
	5 Ctr (Controls)	Nil	Nil
	6 Ctr (Controls)	Nil	Nil
	7 Ctr (Controls)	Nil	Nil
	8 Ctr (Controls)	Nil	Nil
	9 Ctr (Controls)	Nil	Nil
	10 Ctr (Controls)	Nil	Nil
	11 Ctr (Controls)	Nil	Nil
	12 Ctr (Controls)	Nil	Nil

Table S9. Neuropsychiatric information on human samples whose PFC were subjected to proteomic analysis. N/A: not available; Nil: nothing; MDD: major depressive disorder; NOS: depressive disorder not otherwise specified; PTSD: post-traumatic stress disorder.

Trauma <12 years	Code	Substance at death	Last 3 months medication
	1C (<12 years)	Antidepressants (SNRI)	Antidepressants (SNRI)
	2C (<12 years)	Benzodiazepines, Cocaine and metabolites, Opiates, MDMA	Benzodiazepines
	3C (<12 years)	Alcohol, Benzodiazepine, Cocaine + metabolites	Sleeping Rx
	4C (<12 years)	SSRI, Acetone, Cannabis	Antidepressants (SSRI), GABAergic
	5C (<12 years)	Cocaine metabolites	N/A
	6C (<12 years)	Coaïne, Cannabis	Nil
	7C (<12 years)	Antipsychotic	N/A
	8C (<12 years)	Nil	Nil
	9C (<12 years)	Nil	Antidepressant (SNRI)
	10C (<12 years)	Cannabis, Antidepressant (SSRI), Antipsychotics	Unknown Antidepressant, hypnotic
	11C (<12 years)	Alchol, Cocaine, Methamphetamines	N/A
	12C (<12 years)	Nil	Nil

Trauma >12 years	Code	Substance at death	Last 3 months medication
	1D (>12 years)	N/A	Antipsychotics, Antimanic
	2D (>12 years)	Benzodiazepines, Antidepressants (TCA) and metabolites, Alcohol	N/A
	3D (>12 years)	Cocaine,Opioid, Cannabis, Antidepressants (SSRI)	Lithium
	4D (>12 years)	Antidepressants (SNRI), Cannabinol	Opiate, Antidepressants (SNRI), Antipsychotic
	5D (>12 years)	Alcohol	Sleeping Rx
	6D (>12 years)	Alcohol, CNS stimulant, Antidepressants (SARI, SNRI)	Psychostimulant, Antidepressants (SNRI, TCA), Quinolone derived atypical antipsychotic
	7D (>12 years)	Nil	Nil
	8D (>12 years)	N/A	N/A
	9D (>12 years)	Alcohol, Non-Benzodiazepine sedative, SSRI, Atypical antipsychotic, anticonvulsant	
	10D (>12 years)	Antidepressant (SSRI, NDRI), Benzodiazpines, Antipsychotic, Antiepileptic, Cannabis	Antidepressants (SSRI, NDRI), Antipsychotique, Benzodiazepines
	11D (>12 years)	Antidepressant (SNRI), Antipsychotic (Atypical), THC	Antidepressant (SNRI), Antipsychotic

Controls	Code	Substance at death	Last 3 months medication
	1 Ctr (Controls)	Nil	Nil
	2 Ctr (Controls)	Nil	Sedative/Hypnotic
	3 Ctr (Controls)	Nil	Nil
	4 Ctr (Controls)	Morphine, Cannabis metabolites	Nil
	5 Ctr (Controls)	Nil	Nil
	6 Ctr (Controls)	Nil	Nil
	7 Ctr (Controls)	Nil	Nil
	8 Ctr (Controls)	Nil	Nil
	9 Ctr (Controls)	Nil	Nil
	10 Ctr (Controls)	Nil	Nil
	11 Ctr (Controls)	Nil	Nil
	12 Ctr (Controls)	Nil	Nil

Table S10. Information about substance/medication on human samples whose PFC were subjected to proteomic analysis. N/A: not available; Nil: nothing; SNRI: serotonin-norepinephrine reuptake inhibitor; SSRI: selective serotonin reuptake inhibitor; TCA: tricyclic antidepressant; THC: tetrahydrocannabinol; MDMA: methylenedioxy-methylamphetamine.